Characterization of the Alb3/Oxa1/YidC protein family in *Arabidopsis thaliana*

Dissertation der Fakultät für Biologie

der

Ludwig-Maximilians-Universität München

vorgelegt von

Monique Karl

aus Salzgitter

München

2009

Erstgutachter: Prof. Dr. J. Soll
Zweitgutachter: PD Dr. C. Bolle

Tag der mündlichen Prüfung: 22.06.2009

LITTERIS ET FLORIBUS

Abbreviations

2D	two dimensional
AA	amino acid
Alb	Albino
acc.	according (to)
At	*Arabidopsis thaliana*
AGI	*Arabidopsis* Genome Initiative
AOX	mitochondrial alternative oxidase
AP	alkaline phosphatase
ATPase	CF_OCF_1-ATP synthase (complex)
β-ME	β-mercaptoethanol
BLAST	basic local alignment search tool
BN-PAGE	blue-native polyacrylamide gel electrophoresis
bp	basepair
CC	coiled-coil
cDNA	copy-DNA
CF_O	membrane-embedded part of CF_OCF_1 ATP synthase (complex)
CF_1	soluble part of CF_OCF_1 ATP synthase (complex)
Chl	chlorophyll
Col	Columbia
Cox	cytochrome c oxidase
cp	chloroplastidic
C-(terminus)	carboxy terminus
cTP	chloroplast transit peptide
$Cytb_6f$	cytochrome b_6f (complex)
Cyt c	cytochrome c
Da	Dalton
DoMa	*n*-dodecyl-*β*-D-maltoside
DTT	dithiothreitol
ECL	enhanced chemiluminescence
E. coli	*Escherichia coli*
ER	endoplasmic reticulum
Fd	ferredoxin
FNR	ferredoxin-NADP(H) oxidoreductase
GFP	green fluorescent protein
HMW	high molecular weight
IE	inner envelope / inner envelope membrane
IMP	inner membrane protein
IMS	intermembrane space
k, K	kilo, times 1000
LHC(P)	light-harvesting chlorophyll binding (protein)
LMW	low molecular weight
Met	methionine
Mt	mitochondria(l)
mTP	mitochondrial transit peptide
mRNA	messenger-RNA
MS	mass spectrometry
N-(terminus)	amino terminus
OE	outer envelope / outer envelope membrane

OE33	oxygen evolving complex protein of 33 kDa
OEC	oxygen evolving complex (of PSII)
Oxa	cytochrome c oxidase assembly
PAGE	polyacrylamide gel electrophoresis
PCR	polymerase chain reaction
PEG	polyethylene glycol
Ps	*Pisum sativum*
PSI, PSII	photosystem I, II
RACE	rapid amplification of cDNA ends
ret.	retention signal
RNAi	RNA interference
rpm	revolutions per minute
RT	room temperature
RuBisCO	ribulose-1,5-bisphosphate carboxylase/oxygenase
SD	standard deviation
SDS	sodium dodecyl sulphate
Sec	secretory
SP	signal peptide
SRP	signal recognition particle
SSU	ribulose-1,5-bisphosphate carboxylase/oxygenase, small subunit
Tat	twin-arginine translocon
TEM	transmission electron microscopy
Tic	translocon at the inner envelope of chloroplasts
TILLING	targeting induced local lesions in genomes
TM	transmembrane (domain)
Toc	translocon at the outer envelope of chloroplasts
TP	transit peptide
TPR	tetratricopeptide repeat
TX-100	Triton X-100
UTR	untranslated region
v/v	volume per volume
WT	wild-type
w/v	weight per volume
x g	times the force of gravity

Table of contents

Abbreviations ..... **I**
Table of contents ..... **III**
1 Summary **1**
2 Zusammenfassung **2**
3 Introduction **3**
3.1 Chloroplasts, the power house *3*
3.2 Molecular organization of the thylakoid membrane *3*
3.3 Protein translocation into and across the thylakoid membrane *5*
3.4 The Alb3/Oxa1/YidC protein family *7*
3.4.1 Oxa1, the mitochondrial homologue 8
3.4.2 YidC, the bacterial homologue 10
3.4.3 Slr1471 in *Synechocystis* 11
3.4.4 Alb3, the homologue in chloroplasts 11
3.4.5 Alb3.1 and Alb3.2 in *Chlamydomonas* 13
3.4.6 Further homologues in *Arabidopsis thaliana* 13
4 Materials **15**
4.1 Chemicals *15*
4.2 Detergents *15*
4.3 Enzymes *15*
4.4 Kits *15*
4.5 Molecular weight markers and DNA standards *15*
4.6 Antibodies *16*
4.7 Strains, vectors, clones and oligonucleotides *16*
4.8 Plant material *16*
4.9 Clones used in this work *17*
5 Methods **18**
5.1 Growth conditions *18*
5.1.1 Growth of *Arabidopsis thaliana* 18
5.1.2 Growth of *Escherichia coli* 18
5.2 Molecular biological methods *18*
5.2.1 General molecular biological methods 18
5.2.2 Homologous recombination 18
5.2.3 Isolation of genomic DNA from *Arabidopsis thaliana* 19
5.2.4 Characterization of *ALB4* TILLING lines 19
5.2.5 Polymerase Chain Reaction (PCR) 19
5.2.6 RNA isolation, cDNA preparation and real-time PCR 20
5.3 Biochemical methods *21*
5.3.1 General biochemical methods 21
5.3.2 SDS-polyacrylamide electrophoresis (SDS-PAGE) 21
5.3.3 Western blotting and immunodecoration with antibodies 21
5.3.4 Two-dimensional blue native gel electrophoresis / SDS-PAGE and immunoblotting 21
5.3.5 Immunoblot development 22
5.3.6 Extraction of soluble and total membrane proteins from *Arabidopsis thaliana* 23
5.3.7 Protein identification by mass spectrometry (MS) 23
5.4 Cell biological methods *24*
5.4.1 Isolation of *Arabidopsis* chloroplasts 24
5.4.2 Isolation of thylakoid and stroma fractions 24
5.4.3 Separation of stroma thylakoids from grana thylakoids 24
5.4.4 *In vitro* translation in isolated *Arabidopsis* chloroplasts ("*in organello*" translation) 25
5.4.5 Isolation of intact chloroplasts from *Pisum sativum* (pea) 25
5.4.6 Isolation of mitochondria *Pisum sativum* (pea) leaves 25
5.4.7 *In vitro* transcription and translation: 26
5.4.8 *In vitro* import assay into isolated pea chloroplasts 26
5.4.9 *In vitro* import assay into isolated pea mitochondria 27

5.4.10 *In vitro* dual import assay into isolated pea mitochondria and chloroplasts ... 27
5.4.11 Preparation of *Arabidopsis* protoplast and transient transformation ... 28
5.5 Microscopy methods ... 28
5.5.1 Transmission electron microscopy (TEM) ... 28
5.6 Computational methods ... 29
Software, databases and algorithms used in the present study ... 29
6 Results ... 30
6.1 The Oxa gene family in Arabidopsis thaliana ... 30
6.1.1 Seven Alb3/Oxa1/YidC homologues are expressed in *A. thaliana* ... 30
6.1.2 *In silico* characterization of the *Arabidopsis* homologues ... 31
6.2 Sub-cellular localization of Alb3/YidC/Oxa-like proteins in Arabidopsis ... 34
6.2.1 *In silico* analysis ... 34
6.2.2 *In vitro* import ... 35
6.2.3 GFP fusion constructs ... 37
6.3 Physiological role of Alb4 in Arabidopsis thaliana ... 42
6.3.1 *ALB4* TILLING mutants ... 42
6.3.2 Phenotype of *alb4* mutants ... 43
6.3.3 Ultrastructure of *alb4* chloroplasts ... 44
6.3.4 Loss of Alb4 causes a decrease in steady-state levels of ATP synthase subunits ... 45
6.3.5 The role of Alb4 in the assembly of the ATP synthase ... 49
6.3.6 Expression of the *atp* genes is not changed in *alb4* plants ... 51
6.3.7 Sub-thylakoidal localization of Alb4 and ATP synthase ... 52
6.3.8 Alb4 co-migrates with the ATP synthase complex ... 54
6.3.9 Loss of Alb4 influences PSII complexes ... 55
6.3.10 *De novo* synthesis of chloroplast-encoded proteins ... 56
7 Discussion ... 60
7.1 Localization of Alb3/Oxa1/YidC family members in Arabidopsis thaliana ... 60
7.2 The physiological role of Alb4 in Arabidopsis thaliana ... 64
7.2.1 Alb4 is necessary for the proper biogenesis of thylakoid membranes ... 64
7.2.2 Alb4 associates with the ATP synthase but not with cpSec ... 66
7.2.3 The ATP synthase is affected in absence of Alb4 ... 67
7.2.4 Alb4 is likely to promote the assembly and/or stability of the high molecular weight ATP synthase complexes ... 68
7.2.5 Loss of Alb4 results in reduced PSII super-complexes ... 70
7.2.6 Alb4 is a functional member of the Alb3/Oxa1/YidC family ... 72
7.2.7 *De novo* synthesis and assembly of chloroplast-encoded proteins is not impaired by loss of Alb4 ... 73
References ... 75
Danksagung ... 87
***Curriculum vitae* ... 88**
List of publications ... 89
Ehrenwörtliche Versicherung ... 90
Erklärung ... 90

1 Summary

The insertion of membrane proteins in chloroplasts, mitochondria and bacteria is accomplished by an evolutionary conserved pathway. In this pathway, members of the Alb3/Oxa1/YidC family act as membrane integrases and function in the folding and assembly of multi-subunit protein complexes. Prokaryotes and most eukaryotes generally possess one or two homologues of this protein class. In contrast to this, the genome of *Arabidopsis thaliana* was found to contain seven different genes coding for Alb3/Oxa1/YidC-like proteins. Since the sub-cellular localization has been investigated for only three of them so far, one aim of this work was to determine the distribution of all seven homologues in the plant cell. *In vitro* and *in vivo* localization studies establish that four of them, namely AtOxa1a, AtOxa1b, AtOxa2a and AtOxa2b, are present in mitochondria, while Alb3 and Alb4 are located in the chloroplast. AtOxa6, which is identified as a seventh Oxa homologue, is most likely dually targeted to both organelles.

In a second part of this work, the physiological role of Alb4 was investigated in more detail. Next to Alb3, which is known to be essential for the insertion of light-harvesting chlorophyll binding proteins (LHCPs), Alb4 represents a second member of the Alb3/Oxa1/YidC family present in the thylakoid membrane and is shown to be involved in thylakoid biogenesis. Although Alb4 is not essential for survival, *Arabidopsis* knockout plants display retarded growth and an altered chloroplast and thylakoid ultrastructure. Further analyses of the *alb4* mutant lines reveal that the steady state levels of several subunits of the plastidic CF_1CF_O-ATP synthase are reduced, including plastid- and nuclear-encoded components. Transcript analysis as well as *in organello* synthesis of chloroplast proteins indicates that neither transcription nor translation of these subunits is impaired in the mutants. Instead, two-dimensional BN/SDS-PAGE demonstrates that the assembly of the high molecular weight ATP synthase complexes is impaired, resulting in reduced stability of some subunits. Moreover, Alb4 and the CF_1CF_O-ATP synthase are found to form complexes of equal size and to co-localize in the stroma-lamellae of thylakoids, indicating that both might be associated at several stages of the complex assembly. The presented data therefore strongly suggest a role for Alb4 in the assembly and/or stabilization of the plastidic CF_1CF_O-ATP synthase.

2 Zusammenfassung

Der Einbau von integralen Membranproteinen in Chloroplasten, Mitochondrien und Bakterien erfolgt auf einem evolutionär konservierten Weg. Mitglieder der Alb3/Oxa1/YidC-Familie fungieren im Rahmen dieses Weges als Membran-Integrasen und sind in der Faltung sowie Assemblierung von Proteinkomplexen, die aus mehreren Untereinheiten aufgebaut sind, beteiligt. Prokaryoten und die meisten Eukaryoten besitzen im Allgemeinen ein oder zwei Homologe dieser Proteinklasse. Im Genom von *Arabidopsis thaliana* wurden im Gegensatz dazu sieben Gene gefunden, die für Alb3/Oxa1/YidC-Proteine kodieren. Da die subzelluläre Lokalisierung bislang nur für drei von diesen untersucht worden ist, war ein Ziel dieser Arbeit die Verteilung aller sieben Homologe in der Pflanzenzelle zu bestimmen.

Für die vier Proteine AtOxa1a, AtOxa1b, AtOxa2a und AtOxa2b konnte mit Hilfe von *in vitro*- und *in vivo*-Lokalisierungsstudien gezeigt werden, dass sie sich in den Mitochondrien befinden, wohingegen Alb3 und Alb4 in den Chloroplasten lokalisiert sind. AtOxa6, welches als ein siebtes Oxa-Homolog identifiziert werden konnte, wird mit großer Wahrscheinlichkeit zu beiden Organellen geleitet.

In einem zweiten Teil dieser Arbeit wurde die physiologische Rolle von Alb4 genauer untersucht. Neben Alb3, von dem bekannt ist, dass es essentiell für die Integration von Lichtsammelkomplex-Proteinen notwendig ist, repräsentiert Alb4 ein zweites Mitglied der Alb3/Oxa1/YidC-Familie in der Thylakoidmembran, welches an der Thylakoidbiogenese beteiligt ist. Obwohl Alb4 nicht lebensnotwendig ist, zeigen *Arabidopsis* Null-Mutanten verzögertes Wachstum und eine veränderte Ultrastruktur der Chloroplasten sowie der Thylakoidmembranen. Weitere Analysen der *alb4* Mutantenlinien ergaben, dass mehrere, sowohl Plastiden- als auch Zellkernkodierte Untereinheiten der ATP-Synthase in reduzierten Mengen vorliegen. Transkriptanalysen sowie die Untersuchung der Synthese von chloroplastidären Proteinen im isolierten Organell deuten darauf hin, dass weder Transkription noch Translation dieser Untereinheiten in den Mutanten beeinträchtigt ist. Im Gegensatz dazu konnte in zweidimensionalen BN/SDS-Gelen gezeigt werden, dass der Zusammenbau von hochmolekularen ATP-Synthase Komplexen beeinträchtigt ist, was eine verringerte Stabilität einiger Untereinheiten zur Folge hat. Darüber hinaus bilden Alb4 und die CF_OCF_1 ATP-Synthase Komplexe gleicher Größe und sind beide in den Stroma-Lamellen der Thylakoide zu finden, was darauf hindeutet, dass beide an mehreren Phasen der Komplex-Assemblierung assoziiert vorliegen könnten. Die vorgestellten Daten sprechen daher deutlich für eine Funktion von Alb4 im Zusammenbau und/oder der Stabilisierung der plastidären ATP-Synthase.

3 Introduction

3.1 Chloroplasts, the power house

Photosynthesis is one of the major hallmarks of plants, enabling them to convert inorganic metabolites into organic compounds such as sugars by using sunlight as energy source. Since molecular oxygen is released as a side product into the atmosphere, photosynthesis therefore is crucial for life on earth. In photoautotrophic organisms, such as plants and algae, photosynthesis takes place in distinct organelles, called chloroplasts. Chloroplasts are composed of six different compartments: three membrane systems, namely the outer and inner envelopes as well as the thylakoids, which enclose three internal soluble compartments: the intermembrane space, the stroma, and the thylakoid lumen. Besides photosynthesis, many additional essential processes are carried out in chloroplasts, like carbon fixation, amino acid and fatty acid biosynthesis. Moreover, the organelle still maintains a transcription and translation machinery, necessary for the production of chloroplast-encoded proteins. Chloroplasts as well as mitochondria are considered to have originated from an endosymbiotic event, in which a bacterium was taken up by a host cell. Thereby, chloroplasts are believed to have arisen from a cyanobacterial prokaryote, whereas mitochondria are considered to have an alpha-proteobacteria-like ancestor (for review see Gray et al., 1999; Dyall et al., 2004).

During evolution, most of the original prokaryotic genome was either lost or transferred to the nuclear genome. Although mitochondria and chloroplasts still contain their own genomes, the vast majority of their proteins is encoded in the nucleus, synthesized in the cytosol as preproteins and transported post-translationally into the organelles. Targeting to the appropriate organelle is generally mediated by N-terminal targeting peptides and specific protein translocases (for recent reviews see Stengel et al., 2008; Jarvis and Robinson, 2004).

3.2 Molecular organization of the thylakoid membrane

Thylakoids represent the most abundant membrane system in nature and harbor the major photosynthetic complexes: photosystem I (PSI), photosystem II (PSII), cytochrome b_6f ($Cytb_6f$) and the CF_1CF_O-ATP synthase complex (Figure 1) (for review see Leister and Schneider, 2003). These four complexes are composed of at least 70 different proteins encoded in both the nuclear and the chloroplast genome (for review see Ort and Yokum, 1996; Wollman et al., 1999). Over the last years considerable progress has been made regarding their structural resolution (Zouni et al., 2001; Ben Shem et al., 2003; Kurisu et al., 2003). Complex biogenesis and assembly on the other hand are still poorly understood. The

best characterized complex in this respect is the multi-subunit, pigment-containing PSII (Britt, 1996; Goussias et al., 2002). Next to a number of low molecular mass proteins, the core of PSII is comprised of the D1 and D2 proteins, cytochrome b_{559}, as well as the chlorophyll *a* binding antenna proteins CP43 and CP47. The oxygen-evolving complex (OEC) where water oxidation takes place is bound to the luminal surface of the PSII core complex. PSII functions as a dimer, which is further associated with the light-harvesting complex II (LHCII) to form PSII-LHCII super-complexes. These are most likely linked by the minor antenna proteins CP24 (Lhcb6), CP26 (Lhcb5) and CP29 (Lhcb4) (Figure 1). During photosynthesis, the light dependent electron transport is coupled to the synthesis of ATP, which is energetically mediated by an electrochemical proton gradient over the thylakoid membrane. This photophosphorylation is catalyzed by the proton-translocating ATP synthase which has been found to be highly conserved in structure and composition in (eu) bacteria, mitochondria and chloroplasts (for review see Strotmann et al., 1998; Groth and Pohl, 2001). The chloroplast ATP synthase consists of nine different subunits that form two functionally distinct sub-complexes: the transmembrane CF_O part, which mediates the translocation of protons, and the hydrophilic CF_1 part, which contains the catalytic sites involved in ATP synthesis (Figure 1). Five different subunits are found in the CF_1 part, three of which are encoded in the plastome (α, β,ε) and two in the nucleus (γ, δ). The membrane-embedded CF_O section is composed of four subunits (I, II, III, IV), with only subunit II being encoded in the nucleus.

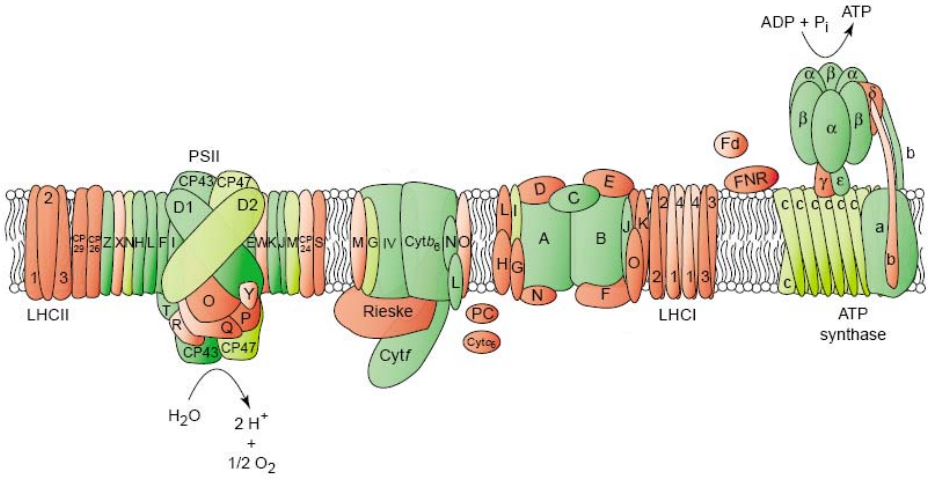

Figure 1. Molecular organization of the thylakoid membrane. Chloroplast-encoded subunits are depicted in green colors and nuclear-encoded subunits in red colors. *PSII*, photosystem II; *Cytb6f*; cytochrom b_6f*; PSI,* photosytem I*; LHCI/LHCII;* light-harvesting complex I/II; *PC*, plastocyanin; *Fd*, Ferredoxin; *FNR*, Ferredoxin NADP Reductase. ATP synthase subunits a, b and c correspond to CF_OI, II and III, respectively.
The picture is modified from Leister and Schneider, 2003.

3.3 Protein translocation into and across the thylakoid membrane

The biogenesis of the thylakoid complexes is an intricate process that requires coordinated targeting and transport to bring the single subunits from their site of synthesis to their final location in the organelle, where they have to be correctly assembled into functional complexes. Nuclear-encoded proteins therefore first have to be transported across the chloroplast envelope by the Toc and Tic complexes (translocon at the outer/ inner envelope membrane of chloroplasts; for review see Stengel et al., 2008; Jarvis and Robinson, 2004). Once in the stroma, protein transport into or across the thylakoid membrane is achieved by one of four different transport pathways that all seem to be of prokaryotic origin. These are designated as (I) the Oxa/Alb and (II) the secretory (Sec) - both working in concert with the signal recognition particle (SRP) pathway – as well as (III) the twin-arginine (Tat) and (IV) the spontaneous integration pathway (Figure 2) (for review see Schünemann, 2007; Aldridge et al., 2009), and each appears to be specific for a subset of thylakoid proteins and operates with a unique mechanism and energy requirement.

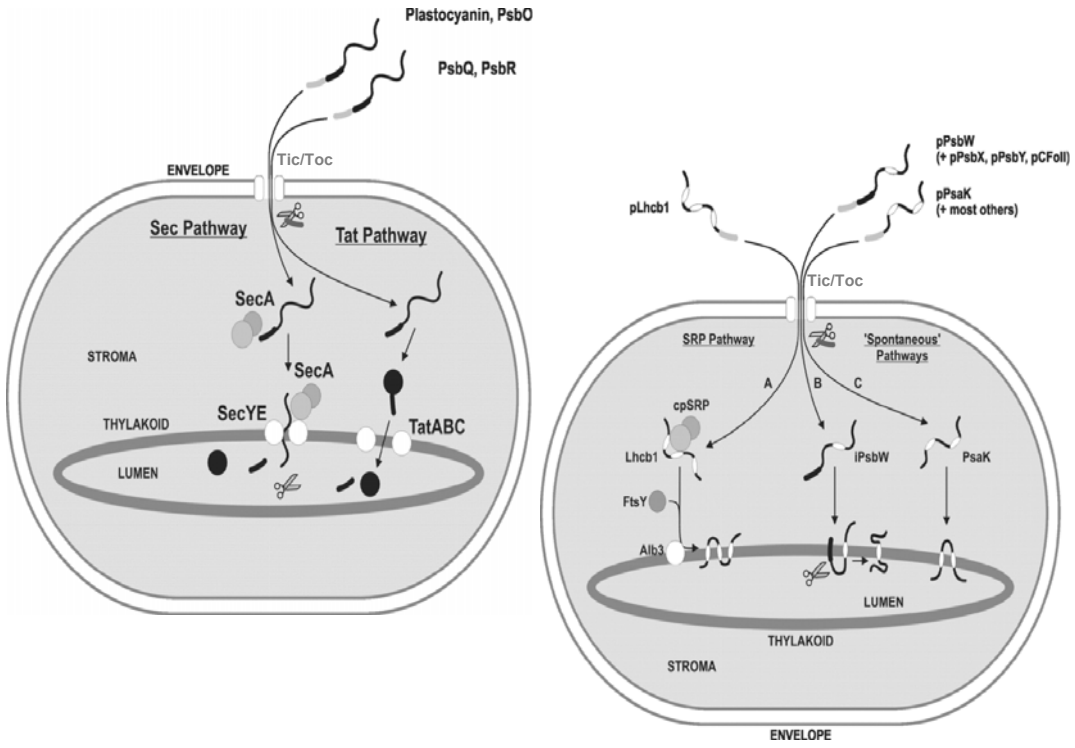

Figure 2. Schematic representation of the intra-organellar sorting of thylakoid proteins. For each of the four protein transport pathways operating at the thylakoid membrane, the stromal and thylakoidal factors involved are shown. Stroma targeting signals are depicted as gray ellipse, thylakoid targeting signals as black ellipse. Likewise the stromal and thylakoidal processing peptidases are shown as scissors. For each pathway, representative substrates are given. The pictures are taken from DiCola et al., 2005.

The transport of hydrophilic proteins destined for the thylakoid lumen is mediated by two of them: the Tat- and Sec-dependent pathways (Figure 2, left side). The Tat pathway is characterized by a number of unique features. First, the translocation process was described to be exclusively driven by the transmembrane proton gradient without the requirement of any soluble factors or nucleoside triphosphates (Mould et al., 1991; Cline et al., 1992), which is why it is also known as the ΔpH-dependent pathway. The second and probably most prominent feature of the Tat pathway is its ability to transport proteins in their folded state across the thylakoid membrane (Clark and Theg, 1997, Marques et al., 2003; Marques et al., 2004).

In contrast to the Tat-system, the chloroplastic Sec-dependent pathway (cpSec) transports unfolded proteins and is energized by the hydrolysis of ATP instead of the ΔpH (Hynds et al., 1998; Hulford et al., 1994; Yuan et al., 1994). The cpSec system is composed of three components, the integral membrane proteins cpSecY and cpSecE and the peripheral cpSecA protein, similarly to the prokaryotic Sec complex (Nakai et al., 1994; Laidler et al., 1995; Schünemann et al., 1999).

Nuclear-encoded thylakoid membrane proteins are transported by either an assisted, SRP-dependent transport pathway (cpSRP) or by an unassisted, possibly spontaneous way (Figure 2, right side). In the cytoplasm of prokaryotes and eukaryotes the co-translational protein transport and membrane insertion is mediated by a SRP pathway related to the chloroplast system, which relies on the presence of ribosomes and a highly conserved RNA component (for review see Luirink and Sinning, 2004). In plants, a unique post-translational SRP pathway exists that does not require any RNA components (Li et al., 1995). The post-translational targeting and integration of members of the nuclear-encoded LHCP (light-harvesting chlorophyll binding proteins) family is characterized best for this process (Schünemann, 2004; Luirink et al., 2005). Whereas in bacteria most inner membrane proteins use the co-translational SRP-dependent way, the post-translational cpSRP way seems to be restricted to LHC proteins in chloroplasts. Targeting of LHCP to the thylakoid membrane requires the association with the cpSRP components cpSRP54 and cpSRP43 to form a soluble transit complex, as well as the membrane bound protein cpFtsY and the integral membrane protein Alb3 (Figure 4C) (Li et al., 1995; Schünemann et al., 1998; Kogata et al., 1999; Moore et al., 2000; Woolhead et al., 2001). Furthermore, protein transport by the SRP pathway requires energy in form of GTP and possibly also the trans-thylakoidal ΔpH.

In addition to the post-translational targeting of LHCPs, the chloroplast SRP pathway is involved in the co-translational insertion of proteins into the membrane (Figure 4C). For this,

one pool of cpSRP54 associates with ribosomes and interacts directly with nascent chains of newly synthesized proteins (Franklin and Hoffman, 1993; Schünemann et al., 1998). A possible substrate for this co-translational protein transport is the chloroplast-encoded D1 protein (Nilsson et al., 1999; Nilsson and van Wijk, 2002). Reminiscent of the SRP-dependent targeting of bacterial membrane proteins, the insertion of D1 into the thylakoid membrane requires the cpSec translocase and maybe also the Alb3 protein (Schünemann, 2004; Zhang et al., 2001).

In contrast to the so far presented pathways, the so-called ´spontaneous` pathway seems to be unique to chloroplasts. Proteins using this route are integral membrane proteins that integrate into the membrane in the absence of any known proteinaceous machinery and without energy requirement (for review see Jarvis and Robinson, 2004; Di Cola et al., 2005). This unassisted pathway was first suggested to be characteristic for single membrane spanning proteins (*e.g.* CF_OII or the PsbW, PsbX subunits of PSII) (Michl et al., 1994, Mant et al., 2001), but some multi-spanning proteins have also been described to insert spontaneously (*e.g.* PSI components PsaK and PsaG or SecE) (Zygadlo et al., 2006; Mant et al., 2001).

3.4 The Alb3/Oxa1/YidC protein family

To be functional in the cell, membrane proteins not only have to be accurately targeted, but also have to obtain their proper topology which in many cases involves the assembly into three-dimensional structures and complexes. As described above, the insertion of most proteins into the membrane is initiated by proteinaceous machineries that support the translocation of hydrophilic domains across the membrane. Furthermore, the folding and arrangement of hydrophobic transmembrane segments often requires membrane chaperones. Since mitochondria and chloroplasts are believed to have prokaryotic ancestors, it is not surprising that there are similarities in their basic mechanisms of protein insertion.

In this context, the biogenesis of membrane proteins in diverse biological membranes has been shown to be mediated by an evolutionary conserved family of integral membrane proteins, the Alb3/Oxa1/YidC family. Members of this family play key roles in the insertion and translocation of membrane proteins, and also in their folding and assembly into multi-subunit protein complexes (for reviews see Kuhn et al., 2003; Dalbey and Kuhn, 2000; Yi and Dalbey, 2005). Representatives have been found in the inner membrane of bacteria and mitochondria, as well as in the thylakoid membrane of chloroplasts, but none has been discovered in the plasma membrane, the endoplasmic reticulum or the Golgi apparatus so far. Alb3/Oxa1/YidC proteins are not very similar in their primary sequences, but they share a conserved core region of five transmembrane domains in the middle of the protein. This

region most likely represents the catalytic active domain needed for the function as an integrase and/or chaperone. In contrast to this conserved structure, the N- and C-terminal regions vary in length depending on the organism (Figure 3) (for review see Kuhn et al., 2003). Over the last years, several members have been studied in some detail, but how exactly the integration of substrates into the membrane occurs as well as the evolutionary origin and organellar distribution of the Alb3/Oxa1/YidC family remains elusive.

Nevertheless, analysis of all sequenced organisms demonstrated that this protein family is ubiquitously distributed throughout all kingdoms (Luirink et al., 2001; Yen et al., 2001; Funes et al., 2009). Prokaryotes in most cases contain just one homologue, but some gram positive bacteria were described to possess two. Even in archea, proteins were found that exhibit homology to the eubacterial Oxa proteins (Luirink et al., 2001). Eukaryotes on the other hand show big variations in the number of homologues, ranging from one to more than six.

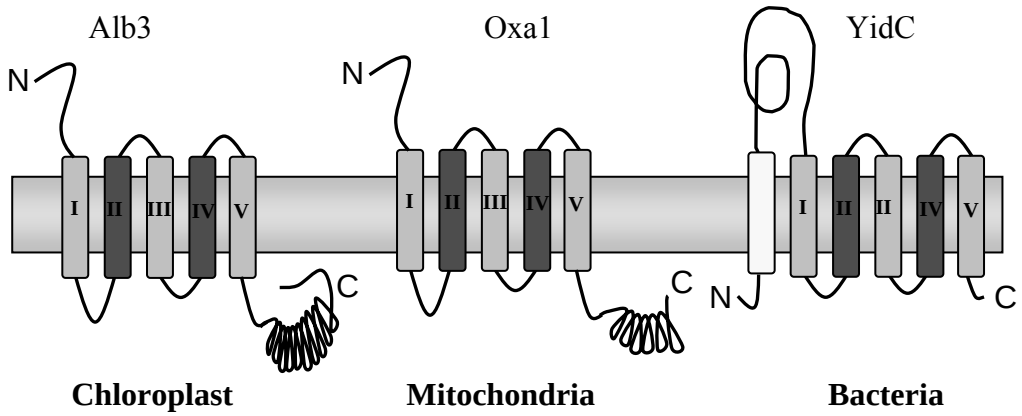

Figure 3. The evolutionary and structurally conserved Alb3/Oxa1/YidC protein family in chloroplasts, mitochondria and bacteria. Shown is the predicted topology of the three best characterized family members: *Arabidopsis* Alb3, yeast Oxa1 and *E. coli* YidC. Transmembrane domains are depicted as rectangles. Dark color represents conserved regions (TMs II, IV), light grey represents non-conserved regions (TMs I, III, V), and white color indicates the unique TM in the YidC protein. *N, C*: N- and C-terminus, respectively.

3.4.1 Oxa1, the mitochondrial homologue

A protein from yeast was the first characterized member of this family. Initially, this protein was discovered in a genetic screen designed to find respiration-deficient yeast mutants (Bauer et al., 1994; Bonnefoy et al., 1994). Since this inner membrane protein was demonstrated to be essential for the assembly of the cytochrome c oxidase (Cox), it was named Oxa1 (oxidase assembly 1). Subsequently, *oxa1* mutants were found to be additionally impaired in the assembly of other respiratory complexes such as the mitochondrial F_1F_O-ATP synthase and

the cytochrome bc_1 complex (Altamura et al., 1996; Kermorgant et al., 1997), indicating that Oxa1 performs essential functions during the biogenesis of inner membrane proteins. Analysis of the Oxa1 protein sequence revealed a characteristic core region of five transmembrane domains next to a long C-terminal tail protruding into the matrix (Figure 3, middle). Oxa1 was first suggested to be specifically involved in the biogenesis of proteins with long hydrophilic N-terminal domains, that need to be translocated across the inner membrane, as *e.g.* the mitochondrial-encoded subunit two of the cytochrome c oxidase complex (Cox2), a subunit of the ATP synthase (Su9) and Oxa1 itself. Surprisingly, although this transport was reminiscent to prokaryotic export systems, it had to occur in a Sec-independent manner since mitochondria lack a Sec complex (He and Fox, 1997; Hell et al., 1997; Hell et al., 1998). Later on, Oxa1 was found not only to catalyze the insertion of inner membrane proteins that are encoded in the mitochondrial genome, but also of nuclear-encoded subunits (Figure 4A) (Hell et al., 2001). Mitochondrial-encoded proteins were demonstrated to be inserted on a co-translational way, in which Oxa1 binds to the large subunit of mitochondrial ribosomes via its C-terminal tail (Jia et al., 2003; Szyrach et al., 2003). In contrast to this, nuclear-encoded proteins are first synthesized in the cytoplasm, post-translationally imported into the matrix and then redirected to the inner membrane to get integrated by Oxa1. However, although Oxa1 seems to be essential for the cell, the Oxa1 pathway is only required for a subset of nuclear-encoded inner membrane proteins, and also mitochondrial-encoded proteins show variations in their dependency on the Oxa translocase (Stuart, 2002).

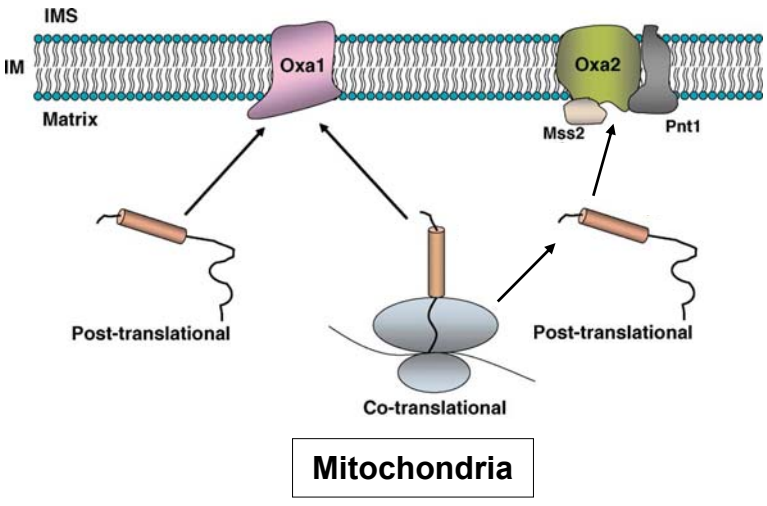

Figure 4A. The Oxa pathway for the insertion into the inner membrane of mitochondria. Mitochondrial-encoded membrane proteins are co-translationally inserted by the Oxa1 translocase (middle). Nuclear- encoded substrates take the post-translational way (left). Oxa2, the peripheral protein Mss2 and the integral membrane protein Pnt1 are involved in the post-translational insertion of Cox2 (right). *IMS*, intermembrane space; *IM*, inner membrane.

Oxa2, the second mitochondrial homologue

A second member of the Oxa1/Alb3/YidC family that was identified in the inner membrane of mitochondria from yeast is Oxa2/Cox18 (Figure 4A) (Souza et al., 2000; Saracco and Fox, 2002; Funes et al., 2004b). Oxa2 likewise functions in the assembly of the cytochrome oxidase complex but seems to be specifically involved in the translocation of the C-terminus of Cox2. Like Oxa1, the Oxa2 protein interacts with nascent mitochondrial-encoded proteins, but since it contains a relatively short C-terminus without a ribosome binding site, its function is restricted to the insertion of proteins in a post-translational manner.

3.4.2 YidC, the bacterial homologue

As already mentioned above, the majority of bacterial inner membrane proteins are targeted to the membrane by the SRP pathway and its receptor FtsY. The integration into the membrane is then mediated by the Sec translocase (Figure 4B) (for review see Herskovits et al., 2000). Moreover, the biogenesis of inner membrane proteins was shown to be dependent on another member of the Alb3/Oxa1/YidC family. Like the Oxa1 protein, the bacterial YidC functions in two different ways. In the co-translational insertion of inner membrane proteins, YidC works in concert with the Sec translocase (Scotti et al., 2000) but it also facilitates the post-translational insertion as a "stand alone" translocase. The best-studied bacterial orthologue is the YidC protein from *E. coli*, which is essential for cell viability (Samuelson et al., 2000). Interestingly, YidC differs in its topology from the organellar proteins. Like all other homologues, it contains the conserved region of five transmembrane helices, but it possesses an additional N-terminal transmembrane span and a large periplasmic domain between the first two transmembrane regions (Figure 3, right side) (Yen et al., 2001). The C-terminus of YidC is not able to bind to ribosomes.

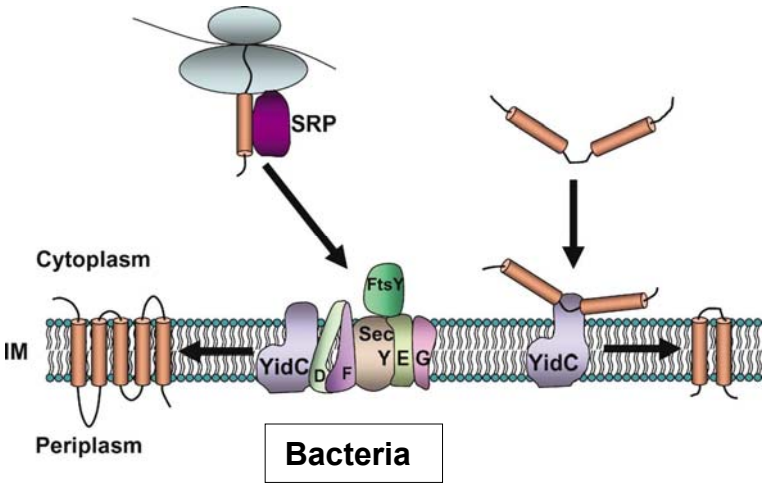

Figure 4B. The Sec/YidC and YidC-only pathways for insertion of bacterial proteins into the inner membrane. The YidC protein is involved in the insertion of Sec-dependent (left) and Sec-independent membrane proteins (right). *IM*, inner membrane.

Initially, YidC was discovered to be responsible for the integration of small phage coat proteins (namely M13 procoat and Pf3 coat protein) that up to then were believed to insert spontaneously into the bacterial membrane (Geller and Wickner, 1985; Ridder et al., 2000; Samuelson et al., 2000). Further analysis revealed that subunits of the cytochrome c oxidase and the F_1F_O-ATP synthase (CyoA and F_Oc, respectively) were endogenous substrates of YidC. The exact function of YidC in the translocation process, however, is still unclear. For some Sec-dependent proteins, YidC seems to interact with hydrophobic regions (Scotti et al., 2000; Chen et al., 2002), whereas it mediates the translocation of hydrophilic parts in other substrates (as *e.g.* for the F_Oc subunit of the ATP synthase) (Samuelson et al., 2000). YidC additionally plays a role in the folding of polytopic membrane proteins (Beck et al., 2001, Nagamori et al., 2004), suggesting that its function varies depending on the particular substrate.

3.4.3 Slr1471 in *Synechocystis*

The cyanobacterium *Synechocystis* possesses a single Alb3/Oxa1/YidC family member, Slr1471 (SynOxa), which was found to be essential for cell viability (Spence et al., 2004; Ossenbühl et al., 2006). Already a reduced level of this protein results in disorganized thylakoid membranes, a strong reduction of photosynthetic pigments (chlorophyll and phycocyanins) and the photosynthetic electron transport process in general. Slr1471 seems to be involved in the integration of the D1 precursor and its subsequent assembly into functional PSII complexes (Ossenbühl et al., 2006). Interestingly, the integral membrane protein Slr1471 was shown to predominantly localize to the plasma membrane and, if at all, only to a minor part to the thylakoid membrane (Gathmann et al., 2008). However, the model that Slr1471 acts as a chaperone in PSII assembly is supported by finding that the initial steps of PSII complex formation in cyanobacteria take place in the plasma membrane. Nevertheless, since there is only one Oxa homologue in *Synechocystis*, it might function in both compartments, the plasma membrane and the thylakoids (Spence et al., 2004).

3.4.4 Alb3, the homologue in chloroplasts

The first hint that an insertion pathway similar to that identified in yeast mitochondria and *E. coli* also exists in the chloroplasts of higher plants came from the identification of the Alb3/Oxa1/YidC homologue Alb3 (Albino3). Alb3 deficient *Arabidopsis* plants show white to yellow cotyledons and leaves with low levels of chlorophyll. Seedlings are not able to survive on soil and only occasionally flower on sugar-containing medium, but are infertile (Sundberg et al., 1997). Analysis of the chloroplast ultrastructure revealed an abnormal morphology with only few thylakoid membranes and hardly any grana stacks, indicating that

thylakoid biogenesis is severely affected in these plants. Alb3 is an integral membrane protein localized in the thylakoids and has a topology similar to the mitochondrial Oxa1 protein, with five central transmembrane regions and a long hydrophilic C-terminus in the chloroplast stroma (Figure 3, left side). Further analysis established that the integration of LHCPs into the thylakoid membrane strictly depends on Alb3, which is consistent with its predicted role in thylakoid biogenesis. As mentioned above, nuclear-encoded LHCPs are targeted post-translationally to the thylakoid membrane by the cpSRP pathway, including cpSRP43 and cpSRP54, as well as the SRP receptor cpFtsY. Integration into the membrane is then mediated by the Alb3 protein (Figure 4 C) (Yuan et al., 2002). Antibody inhibition experiments revealed that the major LHCII protein Lhcb1 and two additional members of the LHCP family, Lhcb4.1 (CP29) and Lhcb5 (CP26) are substrates of the Oxa homologue (Moore et al., 2000; Woolhead et al., 2001). In contrast to this, the transport of luminal proteins by the thylakoid Sec or ΔpH pathway remained unaffected, and *vice versa* the blocking of the Sec component cpSecY had no effect on LHCPs. It was therefore concluded that LCHP integration occurs in an Alb3-dependent way, but independently of the Sec-machinery (Moore et al., 2000; Moore et al., 2003). Nevertheless, the severe phenotype of Alb3 mutants implies that Alb3 has broader functions in thylakoid formation and therefore might participate in the insertion of additional classes of membrane proteins. The observation that Alb3 can functionally complement YidC in *E. coli*, suggested that both homologues may have common functions (Jiang et al., 2002). Moreover, Alb3 was demonstrated to be at least partially associated with cpSecY, indicating that both pathways might work together also in chloroplasts (Figure 4C) (Klostermann et al., 2002; Pasch et al., 2005). Indeed, interactions between Alb3 and several chloroplast-encoded proteins of PSI (PsaA) and PSII (D1, D2 and CP43), as well as with the CF_OIII subunit of the CF_1F_O-ATP synthase, some of which being Sec-dependent substrates, were detected in a yeast split-ubiquitin system, suggesting a role of Alb3 also in the assembly of photosynthetic complexes (Pasch et al., 2005). However, a direct involvement of Alb3 during the co-translational insertion of D1 or other proteins *in planta* has not been demonstrated so far.

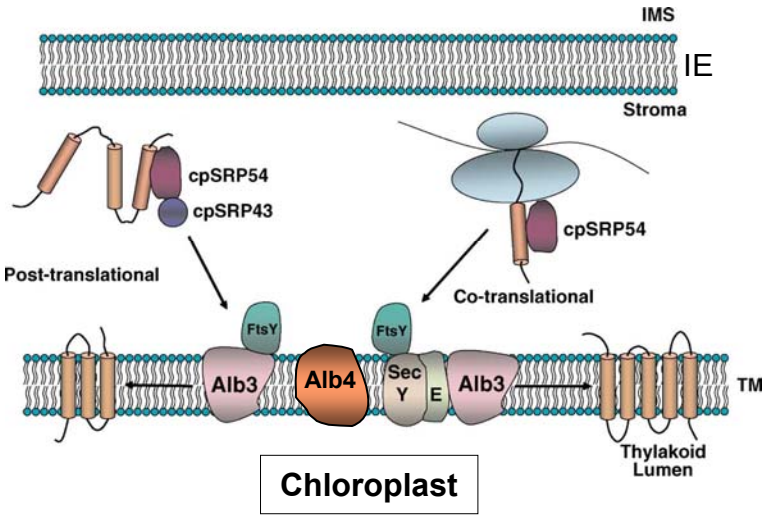

Figure 4C. The Alb3 pathway for the insertion of chloroplast proteins into thylakoid membranes. Plastid-encoded membrane proteins integrate into thylakoids in a co-translational manner (right), involving the Sec machinery and possibly the Alb3 translocase in this process. Nuclear-encoded thylakoid proteins take the post-translational way (left). The function of Alb4 is in thylakoid biogenesis is largely unknown. *IMS*, intermembrane space; *IE*, inner envelope; *TM*, thylakoid membrane. The pictures 4A, B and C are modified from Yi and Dalbey; 2005.

3.4.5 Alb3.1 and Alb3.2 in *Chlamydomonas*

In the green alga *Chlamydomonas reinhardtii*, two Oxa proteins have been identified, which show sequence similarity to the *Arabidopsis* Alb3 protein and were therefore designated Alb3.1 and Alb3.2 (Bellafiore et al., 2002; Ossenbühl et al., 2004, Göhre et al., 2006). Both proteins very likely have non-redundant functions. Mutants deficient for Alb3.1 are able to grow photoautotrophically, but the amounts of PSII and of the light-harvesting complexes from both photosystems (LHCI and LHCII) are drastically reduced. All other photosynthetic complexes (PSI, ATP synthase and $Cytb_6f$), on the other hand, are not affected (Bellafiore et al., 2002). It was therefore suggested that Alb3.1 might assist in the assembly of functional PSII reaction centers, in addition to its specific function in LHCP insertion (Ossenbühl et al., 2004). Alb3.2, in contrast, is essential for cell survival (Göhre et al., 2006). Even a modest decrease of this protein causes a strong reduction of PSI and PSII levels, whereas the LCHPs are almost unaffected. Furthermore, Alb3.2 directly interacts with its homologue Alb3.1 and with the PSII reaction center proteins D1 and D2. The strong phenotype indicates that Alb3.2 has multiple functions during thylakoid biogenesis, but is particularly involved in the assembly of PSI and II (Göhre et al., 2006).

3.4.6 Further homologues in *Arabidopsis thaliana*

In mitochondria and bacteria, Oxa1/YidC proteins play crucial roles in the integration and assembly of a wide range of membrane proteins. In contrast to this, the known functions of Alb3 seem to be more specialized, which might necessitate the presence of additional homologues in the *Arabidopsis* chloroplast. Since Alb4 was identified as a second member of

the Alb3/Oxa1/YidC family that localizes exclusively to thylakoids, it might represent a possible candidate (Fulgosi et al., 2002, Gerdes et al., 2006). Although Alb4 shows high similarity to Alb3, knock-down mutants of Alb4 do not exhibit an obvious phenotype (Gerdes et al., 2006). Nevertheless, an effect on the morphology of chloroplasts was observed in young plants and in particular the thylakoids appear disorganized and less appressed. However, it cannot be ruled out that residual Alb4 protein might have been sufficient for chloroplast function and that much stronger effects might occur at complete loss of the protein. Since Alb4 was found to at least partially complement the mitochondrial Oxa1 in yeast, it probably represents a functional member of the family (Funes et al., 2004a). However, almost nothing is known about its substrates and function *in planta*. Therefore, the primary aim of this work was to define the role of Alb4 in thylakoid protein biogenesis, making use of *Arabidopsis* lines being completely devoid of Alb4 protein.

BLAST searches in the genome of *Arabidopsis* revealed the presence of at least four additional genes coding for proteins with significant homology to the Alb3/Oxa1/YidC family (Funes et al., 2004a). Based on phylogenetic analyses, these proteins were classified into two groups: an Oxa1-like group including proteins with a long C-terminal domain similar to the yeast Oxa1 protein, and an Oxa2-like group that does not contain this domain (Funes et al., 2004a; Yen et al., 2001). Accordingly, these *Arabidopsis* proteins were named AtOxa1a (originally AtOxa1) and AtOxa1b as well as AtOxa2a and AtOxa2b.

However, these annotations have not yet been verified by experimental data, and since many annotations of the *Arabidopsis* genome have been revised over the last years, a number of new gene models and corresponding protein sequences became available. Thus, a second part of the present work was the re-investigation of the *Arabidopsis* genome for the presence of Alb3/Oxa1/YidC-like proteins.

Furthermore, the presence of at least six Oxa- or Oxa-like proteins in the *Arabidopsis* genome provoked the question whether these act independently in separate locations or are present side-by-side in only a limited number of compartments. To answer this, a detailed localization study was performed.

4 Materials

4.1 Chemicals

All used chemicals were purchased in high purity from Sigma-Aldrich (Steinheim, Germany), Fluka (Buchs, CH), Roth (Karlsruhe, Germany), Roche (Penzberg, Germany), Merck (Darmstadt, Germany), AppliChem (Darmstadt, Germany), or Serva (Heidelberg, Germany). Radiolabeled amino acids ([^{35}S]Met) were obtained from DuPont-NEN (Dreieich, Germany). MitoTracker (Orange CMTMRos) was from Invitrogen (Karlsruhe, Germany).

4.2 Detergents

Detergents used in this work were from the following suppliers: *n*-dodecyl-*β*-D-maltoside (DoMa), sodium dodecyl sulphate (SDS), and Triton X-100 (TX-100) were obtained from Roth and digitonin from Calbiochem/Merck.

4.3 Enzymes

Restriction enzymes for cloning, RNA- and DNA-polymerases, and T4-DNA ligases were obtained from Roche (Penzberg, Germany), MBI Fermentas (St. Leon-Rot, Germany), New England Biolabs (Frankfurt a. M., Germany), Qiagen (Hilden, Germany), Eppendorf (Hamburg, Germany), Diagonal (Münster, Germany), GeneCraft (Köln, Germany) and Finnzymes (Espoo, Finnland). Reverse Transkriptase was from Promega (Madison, USA), RNase-free DNase I from Roche and RNase from Amersham Biosciences (Uppsala, Sweden). Cellulase R10 and Macerozyme R10 for digestion of the plant cell wall were from Yakult (Tokyo, Japan) and Serva (Heidelberg, Germany).

4.4 Kits

RNA from plants was isolated using the "Plant RNAeasy Kit" from Qiagen (Hilden, Germany). For high yield DNA purification, the "Plasmid Midi Kit" and for purification of DNA fragments from agarose gels the "Nucleospin Extract II Kit" from Macherey and Nagel (Düren, Germany) was used. *In vitro* translation was performed with the "Flexi Rabbit Reticulocyte Lysate System" from Promega (Madison, USA).

4.5 Molecular weight markers and DNA standards

*Eco*RI and *Hind*III digested λ– Phage DNA (MBI Fermentas) was used as a molecular size marker for agarose-gel electrophoresis.

For SDS-PAGE the "MW-SDS-70L" and "MW-SDS-200" markers from Sigma-Aldrich (Steinheim, Germany) were used and for BN-PAGE the "HMW Native Marker Kit" from GE Healthcare (München, Germany)

4.6 Antibodies

The following antibodies were used in this work:

The α-Alb4 antibody was raised in rabbit against the over-expressed C-terminus of Alb4 (residues 369-499) (Pineda, Berlin, Germany) and was described previously (Gerdes et al., 2006).

The α-Alb3 antibody is raised against the C-terminus and is a kind gift of Prof. Dr. Danja Schünemann (Dept. Plant Physiology, Ruhr-Universität Bochum)

Antisera recognizing Cytf (PetA), and all used antisera against subunits of the CF_1CF_O-ATP synthase ($CF_1\alpha/\beta$; $CF_1\gamma$; $CF_1\delta$; $CF_1\varepsilon$; CF_OI; CF_OII; CF_OIII) were kind gifts of PD Dr. J.Meurer (Dept. Biologie I, Botany, LMU München) and that detecting PsaF was a kind gift of Prof. Dr. D.Leister (Dept. Biologie I, Botany, LMU München).

4.7 Strains, vectors, clones and oligonucleotides

Cloning in *E. coli* was performed in the following strains: DH5α (Invitrogen, Karlsruhe, Germany) and TOP10 (Invitrogen).

For cloning the following vectors were used: pCR2.1 or pCRII (Invitrogen). The vector pOL-GFP for transient transformation of *Arabidopsis* protoplasts was a kind gift of Prof. Dr. U.C.Vothknecht (Dept. Biologie I, Botany, LMU München) and is derived from Mollier et al., 2002). For GFP constructs in the gateway system the vectors pDONR-201 and p2GWF7 (Invitrogen, Karlsruhe, Germany) were used.

Oligonucleotide primers used in this work were ordered in standard desalted quality from either Invitrogen or Operon (Köln, Germany).

Constructs for *in vitro* transcription and translation were inserted into the pSP65 vector from Promega (Madison, USA).

4.8 Plant material

Experiments were performed on *Arabidopsis thaliana* plants, ecotype Col-0 (Lehle Seeds; Round Rock, USA) and ecotype Col-*er*.

The Alb4 TILLING mutant lines CS92437 (#437) and CS95771 (#771) were ordered at the Seattle TILLING Service (http://tilling.fhcrc.org; Till et al., 2003) and purchased from NASC (Scholl et al., 2000). Peas (*Pisum sativum*) var. "Arvica" were ordered from Bayerische Futtersaatbau (Ismaning, Germany).

4.9 Clones used in this work

Table 1. Plasmid DNA clones that were used in this work with additional information on the insert, vector, intended use and source (in case they were not generated by the author)

construct	AGI code	vector	construct info	reference/comments	purpose
pAlb4-GFP	At1g24500	pOL-GFP	full-length	Gerdes et al., 2006	localization
pAlb3-GFP	At2g28800	pOL-GFP	full-length	Gerdes et al., 2006	localization
pAtOxa6-GFP	At1g44890	pOL-GFP	full-length	aggregation	localization
pAtOxa1a-GFP	At5g62050	pOL-GFP	full-length	aggregation	localization
pAtOxa1b-GFP	At2g46470	pOL-GFP	full-length	aggregation	localization
pAtOxa2a-GFP	At1g65080	pOL-GFP	full-length	aggregation	localization
pAtOxa2b-GFP	At3g44370	pOL-GFP	full-length	aggregation	localization
pAtOxa1a-120AS-GFP	At5g66190	p2GWF7	Met-1 to Val-120	this work	localization
pAtOxa1b-120AS-GFP	At2g46470	p2GWF7	Met-1 to Val-120	this work	localization
pAtOxa2a-TM1+5´UTR-GFP	At1g65080	p2GWF7	5`UTR+ Met-1 to Glu-129	this work	localization
pAtOxa2b-TM1 -GFP	At3g44370	p2GWF7	Met-1 to Lys-162	this work	localization
pAtOxa6-110AS-GFP	At1g44890	p2GWF7	Met-1 toVal-110	this work	localization
CFP-PTS1	-	pGEM Teasy	SKL-sequence	Prof. Andreas Weber, Heinrich-Heine-Universität, Düsseldorf	localization peroxisomes
ST-GFP	-	pVKH18En6	*Rattus*-Sialyl-Transferase TM	Dr. Chris Hawes Bookes University, Oxford, UK	localization Golgi
SP+ERret-GFP	-	pMG	SP of *Arabidopsis*-Chitinase +KDEL-retention signal	Dr. Barbara Pickard Washington University, St. Louis, USA	localization endoplasmic reticulum (ER)
dcp.r-GFP	-	pMG	Dr. Barbara Pickard		localization plastid
mito-d2r-GFP	-	pMG	Dr. Barbara Pickard		localization mitochondria
At4g31040-GFP	At4g31040	pOL-GFP	full-length	nuclear-encoded homologue of AtYcf10	localization IE plastid
Alb4	At1g24500	pSP65	full-length	Gerdes et al., 2006	import
Alb3	At2g28800	pSP65	full-length	Gerdes et al., 2006	import
AtOxa6	At1g44890	pSP65	full-length	this work	import
AtOxa1a	At5g62050	pSP65	full-length	this work	import
AtOxa1b	At2g46470	pSP65	full-length	this work	import
AtOxa2a	At1g65080	pSP65	full-length	this work	import
AtOxa2b	At3g44370	pSP65	full-length	this work	import
pSSU	-	were present in the lab			import
pAOX	-	were present in the lab			import
pOE33	-	were present in the lab			import

5 Methods

5.1 Growth conditions

5.1.1 Growth of *Arabidopsis thaliana*

To synchronize germination, seeds of were vernalized for 24h at 4°C in the dark. Seeds were either grown on soil or on MS-plates (Murashige and Skoog, 1962) supplemented with 1% (w/v) sucrose. Before sowing on sterile plates, seeds of *Arabidopsis thaliana* were surface-sterilised in 70% (v/v) ethanol, 0.05% (v/v) Triton X-100 for 10 min, followed by washing in 96% ethanol for 4 x 1 min, and allowed to air-dry in a laminar flow hood. Unless stated otherwise, plants thereafter were grown in a 16 h light (+21°C; 100 µmol photons m^{-2} s^{-1}) and 8 h dark (+16°C) cycle (long-day). Plant material was generally harvested after 2h of light.

5.1.2 Growth of *Escherichia coli*

E. coli was cultivated in LB medium (1% tryptone, 0.5% yeast extract, 1% NaCl and if necessary 1.5% agar) at 37°C in either liquid culture or on agar-plates supplemented with the appropriate antibiotics according to the resistance (Ampicillin 100µg/ml, Kanamycin 50µg/ml, Streptomycin 50µg/ml and Spectinomycin 100µg/ml). Blue-white screening of constructs in pCR2.1 or pCRII was done on LB-plates containing 60 µg/ml X-Gal (Sambrook and Russell, 2001).

5.2 Molecular biological methods

5.2.1 General molecular biological methods

General molecular biological methods like growing of bacteria, DNA precipitation, determination of DNA concentrations and transformation were performed as described (Sambrook et al., 1989). The preparation of chemical competent cells for transformation was done according to the protocol of Hanahan and co-worker (Hanahan, 1983). Preparation of plasmid, DNA restrictions, ligations and agarose gel electrophoresis were conducted as described (Sambrook et al., 1989). Thereby, the reaction conditions were adjusted to the manufacturer's recommendations.

5.2.2 Homologous recombination

Homologous recombination was used for cloning of DNA-fragments / constructs into vectors of the GATEWAY-system (Invitrogen, Karlsruhe, Germany) according to the manufacturer's recommendations. Thereby, *att*B-sequences were added by PCR primers.

5.2.3 Isolation of genomic DNA from *Arabidopsis thaliana*

A small *Arabidopsis* leaf (approx. 0.5-0.75 cm^2) was cut and transferred to a 1.5 ml microtube. 200 µl of extraction buffer (200 mM Tris-HCl (pH 7.5), 250 mM NaCl, 0.5% SDS) was added to the tube and the sample was homogenized using a polytron with a pestle. The homogenate was incubated at room temperature (RT) for 3-5 min and then centrifuged at 13.000 x g for 10 min. 150 µl of the supernatant were transferred to a new tube. To precipitate the genomic DNA, 150 µl of isopropanol (-20°C) was added to the tube, carefully mixed and centrifuged at 13.000 x g for 15 min at 4°C. The pellet was subsequently air-dried and finally resuspended in 50 µl of distilled water.

5.2.4 Characterization of *ALB4* TILLING lines

Genomic DNA of the TILLING lines was screened by PCR genotyping. To identify plants with the point mutation in both alleles (homozygous), gene-specific primers flanking the predicted mutation sites were used (see Table 2). The combination of the two gene-specific primers generates a PCR product of equal sizes in WT and mutant plants. The positions of the point mutations in the *Alb4* TILLING lines #437 and #771 are indicated in Figure 12A. For line #771 PCR products and point mutation sites were verified by sequencing of the amplified DNA fragment. In the mutant line #437 due to the point mutation the restriction site for Bsp143I is modified, resulting in an indigestible PCR fragment.

Table 2. List of used oligonucleotides for PCR genotyping of *Arabidopsis* TILLING lines.

line	primer	seq. (5`-3`)	ordered by No.
alb4-TILLING #437 , #771	ArtTMNotIfor forward	AATGCGGCCGCGGTACATGTTCCTTATTCCTATG	L.Gerdes #53
alb4-TILLING #437	Art-RACE-R1 reverse	GCCTGCAAGGGGATTTATTCCAGCA	L.Gerdes #97
alb4-TILLING #771	Ex12.rev reverse	CGGGGCCCAATGAAAGGGAACAGCCATG	L.Gerdes #4

5.2.5 Polymerase Chain Reaction (PCR)

DNA fragments for cloning into plasmid vectors were generated by polymerase chain reactions (PCR) (Saiki et al., 1988). PCR reactions were carried out as recommended by polymerase suppliers. Flanking restriction sites for cloning were added by the primers used for PCR.

5.2.6 RNA isolation, cDNA preparation and real-time PCR

Three-week-old plantlets were ground in liquid nitrogen (N_2), and total RNA was isolated as recommended in the manual supplied with the RNA Easy Isolation kit (Qiagen, Hilden, Germany). cDNA was prepared from 1 µg samples of DNase-treated RNA using the iScript kit (Bio-Rad, München, Germany). cDNA was diluted 10-fold and a 2 µl aliquot of the dilution was added to 20 µl of iQ SYBR Green Supermix (Bio-Rad). All reactions were performed in quadruplicates with the primers listed below.

The Bio-Rad iQ5 system was used for quantitative three-step real-time PCR. Cycling conditions consisted of an initial step at 95°C for 3 min, followed by 40 cycles of 10 s at 95°C, 30 s at 55°C and 10 s at 72°C. After that a melting curve was performed. RT-PCR was monitored using the iQ^{TM}5 Single Colour Real-Time PCR detection system (Bio-Rad). Adjustment of baseline and threshold was carried out according to the manufacturer's recommendations. The relative abundance of all transcripts amplified was normalized to the expression level of 18S rRNA. Data were analyzed using LinRegPCR (Pfaffl, 2001).

Table 3. List of primers used for real-time PCR.

PCR for	primer	seq. (5`-3`)
*atp*A ($CF_1\alpha$)	forward	ATGCTGGAATCAGACCTGC
	reverse	TCACGCAATCGTTGACCTC
*atp*B ($CF_1\beta$)	forward	AGGATTAGCTGCCAAAGG
	reverse	TGCTACGGTTAAGCGATG
*atp*C1 ($CF_1\gamma$-C1)	forward	AGTCGAGCTCTTGTACAC
	reverse	AATCAGCTGTTGGTGTCC
*atp*C2 ($CF_1\gamma$-C2)	forward	TCTGATCCTGTGATCCAC
	reverse	TGCATCAACGGTGAGATC
*atp*D ($CF_1\delta$)	forward	AACGTCAAGTCATCGAC
	reverse	TCTTTCGCAATCTGAGC
*atp*E ($CF_1\varepsilon$)	forward	AGCAGGATCCGAGGTAT
	reverse	AGTACGGTAGTCGCATC
*atp*F (CF_OI)	forward	TACTTGGGTCACTGGC
	reverse	TAGCTCCTTCACGCAG
*atp*G (CF_OII)	forward	AAGAGAAGCTCGCGAGTG
	reverse	TCTGACTCTCCAAGCTCG
*atp*H (CF_OIII)	forward	ATCCACTGGTTTCTGCTG
	reverse	AGCGCTAATGCTACAACC
*atp*I (CF_OIV)	forward	TACTCACATCAGTAGCCT
	reverse	AGGAACCACTAAAGGTAC
18S rRNA	forward	AACTCGACGGATCGCATGG
	reverse	ACTACCTCCCCGTGTCAGG
*psb*A (D1)	forward	ATACAACGGCGGTCCTTATG
	reverse	AGCAATCCAAGGACGCATAC
*psa*A (PSI core subunit)	forward	TCTTGGGCAGGACATCAAG-
	reverse	AAGGGAGTTGCTCCTTCAG
*rbc*L (RuBisCo)	forward	ACCACCTCATGGTATCC-3'
	reverse	GAAACGGTCTCTCCAAC

5.3 Biochemical methods

5.3.1 General biochemical methods

Determination of chlorophyll concentration was carried out as described by Arnon, 1949.

Determination of protein concentration was performed as follows: For soluble proteins, the concentration was determined with the help of the Bio-Rad Protein Essay Kit (Bio-Rad, München, Germany). Protein concentrations in total membrane samples were determined according to Lowry et al., 1951.

5.3.2 SDS-polyacrylamide electrophoresis (SDS-PAGE)

The electrophoretical separation of proteins in denaturing polyacrylamide gels was carried out according to the method of Laemmli, 1970. Separating gels with polyacrylamide concentrations ranging from 10-15% were used. Before being applied to the gel, proteins were solubilized in sample buffer (Laemmli-buffer) and incubated for 20 min at RT. Gels were stained either by Coomassie Brilliant Blue-R250 (Sambrook et al., 1989) or silver-stained using a protocol according to Blum et al., 1987 with modifications.

5.3.3 Western blotting and immunodecoration with antibodies

For immunodetection, proteins were transferred onto either Nitrocellulose or PVDF membranes by semi-dry-blotting in a Trans Blot Cell (BioRad, München, Germany) in blotting buffer (25 mM Tris-HCl (pH 8.2-8.4), 192 mM glycine, 10-20% MeOH, 0.025% SDS) for 1h at 400 mA as described previously (Towbin et al., 1979). Proteins of the size markers were either stained with Ponceau S solution (nitrocellulose) or amido black solution (PVDF).

Membranes with bound proteins were first incubated for 30 min in blocking buffer containing Casein (0.3% Casein, 0,.03% BSA, 1x TBS (100 mM Tris-HCl (pH 7.4), 160 mM NaCl) or skimmed milk powder (2-5% milk powder, 1x TBS, 0.05% Tween 20). Incubation with the primary antibody (diluted in blocking buffer 1:250-1:4000, depending on the antibody) was done for 2-3h at RT or overnight at 4°C. Non-bound antibody was removed from the membrane by washing for 3x10 min in TBS-T (1x TBS with 0.1% Tween 20). The secondary antibody was selected according to the desired method of visualization (see below).

5.3.4 Two-dimensional blue native gel electrophoresis / SDS-PAGE and immunoblotting

Blue native gel electrophoresis was carried out as described in previously (Schägger and von Jagow, 1991 and Wittig et al., 2006) with the following modifications: Chloroplasts or thylakoid membranes (equivalent to 4-50 µg of chlorophyll (Chl)) were solubilized in 50 mM Bis-Tris/HCl, (pH 7.0), 750 mM 6-aminocaproic acid, 1% *n*-dodecyl β-D-maltoside (DoMa).

After incubation on ice for 15 min, samples were centrifuged at 80,000 rpm for 10 min at 4 °C. The supernatant was supplemented with 0.1 vol. of a Coomassie Blue solution (5% Coomassie Brillant Blue G-250, 750 mM 6-aminocaproic acid) and loaded on a 5-12% (w/v) polyacrylamide gradient gel. Electrophoresis was carried out at increasing voltage (stacking gel: 100 V maximum; separating gel: 15 mA/400 V maximum for a 12 x 14 cm gel, 8 mA maximum for a 6 x 8 cm gel) at 4°C. The cathode buffer contained 0.02% dye and was replaced by buffer lacking dye after approximately one-third of the electrophoresis run. For second dimensions (2D BN/SDS-PAGE) the lanes were cut out after the run and incubated in 1% SDS, 1 mM β-mercaptoethanol (β-ME) for 15 min, followed by 15 min in 1% SDS without β-ME and 15 min in SDS-PAGE electrophoresis buffer (25 mM Tris, 192 mM glycine, 0.1% SDS) at RT. Single lanes were then placed on top of SDS-PAGE (15% polyacrylamide, 4 M urea) and the individual complexes were separated into their constituent subunits by electrophoresis.

For antibody detection, proteins were electro-blotted onto PVDF (Immobilon-P; Zefa, Harthausen) or nitrocellulose membrane (Protran; Whatman, Dassel) using a semi-dry Western blotting system (Hoefer TE 77; Amersham Biosciences, Freiburg) and Towbin buffer (25 mM Tris/HCl (pH 8.2-8.4), 192 mM glycine, 0.1% SDS, 20% methanol). Labeling with protein-specific primary antibodies was carried out by standard techniques, and bound antibodies were visualized either with alkaline phosphatase (AP)-conjugated secondary antibodies (goat anti-rabbit IgG (whole molecule)-AP conjugated; Sigma-Aldrich Chemie GmbH, Taufkirchen, see below) or using a chemiluminescence detection system (see below) in combination with a horseradish peroxidase-conjugated secondary antibody (goat anti-rabbit (whole molecule)-peroxidase conjugated; Sigma).

5.3.5 Immunoblot development

For colorimetric reaction with the alkaline phosphatase (AP) system, the secondary antibody (goat anti-rabbit IgG (whole molecule)-AP conjugated; Sigma-Aldrich Chemie GmbH, Taufkirchen) was applied to the membrane for 1 h. After removal of unbound secondary antibody by washing (3x10 min in wash buffer) and a final wash in western developer (105.7 mM Tris-HCl (pH 9.5), 100 mM NaCl, 50 mM $MgCl_2$,) the immunoreaction was visualized by incubation with western developer containing 66 µl/10ml of NBT (4-Nitro blue tetrazolium chloride, 50 mg/ml in 100% dimethylformamid) and 66 µl/10ml of BCIP (5-Bromo-4-chloro-3-indolyl-phosphate in 100% dimethylformamid). The reaction was stopped by washing in ~5mM EDTA.

For the chemiluminescent method of protein detection (ECL), HRP-conjugated goat anti-rabbit antibody as used as the secondary antibody. Proteins were visualized either with the Pierce ECL Western Blotting Substrate (Thermo Fisher Scientific Inc., Rockford, USA) or according to the following protocol:

Solution 1 (100 mM Tis-HCl (pH 8.5), 1% (w/v) luminol, 0.44% (w/v) coomaric acid) and solution 2 (100 mM Tris-HCl (pH 8.5), 0.018% (v/v) H_2O_2) were mixed in a 1:1 ratio and added to the blot membrane (1-2 ml per small gel). After incubation for 1 min at RT (in the dark) the solution was removed and the luminescence detected with a film (Kodak Biomax MR; PerkinElmer, Rodgau, Germany).

5.3.6 Extraction of soluble and total membrane proteins from *Arabidopsis thaliana*

Arabidopsis rosette leaves of three to five-week-old plants were harvested and flash-frozen in liquid N_2. The frozen leaves were thoroughly ground in liquid nitrogen by using a pre-cooled mortar and pestle. To obtain soluble and membrane-attached proteins the powder was mixed with 400 µl of urea-buffer (50 M Tris (pH 8.0), 0.2 M EDTA, 6 M urea), incubated for 10 min at RT and centrifuged at maximum speed in a microfuge (10 min, 13,000 x g) and the supernatant was saved. To extract the membrane proteins the pellet was resuspended in 200 µl of SDS-buffer (50 mM Tris-HCl (pH 8.0), 0.2 mM EDTA, 1% SDS), incubated for 15 min at RT, centrifuged again at maximum speed and the supernatant containing total membrane proteins was also saved. For the extraction of soluble and membrane proteins in one step, ground samples are extracted by addition of 750 µl SDS buffer (50 mM Tris (pH 8,0), 0.2 mM EDTA, 1% SDS), followed by incubation at RT and centrifugation as described above.

The protein concentration of the supernatants was determined with the Bradford assay.

5.3.7 Protein identification by mass spectrometry (MS)

Coomassie- or silver-stained protein spots were cut from SDS-PAGE gels and send for identification to the "Zentrallabor für Proteinanalytik" (ZfP, Adolf-Butenandt-Institut, LMU München). There, tryptic peptides were detected either by Peptide Mass Fingerprint (MALDI, **M**atrix **A**ssisted **L**aser **D**esorption/**I**onisation) or LC-MS/MS (**L**iquid **C**hromatography with **MS**) runs. Protein identification was then accomplished with a Mascot software assisted database search. Only hits displaying a threshold score of >=60 were analyzed further.

5.4 Cell biological methods

5.4.1 Isolation of *Arabidopsis* chloroplasts

Chloroplasts were isolated according to Aronsson and Jarvis, 2002 with the following modifications: 21-day-old plants grown on soil were homogenized in 25 ml of isolation buffer (0.3 M sorbitol, 5 mM $MgCl_2$, 5 mM EGTA, 5 mM EDTA, 20 mM HEPES/KOH (pH 8.0), 10 mM $NaHCO_3$, 50 mM ascorbic acid). After three homogenisation and filtration steps, the combined homogenate was pelleted at 1000 x *g* for 5 min and resuspended in isolation buffer. Resuspended chloroplasts were separated on a two-step Percoll gradient (30/82% (w/v) Percoll) in a swing-out rotor at 1500 x *g* for 10 min. The lower band comprising intact chloroplasts was washed in 50 mM HEPES/KOH (pH 8.0), 0.3 M Sorbitol, 2 mM DTT. After a final wash, the chloroplasts were pelleted at 1000 x *g* for 5 min and resuspended in 1 ml of wash buffer.

5.4.2 Isolation of thylakoid and stroma fractions

Chloroplasts (equivalent to 150 µg of chlorophyll) were lysed in lysis buffer (10 mM HEPES-KOH (pH 7.8), 5 mM $MgCl_2$) for 20 min on ice. After centrifugation at 7500 rpm the thylakoids were resuspended in lysis buffer. The supernatant contained the stroma fraction. For SDS-PAGE and immunoblot analysis membrane samples corresponding to 2 µg of chlorophyll and 15 µl of supernatant were used (corresponding to 16.5 µg of total protein).

5.4.3 Separation of stroma thylakoids from grana thylakoids

Arabidopsis leaves were homogenized in 25 ml of isolation buffer (0.4 M sorbitol, 0.1 M Tricine/KOH (pH 7.8), 0.3 mM PMSF). After two rounds of filtration through a layer of gauze, the homogenate was pelleted at 1400 x *g* for 10 min at 4°C, resuspended and washed once in isolation buffer. Chloroplasts were resuspended in lysis buffer (25 mM HEPES/KOH (pH 7.8), 5 mM $MgCl_2$, 0.3 mM PMSF) and incubated for 15 min on ice in the dark. After centrifugation at 10,000 x *g* for 10 min at 4°C, thylakoids were resuspended in buffer B (15 mM Tricine/KOH (pH 7.9), 0.1 M sorbitol, 10 mM NaCl, 5 mM $MgCl_2$).

To separate stroma thylakoids from grana thylakoids, the protocol of Ossenbühl et al., 2002 was followed. Briefly, isolated thylakoid membranes (0.2 mg/ml of chlorophyll) were solubilized with 0.1% digitonin in buffer B for 5 min at RT. The incubation was stopped by adding 10 volume of buffer B. Fractionation was obtained by four rounds of centrifugation at 4°C, beginning with 1000 x *g* for 30 min (1K, unlysed chloroplasts), 10,000 x *g* for 30 min (K10, grana), 40,000 x *g* for 1 h (40K, margins) and at 140,000 x *g* for 1.5 h (140K, stroma). The final supernatant was precipitated with TCA. Sub-fractions were used for immunoblots.

5.4.4 *In vitro* translation in isolated *Arabidopsis* chloroplasts ("*in organello*" translation)

Isolated chloroplasts (see 5.4.1) were centrifuged at 2550 x g for 5 min and resuspended in cold medium C (330 mM sorbitol / 50 mM Hepes-KOH (pH 8.0)).

The chloroplasts (0.5 µg/µl chlorophyll) were incubated for 10 min at 23°C in the light in a translation mixture consisting of medium C (330 mM sorbitol, 50 mM Hepes/KOH (pH 8.0), 40 µM of each amino acid except methionine (Met), 2 mM dithiothreitol, 10 mM ATP, 0.2 mM GTP, 5 mM $MgCl_2$, final volume 50 µl). After this pre-incubation time, 2.5 µl of [^{35}S]Met was added.

Pulse-chase experiments

For pulse-chase studies, pulse-labeling was done for 10 min in the light. Following the pulse-labeling period, unlabeled Met (10 mM final concentration) was added to block further incorporation of [^{35}S]Met. Chase periods extended 20-60 min after addition of unlabeled Met. Translation was stopped by adding a 10-fold volume of ice-cold isolation medium. To separate the thylakoid-bound translation products from the stromal products, the chloroplasts were lysed for 45 min in lysis buffer (10 mM Hepes/KOH (pH 7.6), 1 mM PMSF). After centrifugation (7500 rpm for 5 min at 4°C), chloroplasts were washed once in isolation medium and the pellet was resuspended in either 50 µl SDS-PAGE loading buffer and analyzed by SDS-PAGE or used for Blue native (BN)-PAGE.

Although very short (2.5 min) pulses generally are enough for the labeling of proteins and their assembly into bigger-sized complexes the pulse time in these experiments was increased to 10 min followed by a 20-60 min chase to accumulate more radioactivity in the newly synthesized proteins.

5.4.5 Isolation of intact chloroplasts from *Pisum sativum* (pea)

Chloroplasts from pea were isolated from leaves of 9-11 days old pea seedlings (*Pisum sativum* var. Arvica) and purified through Percoll density gradients as previously described (Keegstra and Youssif, 1986 and Waegemann and Soll, 1995).

5.4.6 Isolation of mitochondria *Pisum sativum* (pea) leaves

Pea leaves were ground with 300 ml of grinding medium (0.3 M sucrose, 25 mM tetra-sodium pyrophosphate, 2 mM EDTA, 10 mM KH_2PO_4, 1% PVP-40, 1% BSA, 20 mM ascorbic acid (pH 7.5)) in a pre-chilled mortar. After three rounds of grinding and filtration through one layer of mirocloth, the homogenate was centrifuged for 5 min at 2450 x g at 4°C (all following steps were carried out in the cold or on ice). The supernatant was centrifuged again for 20 min at 17,400 x g. The pellets were resuspended in the residual supernatant and washed once with 1x wash buffer (2x: 0.6 M sucrose, 20 mM TES, 0.2 % (w/v) BSA (pH 7.5)). After

centrifugation for 5 min at 2540 x g the supernatant was centrifuged again for 20 min at 17,400 x g. The pellet was resuspended in 5-10 ml of 1x wash buffer and layered over a 0-4.4% PVP gradient prepared with a standard linear gradient former. The gradient was then centrifuged for 40 min at 35,000 rpm (fixed angle rotor, without brake). The mitochondrial fraction was mixed with 1x wash buffer. After two rounds of washing (centrifugation for 15 min at 27,200 x g) the pellet containing mitochondria was resuspended in wash buffer.

5.4.7 *In vitro* transcription and translation

Transcription of linearized plasmids was carried out as previously described (Firlej-Kwoka et al., 2008).

Translation was carried out using the Flexi Rabbit Reticulocyte Lysate System from Promega (Madison, USA) following the manufacturer`s protocol in presence of [^{35}S]Met for radioactive labeling.

5.4.8 *In vitro* import assay into isolated pea chloroplasts

The translation mixture was centrifuged for 10 min at 19,000 rpm at 4°C and the post-ribosomal supernatant was used for import. After chloroplast isolation the chlorophyll concentration was determined according to Arnon, 1949. A standard import assay into chloroplasts equivalent to 20 µg chlorophyll was performed in 100 µl import buffer (2 mM ATP, 10 mM Met, 10 mM cysteine, 20 mM potassium gluconate, 10 mM $NaHCO_3$, 3 mM $MgSO_4$, 330 mM sorbitol, 50 mM Hepes/KOH (pH 7.6), 0.2% BSA) containing 10% of *in vitro* translated radiolabeled protein. Import was initiated by addition of organelles to the import mixture and was incubated at 25°C in the dark. The reaction was stopped after 20 min in the dark. Intact chloroplasts were reisolated through a Percoll cushion (40% Percoll in 330 mM sorbitol, 50 mM Hepes/KOH (pH 7.6)) and washed once in wash buffer (330 mM sorbitol, 50 mM Hepes/KOH (pH 7.6), 3 mM $MgCl_2$) and used for further treatments.

For thermolysin treatment import reactions were doubled and after washing reactions were resuspended in 100 µl wash buffer II (330 mM sorbitol, 50 mM Hepes/KOH (pH 7.6), 0.5 mM $CaCl_2$) and divided into two equal portions. One portion was incubated with 2 µg thermolysin /10 µg of chlorophyll for 30 min on ice, followed by the addition of 10 mM EDTA to terminate the activity of the protease. After centrifugation (3200 rpm, 1 min) the pellet was resuspended in wash buffer III (330 mM sorbitol, 50 mM Hepes/KOH pH (7.6), 5 mM EDTA) and centrifuged again.

For sub-fractionation into stroma and membrane fractions the pellet was resuspended in 400 µl lysis buffer (10 mM Hepes/ KOH (pH 7.6), 2 mM EDTA, 1 mM PMSF), incubated for 45 min on ice and centrifuged for 10 min at 25,6000 rpm at 4°C. The pellet containing the

membrane fraction was resuspended 30 µl SDS-PAGE loading buffer. Stromal proteins of the supernatant were precipitated with TCA and also resuspended in loading buffer. Samples were analyzed by SDS-PAGE and autoradiography.

5.4.9 *In vitro* import assay into isolated pea mitochondria

In vitro import experiments were carried out with the post-ribosomal supernatant from the translation lysate. After isolation of mitochondria the protein concentration was determined with the Bradford assay.

Mitochondrial import reactions were done according to Whelan et al., 1990; Whelan et al., 1996b. Mitochondrial reactions were carried out in a 200 µl reaction. The incubation buffer contained 1 mM Met, 0.75 mM ATP, 2 mM ADP, 50 mM succinate, 50 mM DTT, 1 mM $MgCl_2$ in import buffer (0.3 M sucrose, 50 mM KCl, 10 mM MOPS (pH 7.4)). Freshly isolated mitochondria, equivalent to 100 µg of protein, were resuspended in import buffer, and then 10 µl translation products (5 µl for AOX) were added. The assay was allowed to proceed for 20 min at 25°C. At the end of incubation, the import mixture was divided into two equal portions. One portion was directly layered onto a 20% (w/v) sucrose cushion, and mitochondria were reisolated by centrifugation at top speed for 5 min in a microcentrifuge at 4°C. The other half was treated with 32 µg/ml proteinase K, incubated at 4°C for 30 min, followed by the addition of 1 mM PMSF to terminate the activity of the protease. The mitochondria were then reisolated as above. The mitochondria of both protease-treated and -untreated portions were washed once with 1 ml of wash buffer and dissolved in 30 µl SDS-PAGE loading buffer. Samples were analyzed by SDS-PAGE and autoradiography.

5.4.10 *In vitro* dual import assay into isolated pea mitochondria and chloroplasts

For imports into the dual import system, mitochondria and chloroplasts were isolated separately, mixed and incubated together with the precursor protein in an import buffer supporting import into both, mitochondria and chloroplasts in a final volume of 100 µl (0.3 mM sucrose, 15 mM HEPES-KOH (pH 7.4) 5 mM KH_2PO_4, 0.5% BSA, 4 mM $MgCl_2$, 4 mM Met, 4 mM ATP, 1 mM GTP, 0.2 mM ADP, 5 mM succinate, 4.5 mM DTT, 10 mM potassium acetate and 10 mM $NaHCO_3$) for 20 min at 25°C with gentle agitation. The samples were transferred to ice and separated into two equal aliquots, one containing 120 µg /ml thermolysin supplemented with 0.1 mM $CaCl_2$ and incubated for 30 min. The thermolysin activity was inhibited by the addition of 10 mM EDTA and each sample was carefully loaded onto a 300 µl 4% (v/v) Percoll gradient in a 400 µl elongated microfuge-tube and centrifuged for 30 sec in a fixed angle Microfuge rotor at 4500 x g. The organelle fractions were collected separately, chloroplasts at the bottom of the gradient as pellet and mitochondria at the top and

washed in 1 ml of wash buffer (0.3 m sucrose, 15 mM Hepes-KOH (pH 7.4), 5 mM KH_2PO_4, 0.5% BSA). The chloroplasts were recovered by centrifugation at 800 x g for 2 min at 4°C and mitochondria for 10 min at maximum speed in a microcentrifuge. Imported products were analyzed by SDS-PAGE and imaged by autoradiography.

Table 4. Sizes of precursor and mature forms of the proteins that were used for *in vitro* import experiments.

name	precursor protein size [kDa]	mature protein size [kDa]
Alb3	50.2	~ 45
Alb4	54.9	~ 50
AtOxa1a	47.9	~ 37
AtOxa1b	47.9	~ 39
AtOxa2a	58.3	~ 45
AtOxa2b	62.8	~ 50
AtOxa6	31	~ 31 (mitochondria) ~ 24 (chloroplasts)
AOX	34	~ 29
SSU	20	~ 14
OE33	36	~ 33

5.4.11 Preparation of *Arabidopsis* protoplast and transient transformation

Mesophyll protoplasts were isolated from leaves of three to four-week-old *Arabidopsis* plants grown on soil and transiently transformed according to the protocol of Jen Sheen (http://opus.mgh.harvard.edu/sheen_lab). GFP fluorescence was observed with a TCS-SP5 confocal laser scanning microscope (Leica, Wetzlar, Germany). Labeling with MitoTracker was done according to the manufacturer's recommendations (Invitrogen, Karlsruhe, Germany).

5.5 Microscopy methods

5.5.1 Transmission electron microscopy (TEM)

Arabidopsis plants (Col-*er*, *ALB4* TILLING #437, #771) were grown on soil and grown under standard long-day conditions (16h light, 100 µmol photons m^{-2} sec^{-1} at +21°C / 8h dark at +16°C) for three weeks. Specimens were taken from rosette leaves.

Distal pieces (approximately 1–2 mm^2) of primary leaves were prefixed in 2.5% (w/v) glutaraldehyde in 75 mM cacodylate buffer (pH 7.0). Leaf segments were rinsed in cacodylate buffer and fixed in 1% (w/v) osmium tetroxide in the same buffer for 2.5h at RT. The specimens were then stained *en bloc* with 1% (w/v) uranyl acetate in 20% acetone, dehydrated in a graded acetone series and embedded in Spurr's low viscosity epoxy resin (Spurr, 1969). Ultrathin sections (60-90 nm thick) were cut with a diamond knife on an LKB Ultratome III

8800 and post-stained with lead citrate (Reynolds, 1963). At least three biological replicates were analyzed. Micrographs were taken at magnifications of 1100x (overviews) and 12,000x (details) at 80 kV on a Zeiss EM109R electron microscope.

5.6 Computational methods

Software, databases and algorithms used in the present study

Table 5: List of used software tools (freeware)

name	version	author/reference	URL
Chromas lite	2.01	Technelysium Pty Ltd.	http://www.technelysium.com.au/chromas_lite.html
Genedoc	2.6.002	Nicholas and Nicholas, 1997	http://www.nrbsc.org/gfx/genedoc/
AnnHyb	4.938	Olivier Friard	http://bioinformatics.org/annhyb
pDRAW32	1.0Rev.1.1.93	Kjeld Olesen	http://www.acaclone.com

Table 6. List of used software tools (licensed)

name	version	Publisher/Licensor	name
Vector NTI	9.1.0	Invitrogen	Vector NTI

Table 7. List of used databases and algorithms (available online)

name	version/ release	author/reference	URL
TMHMM	2.0	Sonnhammer et al., 1998	http://www.cbs.dtu.dk/services/TMHMM/
BLAST		Altschul et al., 1990; Altschul and Koonin, 1998	http://www.ncbi.nlm.nih.gov/BLAST
ARAMEMNON	5.2	Schwacke et al., 2003; Schwacke et al., 2007	http://aramemnon.botanik.uni-koeln.de
NASCArrays			http://affymetrix.arabidopsis.info/narrays/experimentbrowse.pl
AtEnsembl	49	Sanger Institute / EMBL-EBI	http://atensembl.arabidopsis.info/Arabidopsis_thaliana_TAIR/index.html
ExPASy		Gasteiger et al., 2003	http://www.expasy.org/
ClustalW		Higgins and Sharp, 1988; Higgins and Sharp, 1989; Jeanmougin et al., 1998	http://www.ebi.ac.uk/Tools/clustalw/index.html
COILS		Lupas et al., 1991	http://www.ch.embnet.org/software/COILS_form.html

6 Results

6.1 The Oxa gene family in Arabidopsis thaliana

Members of the Alb3/Oxa1/YidC protein family are found in bacteria, mitochondria and chloroplasts and are involved in the biogenesis of integral membrane proteins, as well as their assembly into functional complexes in energy transducing membranes.

6.1.1 Seven Alb3/Oxa1/YidC homologues are expressed in *A. thaliana*

Since extensive studies on the model plant *Arabidopsis* led to several new annotations and corresponding gene models over the last years, it was necessary to revaluate the results of former studies (Funes et al., 2004a). BLAST searches using the new annotations revealed the presence of seven distinct loci in the *Arabidopsis* genome coding for proteins that show significant homology to the Oxa protein family (Table 8; the *Arabidopsis* Information Resource [TAIR]; L.Gerdes & J.Soll, personal communication). Although six of these genes had already been identified in earlier studies, three (AtOxa2a, AtOxa2b and Alb4) displayed major annotational changes.

As mentioned in the introduction, Alb4 (At1g24500) was annotated as a new gene coding for a protein of 497 amino acids (Gerdes et al., 2006). New cDNA sequences for AtOxa2a (At1g65080) and AtOxa2b (At3g44370) resulted in protein sequences that also differed considerably from the previous ones: AtOxa2a gained about 90 amino acids at its N-terminus, giving rise to a new translation start and therefore an altered signal peptide. The size of AtOxa2b, on the other hand, increased from 338 to 566 residues at the C-terminus of the protein (data not shown). In addition to these revised sequences, a new gene, probably representing a seventh Oxa family member in *Arabidopsis*, was identified for the first time and named AtOxa6. The corresponding protein displays weak homology to the other Oxas, although being much smaller and thus likely not a full-length paralogue. It exhibits the highest similarity with the N-terminus of AtOxa1a, with which is shares a sequence similarity of ~44% (Figure 5). Further database analyses demonstrated that all genes coding for putative *Arabidopsis* Oxa proteins, including AtOxa6, are actively transcribed, since expressed sequence tags are reported for all of them (data not shown).

In comparison to yeast and bacteria, where only one or two proteins define this family, this represents a large family size. Since this could imply that *Arabidopsis* uses Oxa-mediated protein insertion in a variety of membrane compartments, the distribution of all seven homologues in the plant cell was studied by *in vitro* and *in vivo* localization experiments.

Table 8. Summary of the *Arabidopsis* Oxa gene family and encoded proteins.
List of all detected homologues with protein name, gene locus (AGI code), length in amino acids, predicted molecular weight (MW in kDa) predicted transmembrane domains (TMs) and presence of the conserved Oxa domain (+: entire domain; *: partial domain). References indicate description in previous studies.

name	AGI code	amino acids	MW [kDa]	TMs	Oxa domain	references
AtAlb3	At2g28800	462	50.2	5-6	+	Sundberg et al., 1997
AtAlb4	At1g24500	497	54.9	5	+	Gerdes et al., 2006
AtOxa1a	At5g62050	429	47.9	4-5	+	Hamel et al., 1997; Sakamoto et al., 2000
AtOxa1b	At2g46470	431	47.9	4	+	Funes et al., 2004
AtOxa2a	At1g65080	525	58.3	4	+	Funes et al., 2004
AtOxa2b	At3g44370	566	62.8	2-4	+	Funes et al., 2004
AtOxa6	At1g44890	281	31.9	1-2	*	-

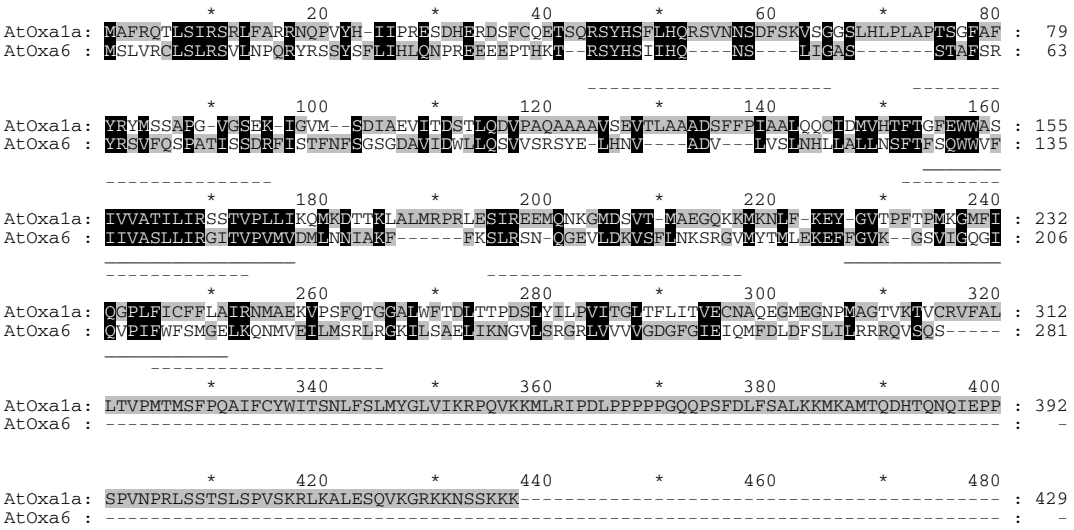

Figure 5. AtOxa6 exhibits sequence similarity to the N-terminus of AtOxa1a. An alignment of AtOxa6 (At1g44890) with AtOxa1a (At5g62050) is shown. Identical amino acids are shown in black and similar ones in grey.

6.1.2 *In silico* characterization of the *Arabidopsis* homologues

For the initial characterization of the genes and their corresponding proteins, detailed *in silico* analyses were performed. Comparison of all seven *Arabidopsis* genes demonstrated that the corresponding proteins range in size from 281 amino acids in the smallest homologue AtOxa6 to 566 amino acids in the AtOxa2b protein (Table 8). The protein sequences were further analyzed for the presence of transmembrane-spanning regions by a total of 15 different prediction programs in the Aramemnon database, including algorithms like TmHMMv2, TMpred, and TopPredv2 (Aramemnon-plant membrane protein database; www.aramemnon.botanik.uni-koeln.de; Schwacke et al., 2003). Figure 6 depicts the

consensus prediction obtained for all seven Oxa proteins. Although members of the Oxa-family usually possess five transmembrane regions, this was only found to be predicted for two of the *Arabidopsis* homologues (AtOxa1a and Alb4). Interestingly, the algorithms detected only four transmembrane regions for three of them (AtOxa1b; AtOxa2a and AtOxa2b) and for one protein (AtOxa6) only two (Figure 6). Moreover, many programs also failed to predict the canonical five transmembrane regions in the well characterized thylakoid protein Alb3, which in this case is believed to have six of these domains. Notably, some of the possible transmembrane helices were predicted only by some of the used programs, resulting in very low scores (indicated by light colors). Therefore, the actual number of transmembrane segments might even be lower than depicted in Figure 6. Further biochemical or structural studies will be necessary to clarify this point.

The conserved core domain of the Alb3/Oxa1/YidC family with its five transmembrane helices has been designated as the Oxa domain (60KD IMP, pfam02096.12; Marchler-Bauer et al., 2007; Marchler-Bauer et al., 2009). Analysis of the *Arabidopsis* sequences established that six of the seven homologues possess the entire Oxa domain, whereas in AtOxa6 only the first part of this domain is present, including the first two putative transmembrane segments (Figure 6). Interestingly, AtOxa2a and AtOxa2b were found to contain additional TPR-domains (tetratricopeptide repeat) in their hydrophilic C-termini. These structural motifs are present in a wide range of proteins and have been described to mediate protein-protein interactions and to be involved in the assembly of multi-protein complexes (Figure 6) (D'Andrea and Regan, 2003).

Alignments of the full-length protein sequences show that always two proteins are more similar to each other than to the other homologues. One of these pairs is represented by Alb3 and Alb4, which show 60% identity and 77% similarity to each other (Gerdes et al., 2006). The others include the AtOxa1a and AtOxa1b pair with 44% identity and 63% similarity in their sequences and finally AtOxa2a and AtOxa2b with 50% sequence identity and 69% similarity (data not shown). The AtOxa6 protein has an exceptional position since it differs both in size and topology from the other Oxa proteins. However, since it exhibits the highest homology in its protein sequence to AtOxa1a, displaying 24% identity and 44% similarity over the first 245 amino acids, it might belong to the group of AtOxa1a and AtOxa1b (Figure 5).

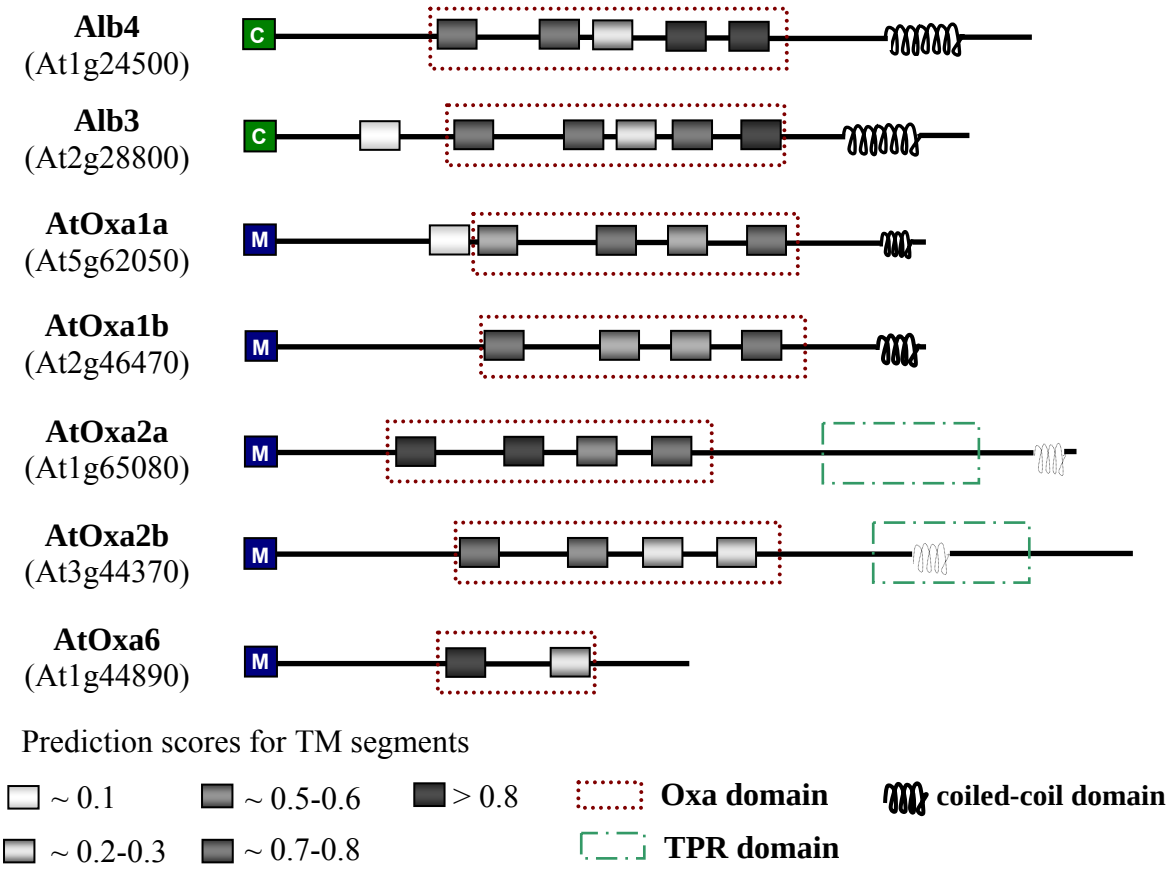

Figure 6. Predicted topology model of the *Arabidopsis* Alb3/Oxa1/YidC protein family members. Names (and AGI gene codes) of the *Arabidopsis* proteins are given at the left. Protein sequences are sketched and oriented with the N-terminus to the left. Green and blue boxes depict targeting signals for chloroplasts (C) and mitochondria (M), respectively. Grey boxes indicate predicted transmembrane domains (light color for weak scores, dark color for strong scores; see above). Predicted coiled-coil domains are shown as helices (dotted for weak prediction). The conserved Alb3/Oxa1/YidC homology domain (Oxa-domain; 60kD IMP) is indicated by purple dotted lines and TPR domains by turquoise dashed lines.

Another criterion for the classification of Oxa proteins is the presence of a coiled-coil like structure in their C-termini. Oxa1 from yeast for instance is predicted to possess such a domain, while the same is missing in the Oxa2 protein (Jia et al., 2003; Szyrach et al., 2003; Funes et al., 2004b). The *Arabidopsis* homologues AtOxa1a/1b and AtOxa2a/2b, respectively, were named according to this trait, which is also in good agreement with the fact that AtOxa1a can functionally complement the mitochondrial Oxa1 protein of yeast (Funes et al., 2004a; Hamel et al., 1997). However, since AtOxa2a, AtOxa2b, and Alb4 were not correctly annotated at this time, and since AtOxa6 was not known, the corresponding predictions had to be repeated. Comparison of the new amino acid sequences of the *Arabidopsis* proteins with family members from other organisms and the prediction of coiled-coil domains (Coils algorithm, www.ch.embnet.org) revealed that the classification is still valid for the *Arabidopsis* homologues: AtOxa1a and AtOxa1b are predicted to have a C-terminal coiled-

coil structure and therefore belong to the so-called Oxa1 group (Figure 6), whereas the newly annotated AtOxa2a and AtOxa2b only exhibit a very weak score and thus most likely do not possess the extended coiled-coil domain, similar to Oxa2 from yeast. Moreover, a C-terminal coiled-coil domain is also predicted for the chloroplast localized proteins Alb3 and Alb4, indicating that these proteins belong to the Oxa1 group at least in this respect (Figure 6). Although being most similar to AtOxa1a in its sequence, AtOxa6 does not contain this structure, indicating that it might represent a C-terminally truncated homolog.

6.2 Sub-cellular localization of Alb3/YidC/Oxa-like proteins in Arabidopsis

6.2.1 *In silico* analysis

Although most of the predicted *Arabidopsis* genes and the deduced protein sequences were already identified some years ago (Funes et al., 2004a), the sub-cellular localization has been determined experimentally only for three of them so far. Alb3 and Alb4 (At1g24500, At2g28800) were shown to be integral proteins located in the thylakoid membrane of chloroplasts. Both are encoded in the nucleus, synthesized in the cytosol as preproteins with cleavable transit peptides and then imported into the chloroplast (Sundberg et al., 1997; Gerdes et al., 2006). AtOxa1a (At5g62050), on the other hand, was demonstrated to be located in the inner membrane of mitochondria (Hamel et al., 1997; Sakamoto et al., 2000), like the yeast Oxa1 and Oxa2 proteins (Herrmann et al., 1997; Kermorgant et al., 1997; Souza et al., 2000; Funes et al., 2004b).

To investigate the localization of the remaining Oxa proteins in *Arabidopsis,* the protein sequences were first analyzed *in silico* by a total of 17 different targeting prediction programs (including *e.g.* TargetP, Predator, Mitoprot, and ChloroP) collected in the Aramemnon database (Schwacke et al., 2007). Finally, a consensus prediction for the sub-cellular targeting is calculated which is depicted in Figure 6 and Table 9. In line with the experimental data, Alb3 and Alb4 received high probability scores for chloroplasts targeting according to the used algorithms (Table 9, Figure 6; Sundberg et al., 1997, Gerdes et al., 2006). In contrast to this, all other *Arabidopsis* homologues were predicted to be located in mitochondria (Table 9), although the prediction was not entirely clear in all cases. Depending on the algorithm, AtOxa2a and AtOxa2b were predicted to be either targeted to mitochondria, chloroplasts or even to both, resulting in relatively high scores also for plastid localization. Furthermore, some programs favored the secretory pathway. Since it is known that these programs occasionally fail to predict the correct localization, these data can only give a first indication and the sub-cellular localization of the proteins of interest has to be determined

experimentally. Therefore, to finally clarify the distribution of the putative *Arabidopsis* Oxa proteins, *in vitro* import experiments and *in vivo* GFP labeling were performed.

Table 9. Summary of the targeting prediction for *Arabidopsis* Oxa proteins. Shown are the protein name, gene locus (AGI code) and the consensus predictions for localization in chloroplasts (Cp), mitochondria (M) or the secretory pathway (SP) based on individual predictions of 17 different predictors as derived from the Aramemnon database and published in Schwacke et al., 2007.

name	AGI code	Cp	M	S P	Prediction consensus
Alb3	At2g28800	**25.0**	1.5	0.0	**Cp**
Alb4	At1g24500	**23.3**	2.0	0.0	**Cp**
AtOxa1a	At5g62050	0.0	**22.2**	0.0	**M**
AtOxa1b	At2g46470	0.0	**22.6**	0.0	**M**
AtOxa2a	At1g65080	11.3	**20.5**	2.1	**M**
AtOxa2b	At3g44370	6.8	**20.4**	0.7	**M**
AtOxa6	At1g44890	0.0	**20.7**	0.3	**M**

6.2.2 *In vitro* import

To address the sub-cellular localization in a first approach *in vitro* import experiments into either chloroplasts, mitochondria or both, were carried out. Since these experiments are best established in *Pisum sativum*, organelles were isolated from pea plants for all experiments.

Initially, the *in vitro* translated and radioactively labeled precursor proteins were incubated with isolated chloroplasts in absence of mitochondria (Figure 7, left panel). Following the reaction, the non-imported preproteins were digested by treatment with the protease thermolysin, and finally the chloroplasts were ruptured and separated into a soluble and a membrane fraction. The uptake into mitochondria was assayed separately. For this, preproteins were incubated with isolated pea mitochondria, followed by treatment with thermolysin.

As Figure 7 illustrates, Alb3 and Alb4 can be successfully imported into chloroplasts *in vitro* (left panel). Precursors of both proteins were found to be processed to a smaller mature protein that was protease resistant and present in the membrane fractions. In both cases, the import behavior was comparable to that of the positive control, the precursor protein of the oxygen evolving complex subunit of 33 kDa (pOE33), which is located in the thylakoid lumen. Since pOE33 is known to have a bipartite transit peptide (Douwe and Weisbeek, 1991; Keegstra and Cline, 1999) an intermediate form could be detected in the stroma fraction (iOE33). A similar product, although in the membrane fraction, was observed for Alb3, which thus might also represent an intermediate (Figure 7). However, no evidence for import into mitochondria could be observed for both Alb proteins, as there were no protease protected

products detectable. Moreover, also the binding to the organelles was very low (Figure 7, right panel).

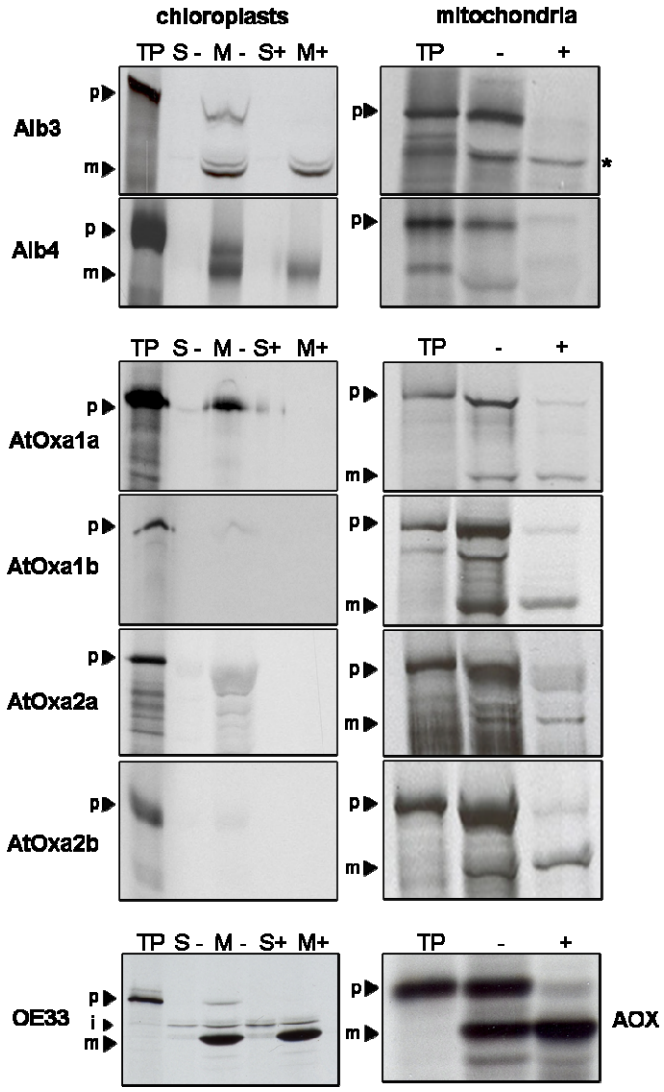

Figure 7. Alb3 and Alb4 are imported exclusively into chloroplasts and AtOxa1a, AtOxa1b, AtOxa2a, and AtOxa2b into mitochondria *in vitro*. *In vitro* translated and radiolabeled precursor proteins of all seven *Arabidopsis* Oxa proteins were incubated with isolated chloroplasts or mitochondria (corresponding to 25 µg Chl or 100 µg of mitochondrial protein, respectively) as described in "methods". Parallel incubations were carried out using the precursors of OE33 as a control for chloroplast import and AOX as a control for uptake into mitochondria. After import into chloroplasts, chloroplasts were either not treated (-) or treated (+) with the protease thermolysin. Then organelles were ruptured and separated into a soluble stroma (*S*) and membrane fraction (*M*). After import into mitochondria, samples were analyzed directly (-) or after treatment with thermolysin (+). All samples were subjected to SDS-PAGE, and labeled proteins were detected by autoradiography. *TP,* 10% of translation product; *p*, precursor; *m*, mature; *i*, intermediate; *, unspecific band from TP.

In contrast, radiolabeled precursors of AtOxa1a, AtOxa1b, AtOxa2a and AtOxa2b were readily imported into purified mitochondria and processed to smaller protease resistant mature proteins (Figure 7, right panel), but none could be imported into isolated chloroplasts (Figure 7, left panel). They thus behaved similar to the mitochondrial control construct, the precursor of the alternative oxidase (AOX, Figure 7; left panel; Whelan et al., 1996a).

Interestingly, the precursor of AtOxa6 was imported into both, chloroplasts and mitochondria, in single import experiments (data not shown). To test, whether AtOxa6 is indeed imported

into both organelles, dual import experiments with isolated pea chloroplasts and mitochondria were carried out, since these are known to increase the specificity of the targeting (Rudhe et al., 2002). The precursors of the small subunit of RuBisCO (pSSU) and AOX (pAOX) were used as controls for the reaction. As shown in Figure 8 (lower panel), pSSU was exclusively imported into chloroplasts while pAOX was only imported into mitochondria, confirming the selectivity of this system. The precursor of AtOxa6, however, was still imported into both organelles (Figure 8, upper panel), resulting in two different sized protease-protected products. In chloroplasts, AtOxa6 was processed to a mature form of approximately 24 kDa, whereas in mitochondria, a 31 kDa product of the same size as the preprotein was observed.

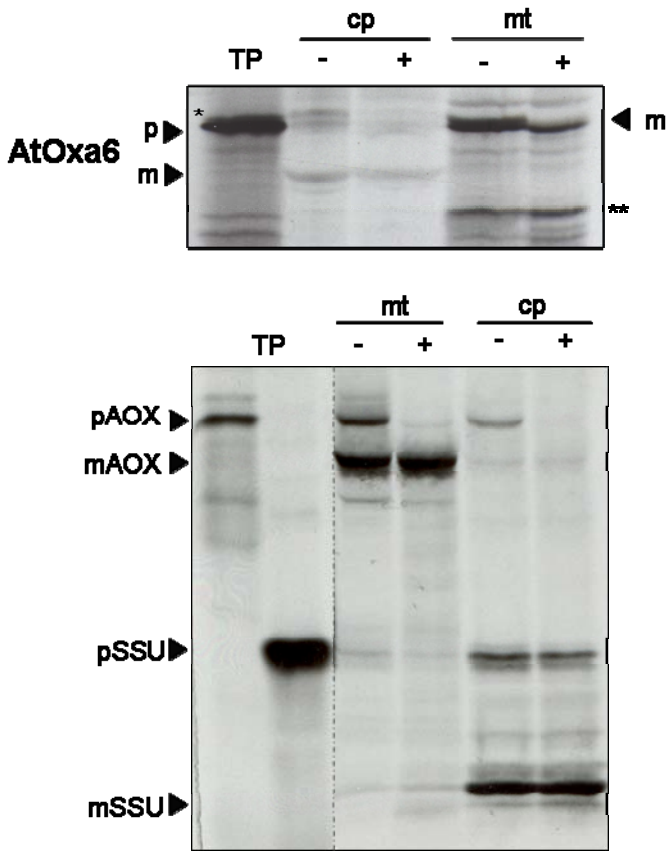

Figure 8. AtOxa6 is imported into both, chloroplasts and mitochondria dual *in vitro* import experiments. Translated and radiolabeled precursors proteins were incubated with isolated pea chloroplasts and mitochondria in parallel (25 µg Chl and 100 µg of mitochondrial protein) as described in "methods". After import, samples were either not treated (-) or treated (+) with the protease thermolysin. Organelles were re-isolated through a 4% (v/v) Percoll cushion. After washing, imported products were analyzed by SDS-PAGE and labeled proteins detected by autoradiography. The translation product of AtOxa6 shows two signals at the size of the precursor protein, of which the lower one is believed to correspond to AtOxa6. Precursors of SSU (pSSU) and AOX (pAOX) were used as controls for import into chloroplast or mitochondria, respectively. *TP,* 10% of translation product; *cp*, chloroplasts; *mt,* mitochondria; *p*, precursor; *m*, mature; */** unspecific bands from TP.

6.2.3 GFP fusion constructs

To corroborate the findings from the *in vitro* uptake assays in a second approach, the sub-cellular localization of the *Arabidopsis* Oxa proteins was further analyzed by transient transformation of mesophyll protoplasts from *Arabidopsis* with GFP fusion constructs. The GFP- and autofluorescence of transformed protoplasts was monitored with a confocal laser

scanning microscope and fluorescence signals subsequently merged. Since chlorophyll emits a red autofluorescence when excited by the confocal laser beam, this signal was used as an indicator for chloroplasts or thylakoids, respectively (Figures 9-11; second panel). Mitochondria were visualized by staining with MitoTracker dye (Figure 10; third panel; see Methods). To get an idea of the cellular distribution and staining pattern of compartments other than chloroplasts and mitochondria, protoplasts were transformed with appropriate GFP/CFP marker proteins (Figures 9 and 11, see Figure legends and methods Table 1). The images for Alb3 and Alb4 in Figure 9 were kindly provided by Dr. L. Gerdes (Gerdes et al., 2006) and are shown as examples for localization of GFP-tagged proteins in thylakoids of chloroplasts. The GFP-signal from these constructs is clearly distinguishable from the pattern obtained with control constructs that are targeted into the stroma or the envelope of chloroplasts (Figure 9; dcp.r-GFP, At4g31040, respectively).

Since C-terminal GFP fusions of full-length constructs from the other *Arabidopsis* Oxa proteins formed aggregates in the cytoplasm (not shown) truncated constructs containing just N-terminal fragments of the proteins, either with or without predicted transmembrane segments or 5`UTR, had to be used (for details, see methods Table 1). Transformation of protoplasts with these shorter constructs resulted in a pattern of numerous small particles for AtOxa1a, AtOxa1b, AtOxa2a, and AtOxa2b, which was similar to the pattern observed with the controls for mitochondria, the endoplasmic reticulum and the Golgi apparatus (Figure 11). However, at closer investigation a clear co-localization of the GFP-fluorescence with the MitoTracker signals could be detected in three-dimensional confocal images, corroborating the mitochondrial targeting for all four Oxa homologues (Figure 10). However, some larger GFP spots were still present, most likely representing residual aggregates that could not be targeted properly.

For AtOxa6, the sub-cellular localization was not as well-defined as for the other homologues. Analysis of a construct comprised of the first 110 amino acids fused to GFP, revealed a spotted GFP pattern that was superficially similar to the signals obtained for the other four Oxa proteins (Figure 10). However, when the GFP and MitoTracker images were merged, these only partially overlapped, while many signals could not be assigned to mitochondria nor to chloroplasts. Since these spots were larger and the signal intensity stronger, they might represent aggregates, as found for the full-length constructs. Another possibility is that the AtOxa6 protein is targeted to additional organelles in the plant cell, as *e.g.* the endoplasmic reticulum, the Golgi apparatus or peroxisomes. However, none of the corresponding markers was found to match with the AtOxa6 signal (Figures 10 and 11). Taken together, the observed

overlap of the AtOxa6 signal with the MitoTracker indicates that at least some of the protein is targeted to mitochondria. Whether AtOxa6 is additionally targeted to another compartment, as *e.g.* implied by the import experiments, could not be answered by this approach and needs further studies.

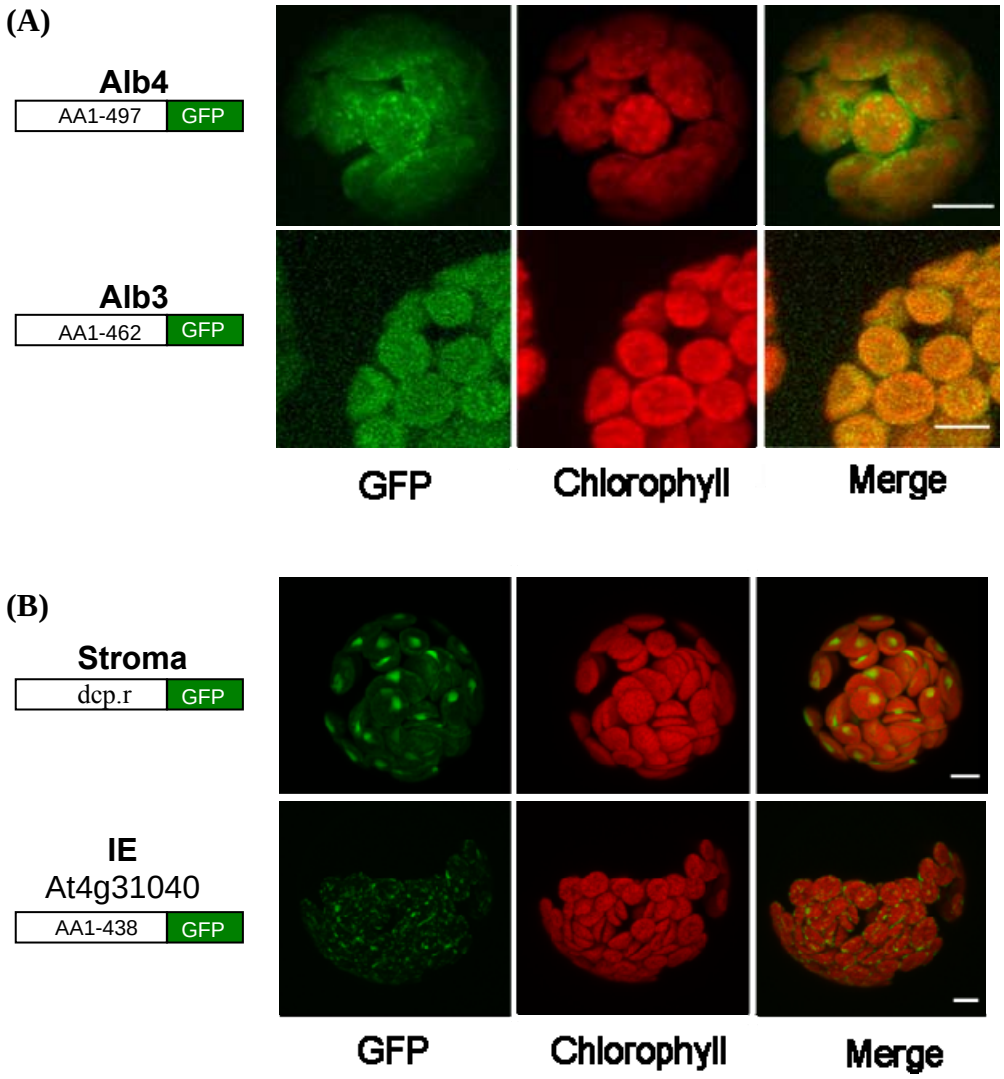

Figure 9. **Alb3 and Alb4 are targeted to chloroplasts *in vivo*.** *Arabidopsis* mesophyll protoplasts were transiently transformed with GFP constructs of (A) full-length Alb3 or Alb4, or (B) markers for chloroplast stroma and inner envelope. Maximum intensity signals from confocal images are shown for GFP fluorescence (GFP), Chl autofluorescence (chlorophyll), and an overlay of both (merge). The used constructs are depicted on the left. *At4g31040*, nuclear-encoded homologue of Ycf10; *dcp.r*, marker for chloroplast stroma; *AA*, amino acids; *bar*, ~ 5 µm. Pictures for Alb3-GFP and Alb4-GFP were previously published in Gerdes *et al*., 2006

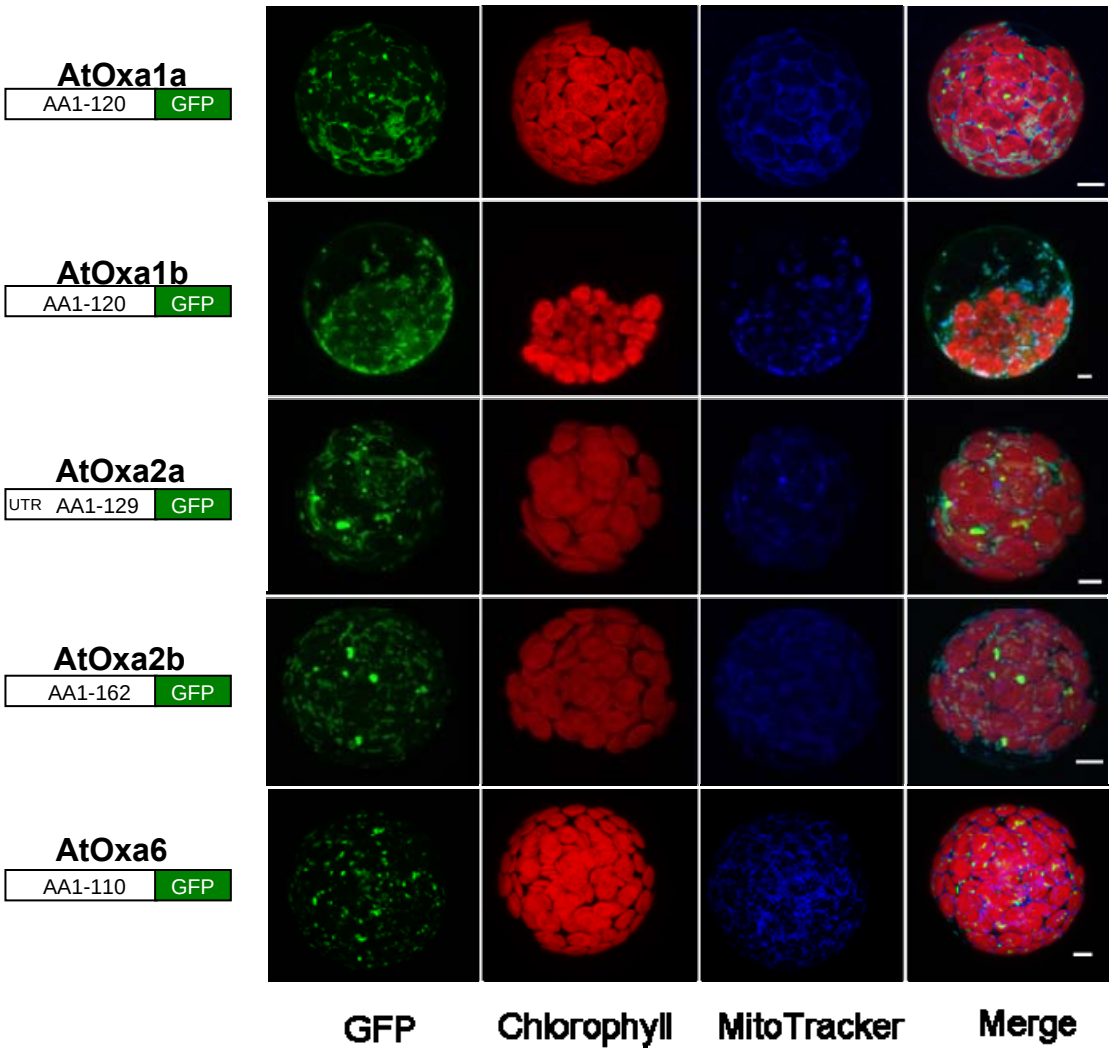

Figure 10. AtOxa1a, AtOxa1b, AtOxa2a, AtOxa2b and AtOxa6 are targeted to mitochondria *in vivo*. The sub-cellular localization of GFP-tagged constructs was assessed by transient transformation of *Arabidopsis* mesophyll protoplasts. MitoTracker labeling was used as a control for mitochondria. Names of the *Arabidopsis* proteins as well as the used constructs are depicted on the left. Maximum intensity signals from confocal images are shown for GFP fluorescence (GFP), Chl autofluorescence (chlorophyll), MitoTracker fluorescence (MitoTracker), and an overlay of all three (merge). *UTR*, 5´untranslated region; *AA*, amino acids; *bar,* ~ 5 µm.

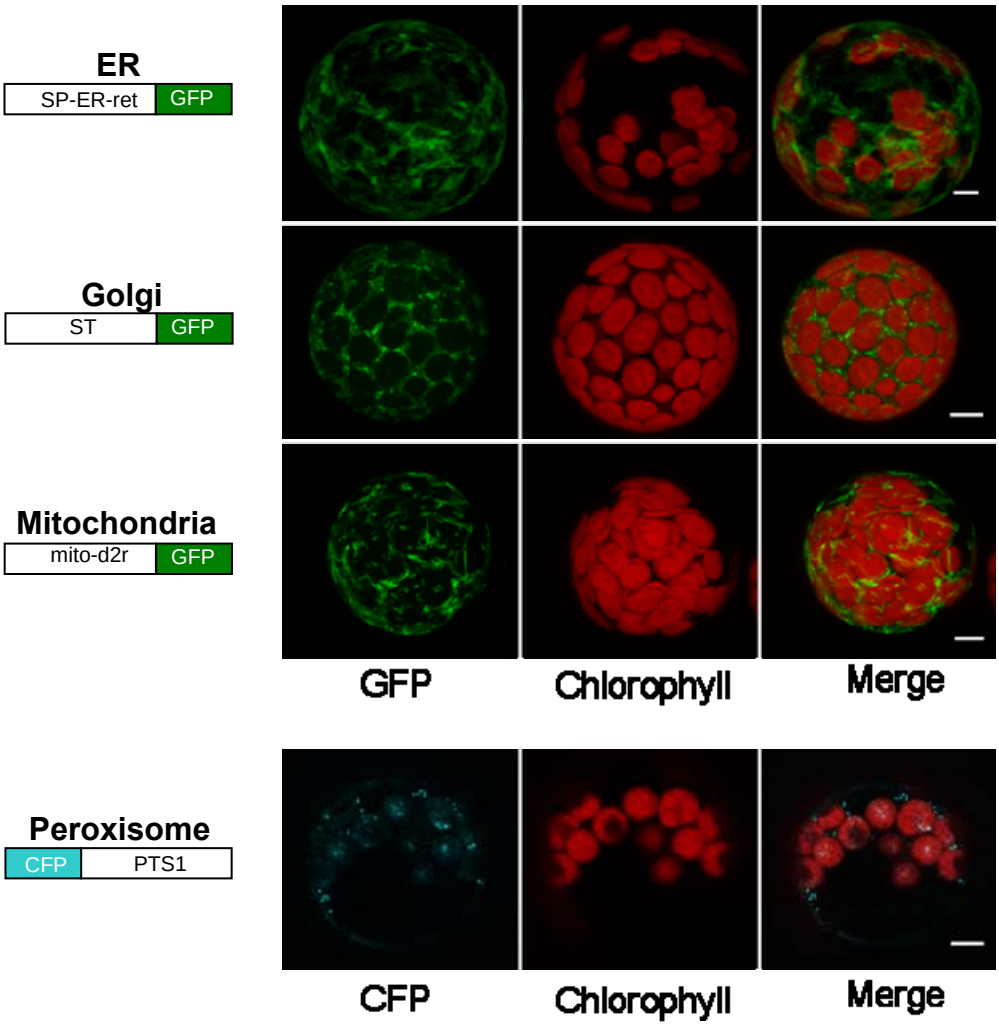

Figure 11. Sub-cellular localization of marker constructs in transiently transformed protoplasts. The localization of marker proteins (fused to GFP or CFP) for sub-cellular compartments or organelles was assessed by transient transformation of *Arabidopsis* mesophyll protoplasts. Maximum intensity signals from confocal images are shown for GFP/CFP fluorescence (panel 1), Chl autofluorescence (chlorophyll), and an overlay of both (merge). *SP-ER-ret*, signal peptide and endoplasmic reticulum retention signal; *ST*, sialyltransferase; *mito-d2r*, marker for mitochondria; *PTS1*, peroxisome targeting signal; *AA*, amino acids; *bar,* ~ 5 µm.

6.3 Physiological role of Alb4 in Arabidopsis thaliana

All members of the Alb3/Oxa1/YidC family characterized so far seem to be essential for survival of the cell, at least under specific growth conditions.

Interestingly, *Arabidopsis* T-DNA and RNA interference lines (RNAi) with a reduced level of Alb4 showed no obvious phenotype, but an altered chloroplast ultrastructure and subtle defects on thylakoid membranes (Gerdes et al., 2006). A more detailed analysis of *Arabidopsis* mutant lines with a complete loss of the Alb4 protein was therefore undertaken to investigate whether these plants display a stronger phenotype and to get insight into the physiological role of Alb4 in the biogenesis of chloroplast membrane proteins.

6.3.1 *ALB4* TILLING mutants

A possibility to generate complete loss-of-function plants is the TILLING approach (*Targeting Induced Local Lesions in Genomes,* Till et al., 2003). This method combines chemical mutagenesis using the mutagen ethyl-methanesulfonate (EMS) with a sensitive DNA screening-technique to identify single point mutations in a gene of interest.

Arabidopsis TILLING lines constructed in a Col-*er* background were thus screened for point mutations in the *ALB4* gene (At1g24500) by a TILLING service (Seattle Arabidopsis TILLING Project, Till et al., 2003). Several independent mutant lines were obtained from this screen, and those lines with mutations in the *ALB4* gene resulting in a truncated or instable protein were chosen for further analysis. Since it is known that EMS mutagenesis can cause several independent mutations leading to diverse genetic backgrounds, two independent mutant lines, which were homozygous for a point mutation in the *ALB4* gene, were analyzed in parallel. For both lines the data of at least two replica experiments were compared and only validated when the results were found to be alike.

The mutation sites in the analyzed lines are depicted in Figure 12A. A point mutation in exon 3 in line CS92437 (#437) introduces a premature stop codon, leading to translation termination after 509 bp. When cDNA from this line was amplified with *ALB4*-specific primers, transcript of WT size was obtained. In contrast, when cDNA from the second line CS95771 (#771) was amplified two transcripts were obtained that differed in size from the WT cDNA. In this line, a C→T transition in intron 2 creates a novel splice site in the *ALB4* gene, which accounts for the variant transcripts observed. The expected point mutations were further confirmed by PCR and restriction analysis, as well as by sequencing of the genomic DNA (data not shown).

To test whether the point mutations cause loss of the Alb4 protein, chloroplasts of the two mutant lines were analyzed in immunoblots using an Alb4 antiserum. As shown in Figure 12B, no Alb4 protein could be detected in either of the mutant lines. As a control, an Alb3-specific antiserum was used which shows an unchanged level of the Alb3 protein in the *alb4* mutants.

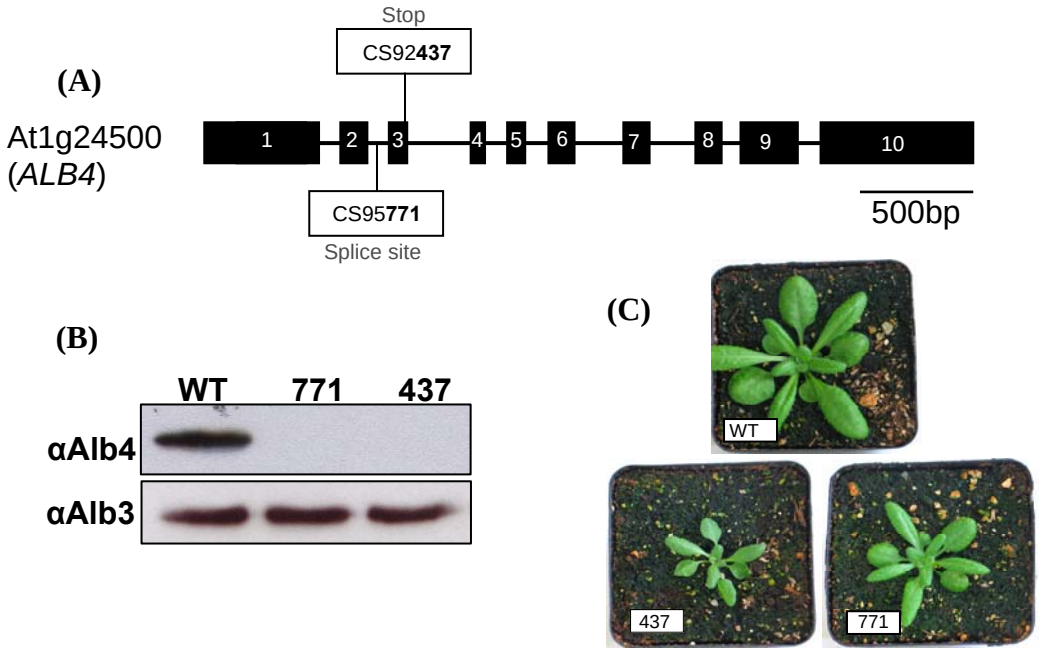

Figure 12. Analysis of *Arabidopsis ALB4* TILLING mutants. (A) Schematic representation of the *Arabidopsis ALB4* gene (At1g24500). Exons are represented as solid boxes and introns as thin lines. Positions of point mutations in the *ALB4* gene are indicated. Line #437 contains a premature stop codon, whereas line #771 shows aberrant splicing behaviour due to a C→T transition in intron 2. (B) Alb4 protein is missing in the *alb4* mutant lines. Chloroplasts (50 µg of total protein) were prepared from mature leaves of three-week-old WT (Col-*er*) and *alb4* mutant plants, fractionated by SDS-PAGE, and subjected to immunoblot analysis using an Alb4 antibody (upper panel). Antiserum against Alb3 was used as a loading control (lower panel). (C) Growth phenotypes of three-week-old WT and *alb4* mutant plants grown on soil under long-day (16h light / 8h dark) conditions.

6.3.2 Phenotype of *alb4* mutants

Arabidopsis alb3 mutants have an albino appearance and do not survive on soil beyond the seedling stage (Sundberg et al., 1997). The loss of Alb4 was found to result in a less severe phenotype than described for the close homologue Alb3. However, although *alb4* plants were not chlorotic, growth of both TILLING lines #437 and #771 was slightly retarded compared to WT during the first three to four weeks of development when plants were grown on soil under long-day conditions (16 h light / 8 h dark; Figure 12C). The same growth defect was also observed under short-day (8 h light / 16 h dark) and 12 h light / 12 h dark conditions

(data not shown). In any case, the *alb4* plants reached the reproductive stage like WT although they stayed slightly smaller. In addition, both mutant lines were completely fertile, and the obtained seeds were viable on soil, indicating that Alb4 is not essential for plant reproduction.

6.3.3 Ultrastructure of *alb4* chloroplasts

To investigate how the complete loss of Alb4 affects the sub-cellular ultrastructure, electron microscopy of three-week-old TILLING plants was performed. Analysis showed that both mutant lines differed from the WT in the numbers of cells per unit area and the mean number of chloroplasts per cell (Figure 13 and Table 10, column 3 and 4). Overviews of the mutant leaf tissue frequently revealed the presence of lacunae, indicating that the mutant cells are smaller than their WT counterparts. As stated in Table 10, the cell density in the mutant tissues was higher, but the number of chloroplasts per cell was reduced. Comparison of the number of starch grains or starch initiation centers in the chloroplasts of several replicas showed that they were less abundant in the mutants compared to the WT, although the variation was higher (Table 10, column 5). The ultrastructural analysis further revealed differences in the development of grana thylakoids and stroma-lamellae (Figure 13). The regular arrangement of well-developed grana stacks and interconnecting stroma thylakoids, which is clearly visible in WT chloroplasts, was less pronounced in the mutants. Grana stacks in the mutants seemed disordered and less well-defined, whereas the luminal space of stroma-lamellae was occasionally swollen.

Table 10. *alb4* mutants display reduced cell size and chloroplast densities. The mean number of cells per unit area (column three) was determined in four to seven non-overlapping areas (column two) of three to four leaves of independent biological replicas. Column four gives the mean number of chloroplasts per cell, based on the areas measured for column three [total chloroplast of area 1/cells of area 1]. Column five gives the mean number of starch or starch initiation centers of all chloroplasts in the analyzed areas. Standard deviations (SD) are given in brackets.

Line	Number of areas (3200 µm^2)	Mean number of cells per area	Mean number of chloroplasts per cell	Mean number of starch or starch initiation centers
Col-*er* (WT)	5	4.2 (±1.3)	5.2 (±2.3)	5.3 (±1.7)
	7	6.6 (±2.2)	5.1 (±1.8)	5.4 (±1.9)
	7	7.1 (±1.6)	5.6 (±0.9)	6.3 (±1.7)
#437	4	6.3 (±1.0)	4.5 (±0.7)	3.8 (±1.0)
	4	7.5 (±1.0)	5.3 (±1.1)	3.5 (±0.5)
	6	7.8 (±2.3)	4.3 (±1.0)	5.0 (±2.0)
	4	9.8 (±1.0)	3.6 (±0.3)	2.3 (±1.2)
#771	6	7.8 (±2.4)	3.2 (±0.7)	1.4 (±0.9)
	4	8.0 (±2.2)	3.3 (±0.5)	3.8 (±2.1)
	4	11.5 (±2.4)	3.0 (±1.0)	7.3 (±2.6)
	7	14.6 (±2.7)	3.6 (±0.5)	5.5 (±3.0)

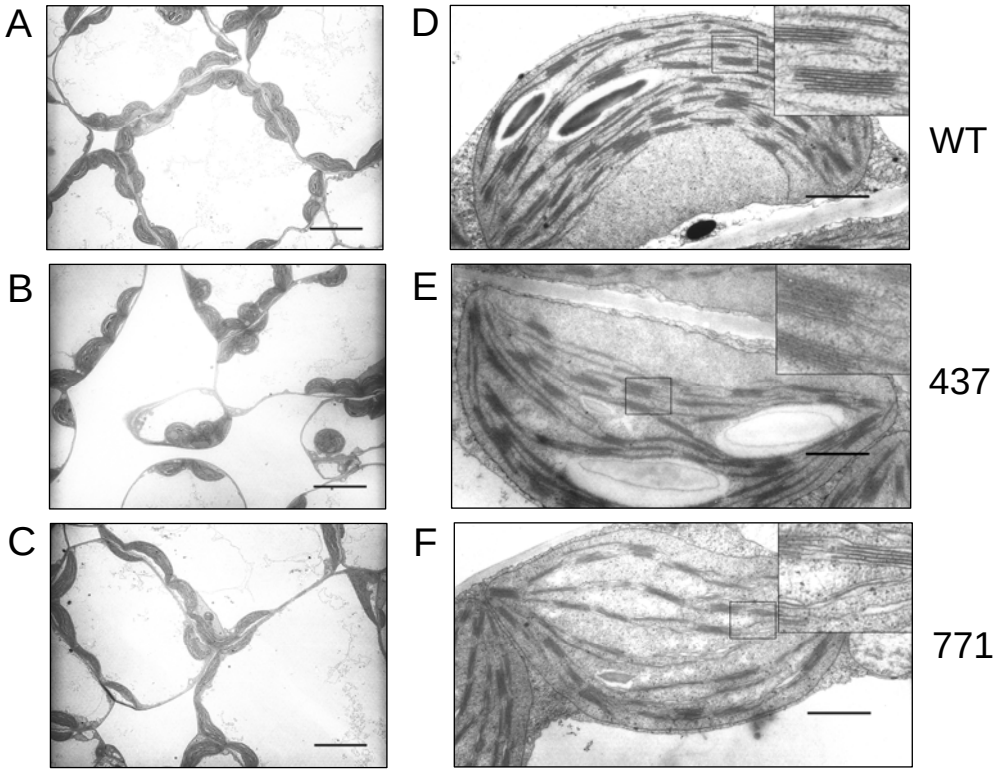

Figure 13. Electron microscopy reveals alterations in the thylakoid structure of *Arabidopsis alb4* mutant lines. (A) – (F) Electron micrographs of mesophyll cells of three-week-old WT and mutant *Arabidopsis* plants. Panels (A) – (C) show overviews of cells from WT (A) and the mutant lines #437 (B) and #771 (C) at a magnification of 1,100x. Bar, 10 µm. Panels (D) – (F) show chloroplast and thylakoid sections (at magnifications of 12,000x and 36,000x, respectively) from WT (D), line #437 (D) and line #771 (F). Bar, 500 nm.

6.3.4 Loss of Alb4 causes a decrease in steady-state levels of ATP synthase subunits

Since members of the YidC/Oxa1/Alb3 protein family are involved in the insertion of proteins into membranes it was tested whether Alb4 is likewise involved in thylakoid membrane protein biogenesis. Therefore, two-dimensional (2D) blue native (BN)/SDS-PAGE was performed, to identify thylakoid membrane complexes that might be affected by loss of Alb4. Chloroplasts isolated from WT and *alb4* mutant lines were solubilized in 1% *n*-dodecyl β-D-maltoside (DoMa) before being separated on a BN-PAGE gradient gel (5-12% polyacrylamide). Separation of complexes by BN-PAGE in the first dimension revealed no obvious differences in complex composition between the WT and the mutant lines. The most prominent complexes found in thylakoid membranes, like PSI and PSII, as well as the $Cytb_6f$ complex and the ATP synthase, were all found to be intact (data not shown).

Identification of single subunits of individual complexes was achieved by SDS-PAGE in a second dimension, followed by staining with either Coomassie or colloidal Coomassie. This way, alterations can be revealed which are not apparent in the first dimension (Figure 14).

Although it appeared that all prominent thylakoid protein complexes (PSI, PSII, Cytb$_6$f and ATP synthase) were present and similarly composed as their WT counterparts, on closer inspection, several proteins were found to differ in abundance between the WT and the mutant lines #437 (Figure 14, white circles) and #771 (data not shown). Most of the protein spots were less abundant in the mutants (D1-D9), whereas two proteins seemed to be increased compared to the WT (I1-2).

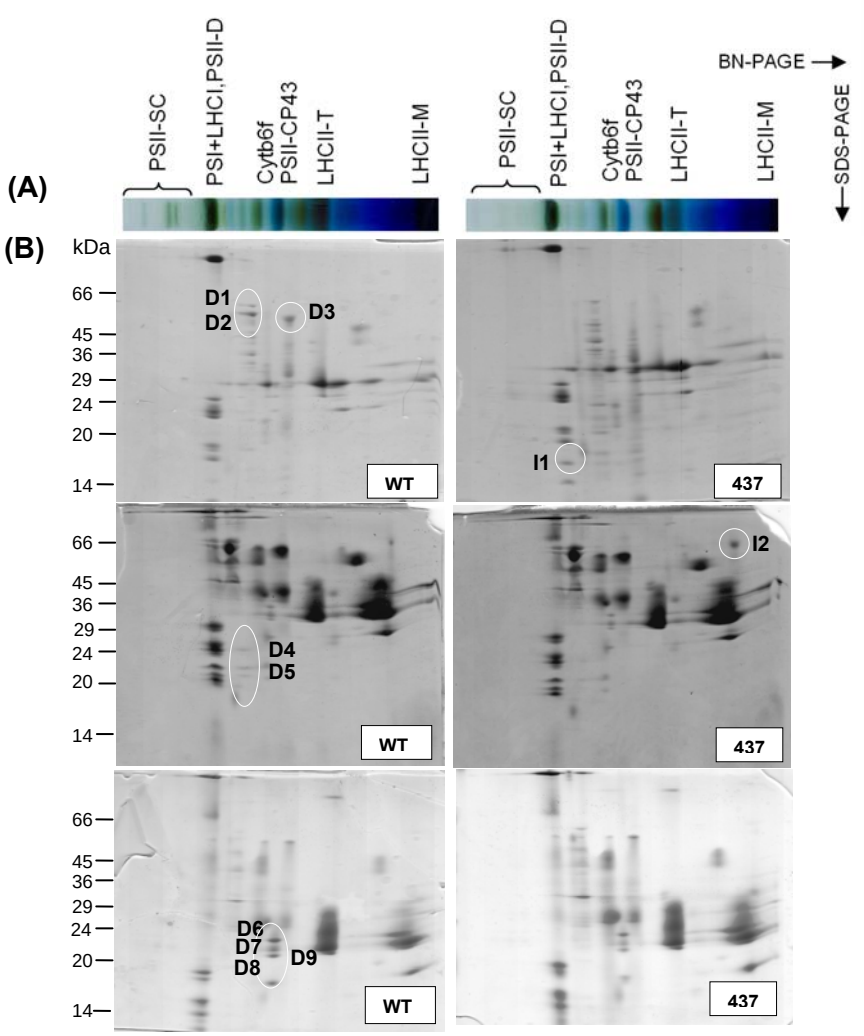

Figure 14. Loss of Alb4 affects the composition of thylakoid complexes. Chloroplasts (row 2 in B) or isolated thylakoids (rows 1 and 3 in B) from three-week-old WT and *alb4* mutant plants were solubilized with 1% DoMa and fractionated by 2D BN/SDS-PAGE. (A) Example lanes from a first dimension BN-PAGE are shown. Macromolecular protein complexes from thylakoids are indicated at the top. (B) Second dimension SDS-PAGE (15% polyacrylamide, 4 M urea). Protein complexes were stained by either Coomassie (rows 1 and 2) or colloidal Coomassie (row 3). Three independent experiments of WT (left side) and one mutant line (437; right side) are presented. Differences between WT and *alb4* mutants are indicated by white circles. *D1-9*, proteins present in decreased amounts relative to WT; *I1/2*, proteins present in increased amounts. Sizes of protein markers are given in kDa on the left. *M*, monomers; *SC*, super-complexes; *D*, dimers; *T*, trimers.

All altered protein spots were cut out and analyzed by mass spectrometry (MALDI-TOF, Zentrallabor für Proteinanalytik, LMU München, Germany). As indicated in table 11, spots D1, D2, and D5 were identified as $CF_1\alpha$+β (D1) and $CF_1\beta$ (D2), respectively, and D5 as subunit CF_OII of the CF_1CF_O-ATP synthase. In addition, subunits of the PSI (PsaD1) and PSII complexes (CP47, Lhcb4.2, CP24 (Lhcb6)), together with proteins of unknown function, were found at reduced levels in the *alb4* mutant lines. Two proteins, which were more abundant in both mutant lines, were identified as the PSI subunit PsaH-1 (I1) and BSA, the latter carried over from the Percoll gradient used for chloroplast isolation (I2). Taken together, the loss of Alb4 causes detectable changes in several thylakoid complexes. In particular subunits of the ATP synthase were decreased in protein level, which might hint at function for Alb4 in the assembly of this complex.

Table 11. Identification of protein spots from 2D BN/SDS-PAGE by mass spectrometry. Coomassie-stained spots from the 2D BN/SDS-PAGE (Figure 14) were cut out and analyzed by mass spectrometry (MALDI-TOF). In the first column the designation of the isolated spots as indicated in Figure 14B is given. The second column gives the estimated sizes of the proteins in kDa. Results of the MALDI-TOF analyses are listed in column three and four, showing the name of the identified protein (column four) and the corresponding gene (column three).

Spot	Size [kDa]	Gene	Protein
D1	55	*ATPA*, *ATPB*	ATP synthase subunit $CF_1\alpha$ + β
D2	50	*ATPB*	ATP synthase subunit $CF_1\beta$
D3	48	*PSBB*	47kDa protein PSII (CP47)
I1	12	*PSAH-1*	PSI reaction center subunit VI
I2	55	-	BSA
D4	20	*PSAD1*	PSI reaction center subunit II
D5	18	*ATPG*	ATP synthase subunit CF_OII
D6	24	*LHCB4.2*	Light-harvesting chlorophyll *a*/*b* binding protein
D7	22	-	unknown
D8	20	-	unknown
D9	14	*LHCB6*	Light-harvesting chlorophyll *a*/*b*-binding protein of minor antenna complex (CP24)

Since the results obtained by 2D BN/SDS-PAGE and MALDI-TOF indicate that plastid- as well as nuclear-encoded subunits of the ATP synthase are affected in the *alb4* mutant lines, Alb4 may influence the assembly of both types of proteins. To test this idea, the steady-state levels of the nuclear-encoded subunits CF_OII, $CF_1\gamma$, and $CF_1\delta$, and the plastid-encoded subunits CF_OIII, $CF_1\alpha$, $CF_1\beta$, and $CF_1\varepsilon$, were analyzed with specific antibodies. To this end, chloroplasts isolated from three-week-old *alb4* mutant lines and the WT were separated by

SDS-PAGE and analyzed by immunoblot using the various antibodies. As shown in Figure 15A, probing with antiserum directed against CF_OII and CF_OIII revealed a reduction of these proteins in both mutant lines, suggesting that the CF_O part of the ATP synthase is indeed affected in the *alb4* mutant lines. Due to either low amounts or unspecific binding of the antibodies raised against CF_OI and CF_OIV, the analysis of other subunits of CF_O was not possible. Similar results were obtained when antisera against the subunits $CF_1\gamma$ and $CF_1\varepsilon$ of the soluble CF_1 sub-complex were used (Figure 15A). Both proteins showed a clear reduction in line #437, while the reduction was less pronounced in the mutant line #771. In contrast to this, subunit $CF_1\delta$ was detectable at WT level in both mutant lines, as was observed with antiserum against Tic62, a component of the translocon of the inner envelope membrane of chloroplast, which was used as loading control. The results obtained with antisera against the subunits $CF_1\alpha$ and $CF_1\beta$ (Figure 15A) showed that the α-subunit was reduced in both mutant lines, whereas the β-subunit was rather unaffected. Interestingly, a protein of about 14 kDa was detected on long exposures of immunoblots of chloroplast membrane- and stroma fractions (Figure 15B, lower panel). This peptide might be an endogenous product of CF_1 turnover, since it is also detectable in WT samples. Based on the intensity of the immunoblot signal, however, the accumulation of this peptide seems to be higher in the mutants than in the WT (Figure 15B). In this experiment, the differences in the protein level of $CF_1\alpha$ and β between WT and mutant lines were not detectable because a much longer exposure was necessary to detect the smaller fragment, which led to saturation of the ECL signal.

Taken together, the presented immunoblot analyses demonstrate that the levels of several nuclear- and plastid-encoded subunits are reduced in both mutant lines, indicating that the assembly of the ATP synthase might be defective in *alb4* plants.

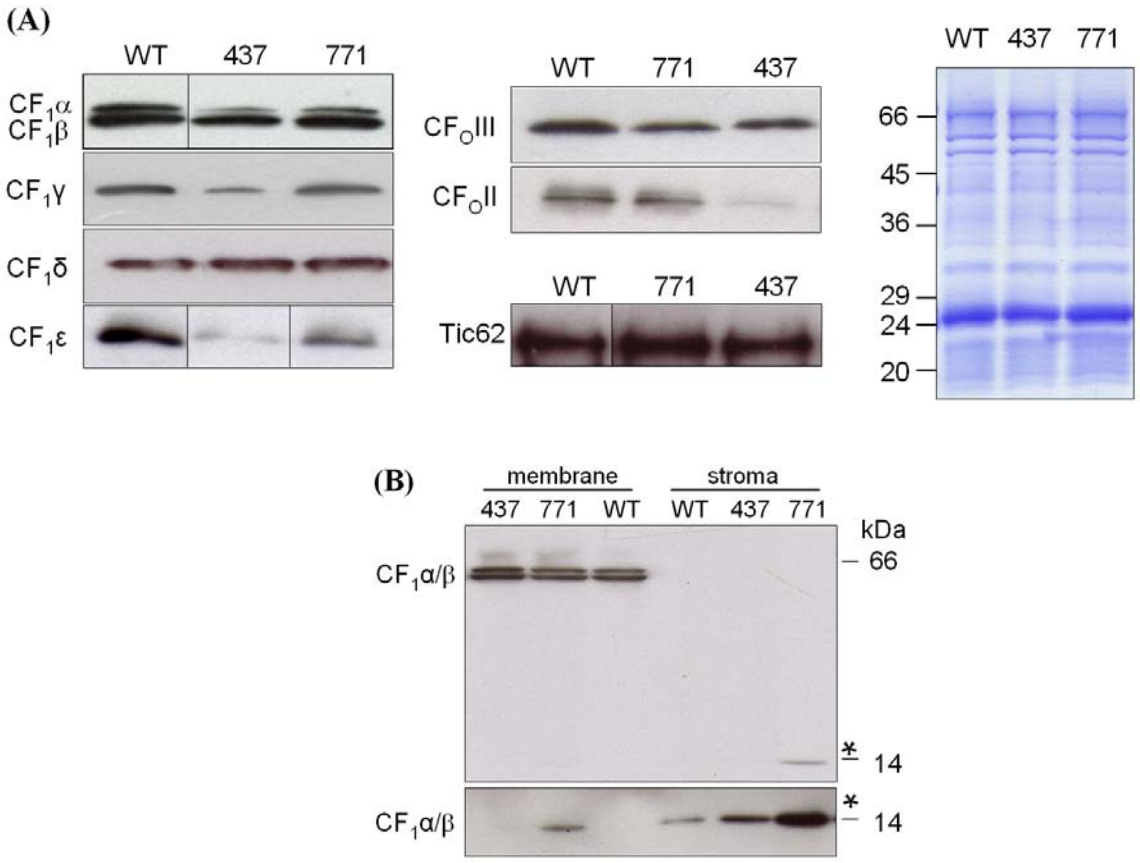

Figure 15. Steady-state levels of ATP synthase subunits are altered in chloroplasts of *alb4* mutants. (A) Chloroplasts were isolated from WT and *alb4* plants grown for three weeks on soil. Samples (10 µg of protein) were fractionated by SDS-PAGE (15% polyacrylamide, 4 M urea), immunoblotted and analyzed with antisera against the indicated subunits of the CF_OCF_1-ATP synthase: subunits of the hydrophilic part $CF_1\alpha/\beta$, $CF_1\gamma$, $CF_1\delta$, and $CF_1\varepsilon$ (left) and membrane-embedded subunits CF_OII, CF_OIII (center). Tic62 antiserum was used as control. As loading control, a Coomassie stained SDS-gel from WT and *alb4* chloroplasts (20 µg of protein) is shown (right). (C) Chloroplasts from WT and *alb4* plants were separated into total membrane and stroma fractions. Membrane (2 µg of Chl) and stroma fractions (16.5 µg of total protein) were fractionated by SDS-PAGE (15% polyacrylamide, 4 M urea), immunoblotted and probed with $CF_1\alpha/\beta$ antiserum. The asterisk (*) indicates a smaller product of $CF_1\alpha/\beta$. The blot in the lower panel is the same as above but was exposed five times longer in order to better visualize the putative degradation products.

6.3.5 The role of Alb4 in the assembly of the ATP synthase

To investigate the effect of decreased levels of some of the ATP synthase subunits on the assembly of the whole complex, isolated chloroplasts from three-week-old WT and both mutant lines (#437 and #771) were solubilized with 1% (w/v) *n*-dodecyl β-D-maltoside, subjected to 2D BN/SDS-PAGE, followed by immunoblot analysis with antisera against $CF_1\alpha$, $CF_1\beta$, $CF_1\gamma$ (head group) and CF_OIII (membrane-embedded complex).

Under the applied conditions, the ATP synthase can be separated into three distinguishable sub-complexes (Choquet and Vallon, 2000). The largest complex migrates at approximately

550 kDa and represents the monomeric form of the ATP synthase, whereas the second complex at approximately 440 kDa corresponds to the assembled CF_1 part (CF_1 complex) of the ATP synthase. Whether the smallest complex, visible at about 140 kDa, contains only free α and β subunits (Drapier et al., 2007) or pre-assembled CF_1 sub-complexes (Choquet and Vallon, 2000) is not entirely clear. As depicted in Figure 16A (row 1), both high molecular weight (HMW) complexes (at 550 and 440 kDa) were visible in the WT. Although the α and β subunits should be present in stoichiomatrical amounts ($\alpha_3\beta_3$), the α-subunit was constantly more abundant than the β-subunit in the smallest complex, which might be a consequence of a higher synthesis rate of $CF_1\alpha$ than $CF_1\beta$ (Drapier et al., 1992). However, less $CF_1\alpha$ was present in the mutant lines as compared to the WT, whereas the overall level of the β-subunit seemed to be increased (Figure 16A), confirming the immunoblot results (Figure 15A). In addition, several intermediate complexes were detected with the $CF_1\alpha/\beta$ antiserum. While in the WT only trace amounts of these intermediates were found, they were more pronounced in the mutant lines (Figure 16A, white arrows).

In the WT control, the same three distinct complexes as for $CF_1\alpha/\beta$ were observed with the antiserum against the $CF_1\gamma$ subunit (Figure 16B). The intermediate complexes, on the other hand, were not visible, indicating that the assembly of $CF_1\gamma$ into CF_1 complexes occurs in a different way than that of the β-subunit. Although all three complexes were detectable in the mutant lines, the overall level of $CF_1\gamma$ was found to be decreased. In line #437, this effect was even more obvious than in the immunoblots (Figure 15A). The observed differences in the ATP synthase complexes were further corroborated with the F_OIII antiserum. In WT thylakoids, the majority of this essential CF_O subunit could be found in the HMW complex at 550 kDa, in addition to several intermediate sub-complexes and low levels in the smallest complex. This is in clear contrast to the *alb4* mutant lines (Figure 16C), in which the CF_OIII subunit was most prominent in the low molecular mass complex. Interestingly, the intermediate forms seemed to be less affected in both mutant lines when compared to the WT. Taken together, it seems that the loss of Alb4 somehow affects the assembly and/or the stability of the ATP synthase, although the formation of the fully assembled complex does occur. In particular the level of the monomeric ATP synthase complex at 550 kDa is reduced, while several assembly intermediates accumulate in the mutants.

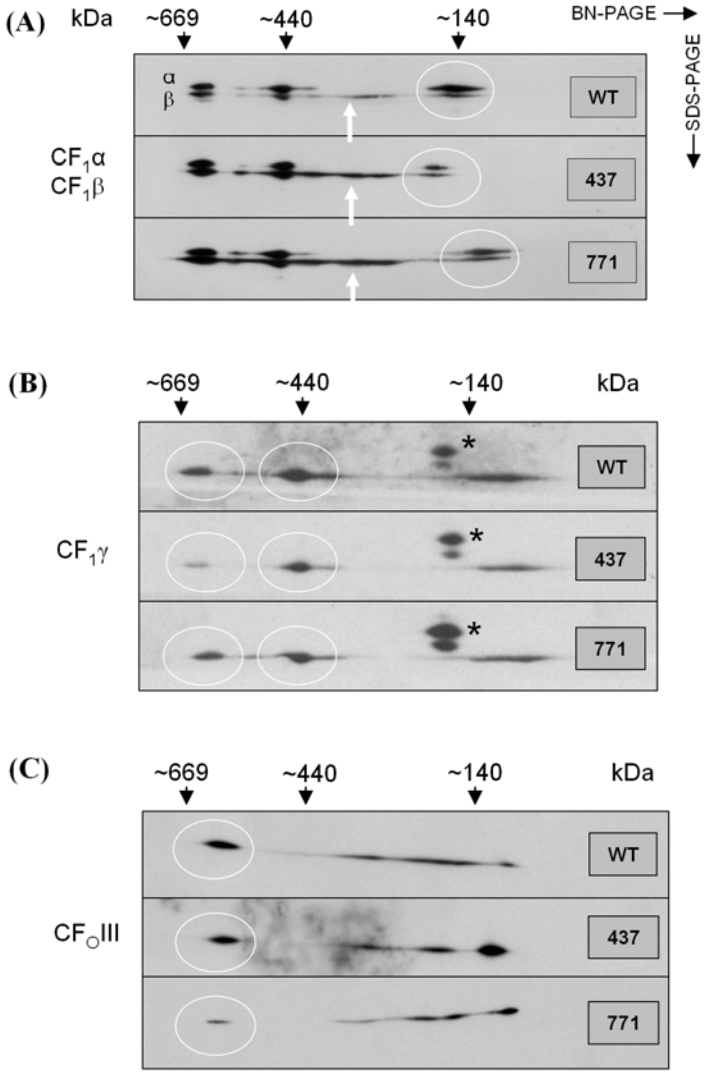

Figure 16. Loss of Alb4 affects the assembly of ATP synthase complexes. Chloroplasts from three-week-old WT and *alb4* mutants (15 µg of Chl) were solubilized with 1% DoMa and fractionated on 5-12% (w/v) BN-PAGE gradient gels. Separated protein complexes were then subjected to SDS-PAGE in a second dimension (15% polyacrylamide, 4 M urea), followed by immunoblot analysis using antisera against ATP synthase subunits of the hydrophilic CF_1 sub-complex $CF_1\alpha/\beta$ (A) and $CF_1\gamma$ (B), or the membrane-embedded CF_OIII subunit. Differences between WT (upper panel) and *alb4* mutants (437, 771) are indicated by white arrows and circles, respectively. The asterisk (*) indicates an unidentified soluble protein complex recognized unspecifically by the $CF_1\gamma$ antiserum, which was used as an internal loading control. Size markers (in kDa) are indicated on top.

6.3.6 Expression of the *atp* genes is not changed in *alb4* plants

Since protein levels of several ATP synthase subunits were found to be decreased in *alb4* mutant lines (see above) the transcription activity of the corresponding *atp* genes was determined to investigate whether this is likewise affected by the loss of Alb4. To this end, total RNA was isolated from rosette leaves harvested from WT and mutant lines that were grown on soil for three weeks and the transcript levels from both nuclear- and plastid-encoded *atp* genes were measured by quantitative real-time PCR. To see whether the mutations in the *alb4* gene have an influence on other chloroplast localized proteins, three additional genes, the *psa*A gene as a representative of the PSI, *psb*A (coding for the D1 protein) as a representative of PSII and *rbc*L (coding for the large subunit of RuBisCO) as a stromal protein were included into this analysis. As summarized in Figure 17, the expression pattern of all mRNAs coding for subunits of the soluble CF_1 part of the ATP synthase (genes *atp*A-E) as well as those coding for subunits of the CF_O part (genes *atp*F-I) were not altered in the *alb4* depletion

lines relative to WT, although overall levels were slightly higher in line #771. Analysis of the *psa*A, *psb*A and *rbc*L transcripts demonstrated that these were also unchanged in the mutants, indicating that loss of Alb4 has no effect on genes coding for PSI, PSII and RuBisCO. In summary, these results suggest that the reduction of the steady-state protein level observed for several ATP synthase subunits in the mutant lines (Figure 17) is not due to regulation at the transcript level, but rather takes place post-transcriptionally.

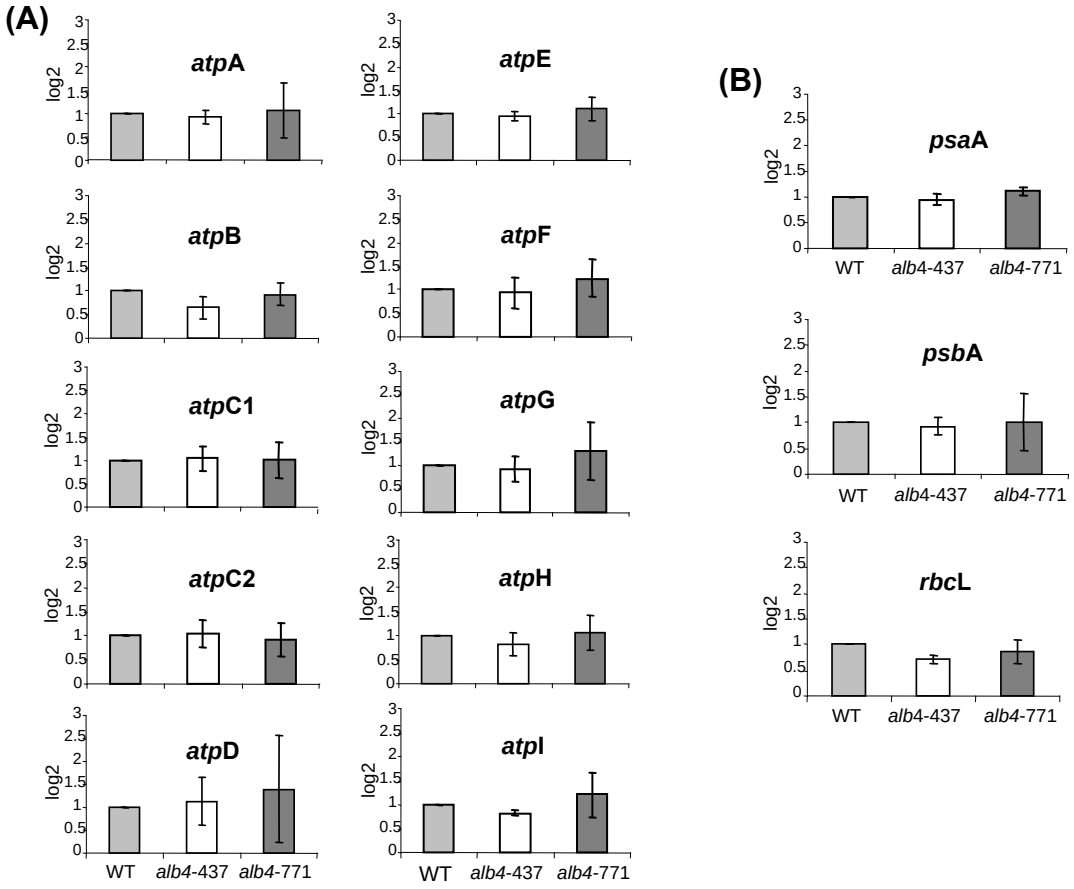

Figure 17. The transcript levels of genes coding for ATP synthase subunits are not affected in the *alb4* mutants. cDNA was synthesized from three-week-old WT and *alb4* mutant lines and analyzed by real-time PCR using appropriate primers. As an internal standard, 18S rRNA was amplified. Each bar represents the mean (±SD) of at least three independent experiments. Expression levels of genes coding for subunits of the hydrophilic CF_1 (*atp*A-E) and the membrane-embedded CF_O part (*atp*F-I) were determined. *atp*A-E encode $CF_1\alpha$, $CF_1\beta$, $CF_1\gamma$ (two isoforms in *Arabidopsis*), $CF_1\delta$, and $CF_1\varepsilon$, respectively; *atp*F-I encode CF_OI, CF_OII, CF_OIII, and CF_OIV, respectively. (B) Expression levels of genes coding for chloroplast-encoded proteins: *psa*A (PsaA, core subunit of PSI), *psb*A (D1, core subunit of PSII) and *rbc*L (LSU, large subunit of RuBisCO).

6.3.7 Sub-thylakoidal localization of Alb4 and ATP synthase

Thylakoid membranes (T) can be sub-fractionated by differential centrifugation into enriched grana thylakoids (10K), intermediate and margin regions (40K), and stroma thylakoids (140K). In addition, a final supernatant (SN) contains loosely attached membrane proteins,

that are readily released during the fractionation. Using this approach, it is possible to analyze the sub-thylakoidal localization of individual proteins and complexes. Alb4 is known to localize to the thylakoid membrane, but whether it is located in the same sub-compartment as the ATP synthase has not been determined yet.

The success of the fractionation can be estimated by separation of the different fractions by SDS-PAGE, followed by either Coomassie staining or immunoblot analysis as well as by determination of the chlorophyll *a:b* ratio, which increases with the enrichment of PSI/LHCI (Figure 18).

The resulting fractions can be furthermore distinguished by characteristic marker proteins that are already visible in the Coomassie-stained gel. PSII super-complexes are known to be enriched in grana thylakoids. Accordingly, components of PSII, such as LHCII and D1/D2, were preferentially found in the 10K fraction, whereas subunits of the PSI complex, as well as the ATP synthase (CF_1 α+β and CF_OI) accumulated in the stroma thylakoid fraction (140K) or, to a lesser extent, in the margins (40K) as shown in Figure 18A.

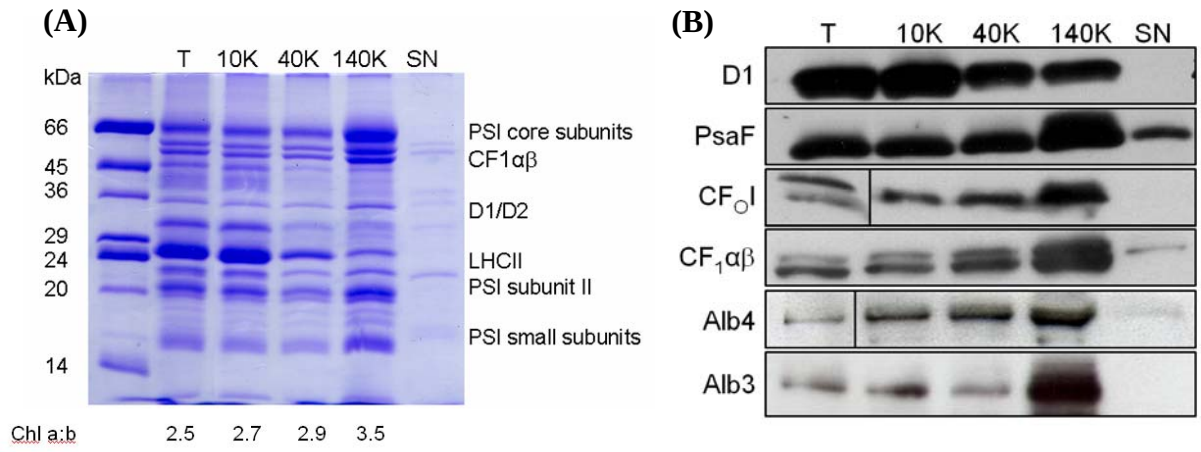

Figure 18. Alb4 and ATP synthase are localized in stroma thylakoids. Isolated thylakoids from three-week-old WT plants were solubilized with 0.1% digitonin and fractionated by centrifugation at 10,000 x g, 40,000 x g and 140,000 x g, respectively, into grana thylakoids (10K), margins (40K) and stroma-lamellae (140K), acc. to Ossenbühl et al. 2002. Thylakoid fractions (5 µg of Chl), and TCA-precipitated soluble proteins (20 µl) were subjected to SDS-PAGE (13% polyacrylamide, 4 M urea) and visualized either by Coomassie staining (A) or by immunoblot analysis (B). (A) Thylakoid proteins visible after Coomassie stain are indicated on the right. The ratio of Chl *a* to Chl *b* is given below of the gel. (B) Immunoblot analysis with antisera specific for Alb4, Alb3, and the ATP synthase subunits CF_OI and $CF_1α/β$. PsaF, a protein of PSI, was used as marker for stroma-lamellae, and PSII core protein D1 as a marker for grana thylakoids. *T*, solubilized thylakoids; *SN*, final supernatant. The sizes of the protein markers are given in kDa on the left.

To analyze the localization of Alb4 and the ATP synthase more precisely, immunoblots of the respective fractions were probed with antisera against Alb4, $CF_1\alpha/\beta$ and CF_OI, together with marker proteins for the grana thylakoids (D1) and the non-appressed stroma thylakoids (PSI subunit PsaF). As expected, D1 was clearly detectable in the 10K fraction, while PsaF was predominantly found in the 140K fraction, corroborating that the sub-fractionation of thylakoid membranes had been successful. ATP synthase subunits were mainly associated with the stroma thylakoids (Figure 18B, panel 3-4), which is in good agreement with published data (Boekema et al., 1999, Aro et al., 2005). Analysis of the distribution of Alb4 revealed a very similar pattern to the ATP synthase, demonstrating that Alb4 co-localizes with this complex in the stroma-lamellae (Figure 18B, panel 5). Smaller amounts of Alb4, ATP synthase subunits and all other analyzed proteins were also detected in the intermediate margin fraction (40K), which is known to contain a mixture of all photosynthetic complexes.
The sub-thylakoidal localization of the Alb3 protein revealed a fractionation pattern resembling that of Alb4 and the ATP synthase (Figure 18B, panel 6).

6.3.8 Alb4 co-migrates with the ATP synthase complex

Since Alb4 and the ATP synthase were found to be located in the same thylakoid sub-compartment, it was investigated whether they are furthermore present in similar complexes.
When thylakoids from three-week-old WT plants were thus analyzed by 2D BN/SDS-PAGE and immunoblotting, Alb4 was mainly found in a complex of approximately 120-140 kDa next to some larger complexes (Figure 19, panel 1). Comparison of these latter complexes with those obtained for the ATP synthase, revealed that the two HMW complexes, corresponding to the monomeric ATP synthase complex at 550 kDa and the CF_1 complex at 440 kDa, are of identical size. These findings suggest that Alb4 co-migrates with $CF_1\alpha$, $CF_1\beta$ and $CF_1\gamma$ (Figure 19, panel 2). Moreover, analysis of CF_OIII revealed that, next to HMW signals, considerable amounts of this subunit were also present in a complex of 120-140 kDa, reminiscent of what was found for Alb4 (Figure 19, panel 3). In summary, these results demonstrate that Alb4 co-migrates with at least four subunits of the ATP synthase in several complexes, indicating that Alb4 might be associated with the ATP synthase complex at several stages of its assembly process.

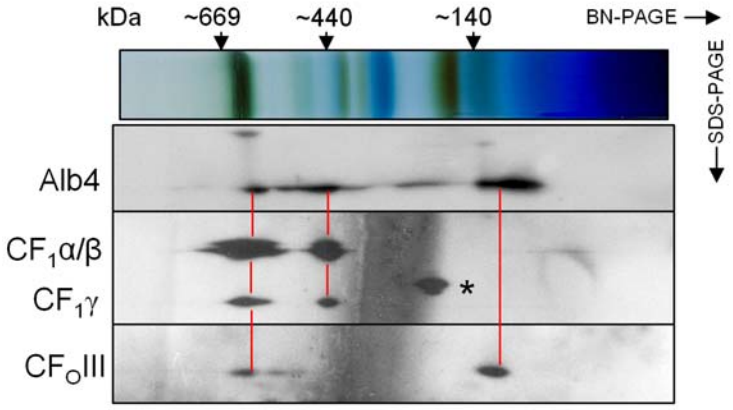

Figure 19. Alb4 co-migrates with the ATP synthase complex. Thylakoids (10 µg of Chl) isolated from leaves of three-week-old WT plants were solubilized with 1% DoMa, fractionated by 2D BN/SDS-PAGE (5-12% polyacrylamide gradient gel in the first dimension and 15% polyacrylamide, 4 M urea in the second dimension), and analyzed by immunoblots using antisera specific for Alb4 and the ATP synthase subunits CF_OIII, $CF_1\alpha/\beta$ and $CF_1\gamma$. The asterisk (*) indicates an unspecific signal obtained with the $CF_1\gamma$ antiserum. Protein size markers (in kDa) are indicated on top.

6.3.9 Loss of Alb4 influences PSII complexes

Reduced levels of PSII components as detected by MALDI-TOF analysis (Table 11) indicated that the PSII complex could be affected in the *alb4* mutant lines. To investigate this in more detail, isolated chloroplasts were subjected to 2D BN/SDS-PAGE as described above, this time using specific antibodies against LHC proteins (Figure 20). In WT and the mutants, complexes corresponding to PSII monomers and dimers were clearly detectable at approx. 370 kDa and 700 kDa, respectively. Strikingly, however, HMW super-complexes were barely detectable in the mutant lines, while they were well visible in the WT. Thus, it seems that Alb4 depletion not only affects the assembly and/or stability of HMW ATP synthase complexes, but also of PSII (super-) complexes.

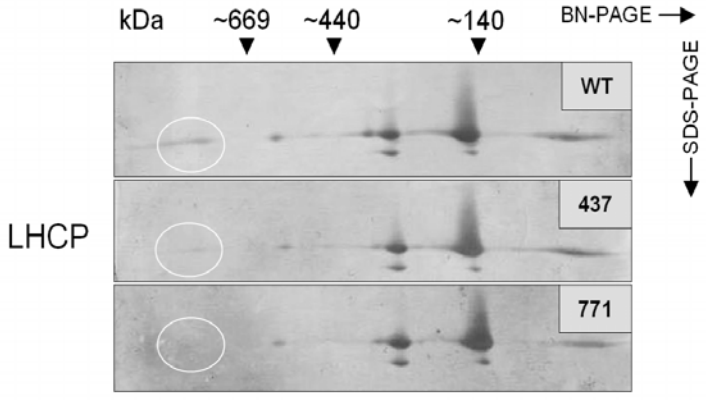

Figure 20. Loss of Alb4 affects the assembly or stability of high molecular weight complexes containing light-harvesting complex proteins. Thylakoids of three-week-old WT and *alb4* plants (4 µg of Chl) were solubilized with 1% DoMa and complexes separated on a 5-12% polyacrylamide BN-PAGE in a first dimension and an SDS-PAGE (15% polyacrylamide, 4 M urea) in a second dimension, followed by immunoblot analysis using antiserum against light-harvesting complex proteins (LHCP). Differences in the high molecular weight complexes between WT and mutants are indicated by white circles. Size markers (in kDa) are indicated on top.

6.3.10 *De novo* synthesis of chloroplast-encoded proteins

Since at least some plastid-encoded thylakoid proteins were found to be less abundant in the *alb4* mutants (Figure 15A), a suitable assay had to be developed to investigate whether Alb4 is involved in the co-translational insertion pathway. The *de novo* synthesis and assembly of thylakoid proteins had been investigated in an *in vitro* system before, using chloroplasts from spinach (*Spinacea oleracea*; Zhang et al., 1999; Rokka et al., 2005) and barley (*Hordeum vulgare* L; Eichacker et al., 1992) To perform these experiments in the *alb4* mutant background, an *Arabidopsis* "*in organello"* translation system was therefore established, adapted from these protocols (see methods, section 5.4.4). Conditions were chosen that allowed the incorporation of [^{35}S]Met not only into the D1 protein (displaying a high turnover rate) but also in other protein subunits of the thylakoid membrane complexes (Mattoo et al., 1984). After translation, both in presence (pulse) and absence (chase) of radiolabeled [^{35}S]Met, the samples were first analyzed in 1D SDS/PAGE gels to reveal whether there are any differences in the pattern of newly synthesized polypeptides between the WT and the mutant chloroplasts. As shown in Figures 21A and 22A, radiolabeling of chloroplast proteins revealed some major signals corresponding most likely to PsaA and PsaB of PSI, $CF_1\alpha$ and $CF_1\beta$ of the ATP synthase and the subunits D1, D2, CP43, and CP47 of PSII. In addition, after 20 min chase a number of transient intermediates were observed (Figure 21A) that vanished after an extension of the chase time to 60 min, with D1 as the most abundant protein synthesized (Figure 22A) However, no consistent differences could be detected when the labeling pattern of WT and mutant lines of several independent approaches were compared, indicating that the loss of Alb4 does not affect the translation of these proteins.

Since the *de novo* synthesis was not affected, it was further tested whether the assembly of labeled proteins into HMW complexes was inhibited in the mutants. To this end, either intact chloroplasts (Figures 21B/C and 22B) or isolated thylakoids (Figure 22C) were solubilized in 1% *n*-dodecyl β-D-maltoside following the *in organello* translation and the newly synthesized proteins analyzed by 1D BN- or 2D BN/SDS-PAGE.

Since the PSII core protein D1 exhibits the highest rate of translation and is rapidly assembled into PSII complexes, mainly radiolabeled PSII was detectable in various assembly intermediates in the first dimension (Figures 21B and 22B) (van Wijk et al., 1995; Rokka et al., 2005). However, the assembly of newly synthesized proteins in higher (PSII) complexes was not impaired in the mutant lines as exemplified by a WT-like labeling pattern.

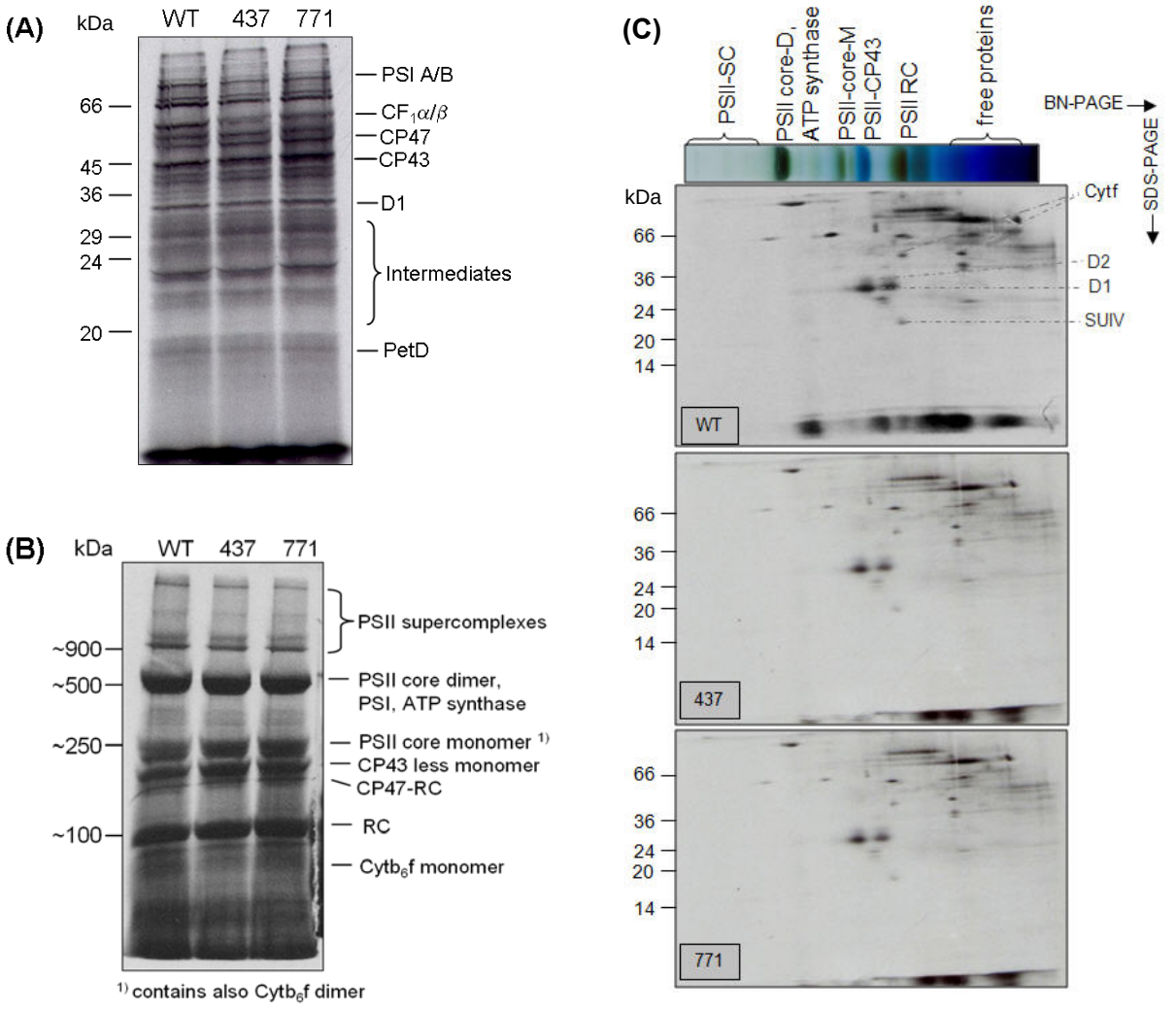

Figure 21. *De novo* synthesis and assembly of thylakoid membrane protein complexes in chloroplasts of *alb4* mutants is not affected (10 min pulse / 20 min chase). Chloroplasts isolated from three-week-old *Arabidopsis* plants were pulse-labeled for 10 min in the presence of [^{35}S]Met followed by a chase of 20 min. (A) Chloroplasts samples (7.5 µg of Chl) were separated by SDS-PAGE and radiolabeled proteins visualized by autoradiography. (B) Chloroplasts (10 µg of Chl) were solubilized with 1% DoMa and newly assembled chloroplast protein complexes separated by BN-PAGE (5-12% polyacrylamide gradient gel) and visualized by autoradiography. Detected complexes are indicated on the right: PSII core dimer co-migrates with PSI and the ATP synthase and the PSII core monomer with the Cytb$_6$f dimer. Sizes of protein markers are given on the left (in kDa). (C) Lanes of a BN-PAGE gel (30 µg of Chl) were subjected to SDS-PAGE (15% polyacylamide, 4 M urea) in a second dimension. Labeled proteins were assigned according to their abundance, apparent molecular weight, as well as to Van Wijk et al. 1995 and Rokka et al. 2005. Identified proteins are designated at the right. Protein size markers are indicated on the left (in kDa). *RC*, reaction center; *M*, monomers; *SC*, super-complexes; *D*, dimers; *T*, trimers.

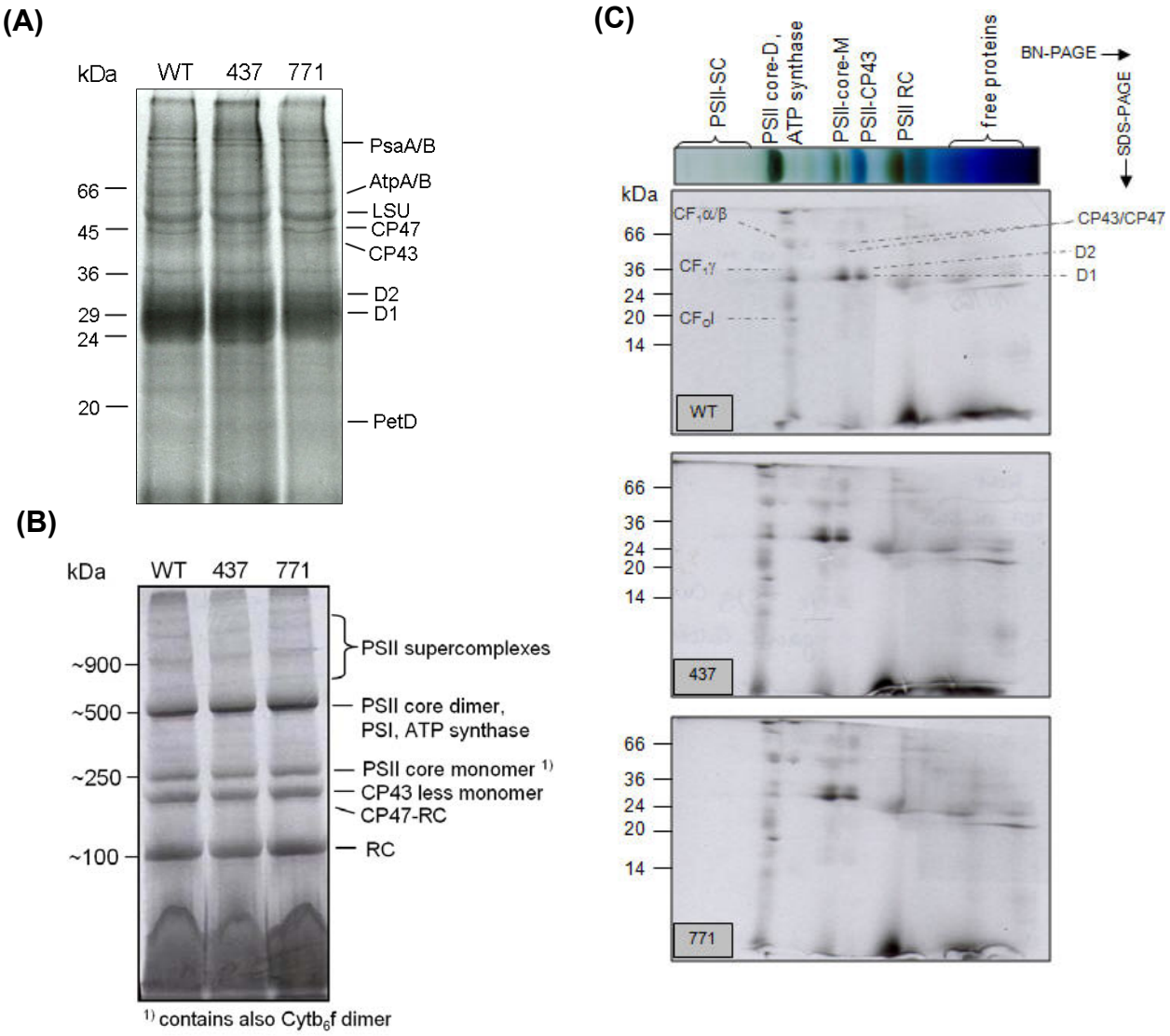

Figure 22. *In organello* translation and assembly of thylakoid membrane protein complexes is not impaired in *alb4* mutants. Experimental procedure was as in Figure 21, except that chloroplasts were pulse-labeled for 10 min followed by a chase of 60 min. (A) SDS-PAGE and autoradiogram of labeled chloroplasts samples (7.5 µg of Chl). (B) BN-PAGE (5-12% polyacrylamide gradient) and autoradiogram of labeled chloroplasts (10 µg of Chl). (C) 1D BN-PAGE gels with separated thylakoids (30 µg of Chl) were subjected to SDS-PAGE (15% polyacylamide, 4 M urea) in the second dimension. For details see Figure 21 and section "methods". *RC*, reaction center; *M*, monomers; *SC*, super-complexes; *D*, dimers; *T*, trimers.

To take a closer look at the newly synthesized and assembled polypeptides in each (sub-) complex, the lanes of the BN-PAGE gel were further subjected to SDS-PAGE in the second dimension. As can be seen in Figures 21C and 22C, the autoradiogram exhibits several distinct signals representing chloroplast-encoded subunits of thylakoid complexes. Besides D1 and D2 in different PSII sub-complexes, the Cyt*f* and subunit (SU) IV proteins were found to be assembled into the $Cytb_6f$ complex at 20 min chase time (Figure 21C). With increasing

chase time, the PSII proteins CP43 and CP47 were labeled. Moreover, several chloroplast-encoded subunits of the ATP synthase ($CF_1\alpha$, $CF_1\beta$, $CF_1\gamma$ and CF_OI) were found to be assembled into the monomeric complex, as well as the Cyt*f* and SUIV proteins into the $Cytb_6f$ complex (Figure 22C). Similar to the first dimensions however, comparison of the autoradiograms of WT and the mutant lines did not reveal any differences.

Taken together, the results from the *in organello* assays indicate that Alb4 presumably is not essential for the translation and assembly at least of chloroplast-encoded thylakoid proteins. However, a more subtle and accessory function cannot be ruled out based on these data. A kinetic analysis of the assembly process might be useful to elucidate this with better resolution in the future.

7 Discussion

7.1 Localization of Alb3/Oxa1/YidC family members in Arabidopsis thaliana

Proteins of the Alb3/Oxa1/YidC family were found in the genomes of every fully sequenced organism (Yen et al., 2001; Luirink et al., 2001). Most prokaryotes contain only one or two homologues (*e.g.* gram positive bacteria like *Bacillus* and *Streptococcus* species), whereas some eukaryotes possess as few as one, but others as many as six or seven such homologues. One such example is the model plant *Arabidopsis thaliana. In silico* analyses showed that at least six members of the Oxa/Alb protein family are expressed in *Arabidopsis* (Yen et al., 2001; Funes et al., 2004a). A legitimate question therefore is whether all these have overlapping functions or are non-redundant like it was shown for other family members (*e.g.* yeast Oxa1 and Oxa2; *Chlamydomonas* Alb3.1 and Alb3.2). A prerequisite to answer this was to define whether they act together in a limited number of compartments, individually in separate locations or at different developmental stages. Moreover, since several annotations of the *Arabidopsis* genome were revised over the last years, a revaluation of the *Arabidopsis* genome for the presence of Oxa/ Alb-like proteins was additionally required.

BLAST searches performed in this study revealed that *Arabidopsis* comprises seven different Oxa homologues (Table 8 and Figure 6). Six of these genes, namely AtOxa1a/1b, AtOxa2a/2b and Alb3/4, had already been identified in the earlier BLAST analyses (Funes et al., 2004a), but for three of them (AtOxa2a, AtOxa2b and Alb4) new gene models and corresponding protein sequences were available, which differed considerably from the former ones. The so-called AtOxa6 protein (At1g44890) on the contrary was identified for the first time. Interestingly, AtOxa6 is still annotated as an unknown protein in the TAIR database, but BLAST analysis revealed that this protein shows weak homology to the AtOxa1a protein and therefore might represent a new and additional member of the Oxa family in *Arabidopsis* (Figure 5; L.Gerdes & J.Soll, personal communication). Furthermore, AtOxa6 is an actively transcribed gene, since expressed sequence tags are reported in the database and the corresponding cDNA sequences have been confirmed by RT-PCR and 5`-RACE experiments (data not shown). Due to these lines of evidence, the Oxa6 protein was included in the localization studies.

Although the genes coding for AtOxa1a/b, AtOxa2a/b, and Alb3/4 are known for some years (Funes et al., 2004a), the sub-cellular localization and function in the cell has been studied experimentally only for three of these. AtOxa1a was demonstrated to be essential for the respiratory complex assembly in *Arabidopsis* (Hamel et al., 1997) and was localized to the

mitochondrial inner membrane (Sakamoto et al., 2000). The other two proteins studied are the close homologues Alb3 and Alb4, which are both localized in the thylakoid membrane of chloroplasts (Sundberg et al., 1997; Gerdes et al., 2006). For all other *Arabidopsis* homologues, only annotations according to databases and *in silico* predictions are available (Table 8 and 9; Figure 6).

As depicted in Figure 6, *in silico* targeting prediction suggests that five of the encoded *Arabidopsis* Oxa homologues are mitochondrial proteins, possessing putative mitochondrial presequences, whereas Alb3 and Alb4 are predicted to be localized in chloroplasts. However, prediction algorithms are not 100% reliable, and the prediction scores for the new gene annotations in some cases differed considerably from those for the old gene models (data not shown). Moreover, in case of AtOxa2b there was some disagreement between a number of the programs, resulting in a relatively high score for chloroplast localization (Table 9). To finally clarify these mentioned uncertainties and substantiate the predictions, it was necessary to confirm the sub-cellular localization of the Oxa homologues experimentally.

Since the sub-cellular targeting of AtOxa1a, Alb3, and Alb4 had already been investigated (Sakamoto et al., 2000; Sundberg et al., 1997; Gerdes et al., 2006), they were included as controls in this study. The employed localization studies clearly favor a mitochondrial targeting for AtOxa1a/b and AtOxa2a/b, both *in vitro* and *in vivo*, whereas Alb3 and Alb4 are directed to chloroplasts, corroborating earlier results (Figures 7, 9 and 10; Gerdes et al., 2006). For all proteins, successful import into the respective organelles and subsequent processing to their mature size could be shown, and also in transgenic plants, the GFP fusion proteins were clearly targeted to either chloroplasts (Albs) or mitochondria (Oxas). However, for the mitochondrial proteins it was necessary to use C-terminally truncated constructs in order to avoid unspecific aggregation in the cytosol, probably due to the high hydrophobicity of the proteins in combination with the artificial overexpression in this system. Moreover, the 5´UTR had to be included in the GFP construct of AtOxa2a to achieve proper targeting. Obviously in this case the canonical presequence is not sufficient and additional information contained in the 5´untranslated region is essential for the process. These might be structural features needed for the post-transcriptional regulation of gene expression, including modulation of the mRNA transport out of the nucleus, translation efficiency, sub-cellular localization and stability (for review see Mignone et al., 2002).

In contrast to the other *Arabidopsis* proteins, AtOxa6 did not display a distinct localization. In dual import experiments for instance, AtOxa6 is imported into both, chloroplasts and mitochondria, but exhibits differential processing in the respective organelles (Figure 8).

About 50 proteins have been shown to be dually targeted so far, the majority possessing the same processing sites in both organelles, but there are also examples which deviate from this rule (for review see Carrie et al., 2009; Pujol et al., 2007). Interestingly, AtOxa6 might even completely lack a recognition site for processing peptidases in mitochondria, since precursor and mature form have a very similar size. The vast majority of mitochondrial matrix proteins and several inner membrane proteins possess cleavable N-terminal targeting signals. In contrast to this, proteins destined for the mitochondrial outer membrane as well as some inner membrane proteins, such as metabolite carrier or preprotein translocases (*e.g.* Tim17 and Tim23), are synthesized with internal targeting signals that do not need to be cleaved (for review see Rapaport, 2003, Becker et al., 2009). Since α-helical membrane proteins are known to be present in the mitochondrial outer membrane, it might be possible that AtOxa6, which has two predicted TM helices (Figure 6), is also targeted to this compartment. However, further import studies are necessary to determine the exact localization of AtOxa6 in the membranes and support this notion.

Although AtOxa6 can be taken up into both organelles *in vitro*, targeting of GFP fusion constructs into *Arabidopsis* protoplasts only results in mitochondrial localization (Figure 10). Generally, GFP tagging has the potential to reveal dual targeting, since GFP can be detected in both organelles, but several factors can interfere with one or the other process as *e.g.* observed for the *Arabidopsis* ascorbate peroxidase or the σ factor of maize (Beardslee et al., 2002; Chew et al., 2003). As discussed above, GFP-tagged proteins are usually expressed at very high levels, promoting the formation of aggregates that can not be targeted properly, as observed for all full-length constructs of the mitochondrial Oxa homologues. To avoid this, often only parts of the proteins of interest can be used, potentially removing essential information contained in the mature sequence. This is exemplified by the alternative NAD(P)H dehydrogenase NDC1, which was found to localize exclusively to mitochondria when the targeting signal of 83 amino acids is used, but is dually targeted in presence of the full-length protein (Carrie et al., 2008). Correspondingly, since only the N-terminal half of AtOxa6 (residues 1-110) was contained in the GFP fusion constructs due to aggregation of the full-length protein, this might provide an explanation for the single targeting of Oxa6. Finally, the membrane topology of the investigated protein is crucial for the successful localization by GFP-fluorescence, because targeting to the thylakoid lumen or the intermembrane space was described to interfere with the proper folding of the GFP, most likely as a consequence of either the acidic environment or the absence of appropriate chaperones (Tsien, 1998). Since the membrane topology and sub-organellar localization of AtOxa6 is not yet known, the

possibility can not be excluded that its C-terminus, and therefore also the GFP, is oriented towards the lumen or the intermembrane space of the plastids. Therefore, the protein could be invisible, although present in the correct compartment. Considering all the factors that might inhibit dual targeting in the *in vivo* localization approach and the fact that mistargeting to chloroplasts has not been observed in *in vitro* dual import experiments (Rudhe et al., 2002), the presented results suggest that AtOxa6 might indeed represent the first dually targeted member of the Oxa family. However, to further substantiate the sub-cellular localization and especially the dual targeting of AtOxa6, immunological assays have to be performed, which have not been possible so far. According to microarray data available in the internet ((http://bbc.botany.utoronto.ca/efp/cgi-bin/efpWeb.cgi) the absolute transcript of all mitochondrial homologues, including AtOxa6, is rather low, indicating that the corresponding proteins might also be low abundant in the plant tissue. Furthermore, they seem to be differentially expressed in the various tissues. Analysis of T-DNA insertion lines for all mitochondrial homologues, as well as immunoblot studies with specific antibodies will shed more light on this family in the future.

The experimental localization of the Oxa homologues resembles the phylogenetic classification into different sub-branches of the Alb3/Oxa1/YidC family. The clustering pattern in phylogenetic trees usually reflects the evolutionary origin of proteins, but in the case of eukaryotes it can additionally indicate the organellar localization. Phylogentic trees generated from alignments of the *Arabidopsis* homologues display two separate clusters (Funes et al., 2004a): one including the highly homologous proteins Alb3 and Alb4, which are present in the chloroplast (Gerdes et al., 2006), and a second one including all other Oxa homologues that were shown to be targeted to the mitochondria. This is likewise represented in an extended phylogenetic analysis using the known Oxa homologues from all sequenced organisms (Yen et al., 2001). In this tree, all eukaryotic forms are found in two primary clusters: the *Arabidopsis* Alb3 and Alb4 proteins are found in a small cluster that branches from the prokaryotic side of the phylogentic tree, whereas the second cluster contains the mitochondrial proteins. Interestingly, this illustrates the fact that the chloroplast homologues Alb3 and Alb4 are more closely related to the bacterial YidC, whereas the mitochondrial *Arabidopsis* homologues can be found in association with the Oxa1 protein from yeast. From these results it was hypothesized that Alb3 and Alb4 are derived from the cyanobacterial ancestor. In contrast to this, the mitochondrial Oxa1 paralogs might have arisen as a result of very early gene duplication events, since the corresponding cluster branches at a distant point

from the center of the prokaryotic tree and includes proteins that are likewise very distant in sequence.

Since the presence of at least four Oxa proteins in the mitochondria of *Arabidopsis* could be established, the question remains whether these perform independent functions or rather act in a redundant fashion. Sequence comparisons might already provide some indications for separate functions. Interestingly, always two *Arabidopsis* proteins are found to be highly similar in terms of size and sequence and thus most likely represent paralogs of each other: just like Alb4 resembles Alb3, AtOxa1a resembles AtOxa1b and AtOxa2a is highly similar to AtOxa2b. Only for AtOxa6 no paralog was found in the *Arabidopsis* genome, but since it exhibits highest homology to AtOxa1a, it probably derived from a duplication and subsequent specialization event of this homologue. Additionally, the Alb3/Oxa1/YidC family can be classified into two groups, according to the structure of their C-terminal parts. In yeast it was shown that Oxa1 and Oxa2 have different functions in protein insertion processes, dependent on the presence of a C-terminal coiled-coil domain: both are involved in post-translational insertion processes, although acting in different steps, but Oxa1 can additionally function in the co-translational pathway, mediated by binding to the large subunit of mitochondrial ribosomes via its C-terminus. In *Arabidopsis*, AtOxa1a and AtOxa1b, as well as Alb3 and Alb4 contain a predicted coiled-coil domain at their C-terminus, reminiscent to the one found in the yeast Oxa1 protein, and therefore belong to the Oxa1 group. In the remaining Oxas, this domain is either missing (AtOxa6) or only weakly predicted (AtOxa2a and AtOxa2b), making them structurally more similar to Oxa2 from yeast (Figure 6).

7.2 The physiological role of Alb4 in Arabidopsis thaliana

In this work, it is reported that the thylakoidal Alb3/Oxa1/YidC homologue Alb4 promotes the assembly and/or stabilization of the CF_1CF_O-ATP synthase complex in *Arabidopsis* chloroplasts. Alb4 was found to localize to the same thylakoidal sub-compartment and to associate with the holo-enzyme. Loss of Alb4 results in retarded growth and defects in the thylakoid ultrastructure. Steady-state levels of several ATP synthase subunits are decreased, as well as the assembly and/or stability of HMW complexes.

7.2.1 Alb4 is necessary for the proper biogenesis of thylakoid membranes

The first member of the Alb3/Oxa1/YidC protein family identified in *Arabidopsis thaliana* was the Alb3 protein (Sundberg et al., 1997). Only recently, Alb4 was described as a second homologue and localized in chloroplasts (Gerdes et al., 2006). Both proteins are expressed in

the green tissue of *Arabidopsis* and are located in the same compartment, the thylakoid membrane. Furthermore, with 72% similarity and 55% identity, Alb3 and Alb4 display a high degree of conservation.

Phenotypic analysis of two independent Alb4 depletion lines revealed a clear but modest growth defect (Figure 12C), which is most pronounced during the first three to four weeks of plant development and when plants are grown under short-day conditions. Long-day conditions help to attenuate this defect, though it is not eliminated entirely.

Moreover, by electron microscopy, a clear phenotype could also be observed on the level of the chloroplast ultrastructure: chloroplasts of *alb4* plants display less organized thylakoid membranes, grana stacks are smaller and more disordered and stroma thylakoids appear slightly swollen (Figure 13). Mutants with a strong reduction of the Alb4 protein level had a similar appearance (Gerdes et al., 2006), although the phenotypes are difficult to compare due to a different WT background: the TILLING mutants used in this work are Col-*er105* and already exhibit a compact growth habit, while the background was Col-0 in the knock-down plants. In addition, primary leaves from three-week-old soil-grown plants were used for electron microscopy here, whereas cotyledons from 10-day-old plants grown on sugar containing medium were used in the previous study (Gerdes et al., 2006). However, the fact that the complete loss of Alb4 did not result in a stronger phenotype than observed in the knock-down plants, implies that the Alb4 protein is not essential for the function of chloroplasts, at least at this stage of development.

Loss of Alb3 in contrast results in a more severe phenotype, since *alb3* seedlings are highly albinotic and not able to grow photoautotrophically (Sundberg et al., 1997). Chloroplasts of *alb3* plants possess severely disorganized thylakoids with hardly any grana stacks, indicating that Alb3 is indispensable for chloroplast development. The visible difference in the extent of the phenotypes indicates that Alb4 is not able to fully compensate for the loss of Alb3. One possible explanation might be that Alb4 has a specialized function in thylakoid biogenesis, whereas Alb3 plays a much more general role that cannot completely be taken over by its close homologue. Alternatively, the protein level of Alb4 might not be sufficient high to fulfill the function(s) of Alb3. Microarray data demonstrate that the absolute content of *ALB3* transcript in all analyzed tissues is much higher than that of *ALB4* (http://bbc.botany.utoronto.ca/efp/cgi-bin/efpWeb.cgi). In addition, both genes are differently expressed in the various tissues. While Alb3 is highly expressed in green leaves, Alb4 reaches its maximum expression level in the very late stages of seed development and dry seeds as well as in senescent leaves, indicating that Alb4 indeed might have specialized functions

during plant development. However, it should be noted that the transcript level of a gene does not necessarily directly correlate with its protein level, since eukaryotes often regulate the protein amount in a post-translational manner. This might be the case for Alb4, since the protein can be detected in all analyzed tissues, although the corresponding gene expression is very low (data not shown). Thus, although Alb4 is obviously not able to fully complement Alb3, it cannot be excluded that the mild phenotype of the Alb4 mutants analyzed in this study is caused by a functional replacement with the highly abundant Alb3 protein (Sundberg et al., 1997, Gerdes et al., 2006). Moreover, the fact that *alb3* plants are still viable to some extend might indicate that at least a small amount of activity remains due to the presence of Alb4. The analysis of double knockout mutants or overexpression lines will help to answer these questions in the future.

A similar situation as in *Arabidopsis* can be found in *Chlamydomonas reinhardtii.* In the thylakoid membrane of this green alga, two Oxa homologues, Alb3.1 and Alb3.2, were identified, which are closely related to Alb3 and Alb4 from *Arabidopsis* (Bellafiore et al., 2002). While the *alb3.1* mutant strain is able to grow photoautotrophically, the Alb3.2 protein from *Chlamydomonas* is essential for survival, suggesting a more general function in the cell (Bellafiore et al., 2002; Göhre et al., 2006). Likewise reminiscent of Alb4 deficient plants, growth of *alb3.1* mutants is significantly reduced under low-light conditions, whereas growth rates reach almost WT levels under standard-light levels. (Bellafiore et al., 2002). Apparently, a certain threshold of light is required for normal growth of both mutants.

Taken together, loss of Alb4 results in a less severe phenotype than observed in *alb3* plants. Nevertheless, thylakoid biogenesis is clearly affected in both mutants, indicating that Alb3 and Alb4 are functionally involved in establishing and maintaining the thylakoid membrane structure.

7.2.2 Alb4 associates with the ATP synthase but not with cpSec

In the present work, several indications were found for a physical association of Alb4 with the CF_1CF_O-ATP synthase complex. First, thylakoid sub-fractionations demonstrate that both localize to the same sub-compartment, the stroma-lamellae (Figure 18). Furthermore, both were found to co-migrate in native PAGE, indicating that they might be part of the same complexes (Figure 19). Since several spots between 120 kDa and 550 kDa displayed a co-migration behavior, some of these might represent assembly intermediates. Stable co-migration of Alb4 and the ATP synthase could be confirmed by gel filtration of solubilized WT thylakoids performed by Thomas Bals in the group of Prof. D. Schünemann. In these experiments, Alb4 was detected to co-elute with the ATP synthase subunits $CF_1\beta$, CF_OII and

CF_OIII (data not shown, personal communication). In further chemical cross-linking studies, Alb4 could be cross-linked to the main CF_1 subunits α and β (Thomas Bals, personal communication), indicating that they are in close physical proximity, possibly directly interacting with each other.

Since the Alb3 protein localizes to the stroma-lamellae as well (Figure 18) (Asakura et al., 2008), it cannot be excluded that it also plays a role in the assembly of the ATP synthase complex. The experiments done by Thomas Bals, however, support the assumption that Alb4 and Alb3 have non-redundant functions in thylakoid biogenesis, since no association of Alb3 with the ATP synthase was detected in both assays. By contrast, the majority of Alb3 co-migrated with complexes containing cpSecY, whereas no interaction with components of the chloroplast Sec machinery could be shown for Alb4. Interestingly, although this had been suggested before, also no interaction was observed between the *Arabidopsis* homologues Alb3 and Alb4 (Thomas Bals, personal communication). This is in contrast to the thylakoidal homologues Alb3.1 and Alb3.2 in *Chlamydomonas* that were shown to interact with each other (Göhre et al., 2006).

7.2.3 The ATP synthase is affected in absence of Alb4

As exemplified by the strong phenotype, Alb3 most likely exerts a more general function in thylakoid biogenesis than Alb4. However, the only established function known for Alb3 to date is the integration of some of the light-harvesting complex proteins (LHCPs) into the thylakoid membrane in a post-translational manner (Moore et al., 2000, Woolhead et al., 2001). In *Chlamydomonas*, all substrates of Alb3.1 and Alb3.2 identified so far belong to the PSI and PSII complexes (Bellafiore et al., 2002; Ossenbühl et al., 2004; Göhre et al., 2006). In contrast, none of the thylakoidal Alb3 homologues has been shown to be involved in the assembly of the $Cytb_6f$ or the CF_1CF_O-ATP synthase complex so far. Analysis of the *alb4* mutants, on the other hand, revealed that the steady-state levels of several CF_1CF_O-ATP synthase subunits are reduced compared to the WT (Figure 15A). In addition, the assembly of the ATP synthase complex seems to be affected (Figure 16), indicating that Alb4 functions in this process.

Therefore, Alb4 seems to be functionally more closely related to the yeast Oxa1 and *E. coli* YidC in this respect, since these two proteins have already been shown to interact with subunits of the ATP synthase. In *E. coli*, YidC is involved in the co-translational insertion of the channel subunit F_Oc, the bacterial CF_OIII homologue, into the inner membrane, which is a critical step in the assembly of the F_1F_O-ATP synthase (van der Laan et al., 2004). Oxa1, on the other hand, was argued to associate with the mitochondrial CF_OIII homologue Atp9, in

order to maintain the competence of assembly intermediates (Atp9-F_1 sub-complexes) for association with further subunits (Jia et al., 2007). These observations emphasize that the function of Alb3/Oxa1/YidC family members is not restricted to the integration of hydrophobic ATP synthase subunits into the membrane, but that they are likewise involved in the formation of the holo-complex. Further examples for these separate functions have been observed in other cases. For the mitochondrial Oxa1 for example, the function as an assembly chaperone for multi-subunit protein complexes (*e.g.* the mitochondrial ATP synthase) seems to be distinct from its translocase activity needed for the insertion of proteins into the membrane (such as the Cox subunits) (Jia et al., 2007). Likewise, YidC is believed to function as both, an integrase for membrane proteins as well as a chaperone for the assembly of membrane protein complexes (for review see Dalbey and Kuhn, 2004). However, that it is difficult to distinguish between these two functions is exemplified by the case of Oxa1: although not the integration but rather the assembly of the ATP synthase is mediated by this protein, loss of Oxa1 nevertheless also results in reduced levels of all three membrane-embedded subunits Atp4 (CF_OI), Atp6 (CF_OIV), and Atp9 (CF_OIII) (Altamura et al., 1996; Szyrach et al., 2003). Also in *alb4* mutants, subunits of both, the membrane-embedded CF_O part as well as the hydrophilic CF_1 part of the ATP synthase complex, were found to be affected. Therefore, although a function for Alb4 in the integration of hydrophobic subunits cannot be excluded, a role in the further assembly and/or stabilization of the complex would be in agreement with the observed molecular phenotype as well.

Furthermore, not only plastid-encoded but also nuclear-encoded subunits are affected upon depletion of Alb4. This has already been reported for the Oxa1 protein, which facilitates membrane insertion processes by interacting in a co-translational manner with the mitochondrial-encoded Cox subunits (Hell et al., 2001), whereas the interaction with Atp9 occurs post-translationally (Jia et al., 2007).

7.2.4 Alb4 is likely to promote the assembly and/or stability of the high molecular weight ATP synthase complexes

Up to date, the assembly process of the chloroplast ATP synthase is still not fully understood (for review see Wollman et al., 1999). CF_OIII is known to pre-assemble into a homo-oligomeric complex of about 120 kDa in the thylakoid membrane (Seelert et al., 2000). By analogy to the bacterial enzyme, it is assumed that the hydrophilic CF_1 part accumulates independently and is then associated to the CF_O oligomers to constitute a functional complex (Klionsky and Simoni, 1985). However, in *alb4* mutants, the pre-assembled 120 kDa complex of the membrane-embedded CF_OIII was found to be present and is even slightly more

abundant than in the WT (Figure 16), indicating that oligomerization of CF_OIII is not impaired.

In contrast to this, the assembly or stability of the CF_1 portion of the enzyme seems to be affected by the loss of Alb4. Whereas three distinct complexes - the ATP synthase monomer, the CF_1 part, and low molecular CF_1 pre-complexes - can be detected in the WT, the fully assembled enzyme seems to be reduced in the mutants. This is exemplified by the diminished amounts of HMW complexes detected for the $CF_1\gamma$ subunit (Figure 16B) as well as for CF_OIII (Figure 16C). Moreover, for CF_OIII and $CF_1\beta$, several additional complexes are detectable in the *alb4* mutants, which probably represent assembly-intermediates (Figure 16A and 16C). The fact that almost no intermediate complexes containing the nuclear-encoded $CF_1\gamma$ subunit are visible implies that the association of $CF_1\gamma$ to pre-assembled ATP synthase complexes occurs at a different stage than that of $CF_1\beta$ and CF_OIII.

Interestingly, further investigation of the main CF_1 subunits revealed that the abundance of the 54 kDa $CF_1\beta$ subunit remains relatively unaffected, whereas the $CF_1\alpha$ subunit is decreased (Figure 15A and 16A). Furthermore, immunoblot analysis of stroma fractions showed the accumulation of a putative degradation product, which might indicate higher turnover rates for one or both of the $CF_1\alpha/\beta$ proteins in *alb4* mutant lines (Figure 15B).

Taken together, Alb4 activity is most likely required downstream of the insertion and oligomerization of the CF_OIII subunit. The higher turnover rate as observed for CF_1 indicates a function for Alb4 in the assembly or stabilisation of the CF_1 complex. It is likely that the CF_1 assembly is abnormally slow or, alternatively, that $CF_1\alpha/\beta$ (sub-) complexes are unstable in absence of Alb4 and therefore a target for degradation. Another possibility is that Alb4 holds pre-assembled complexes in a competent state for the recruitment of additional subunits, such as $CF_1\gamma$ or $CF_1\varepsilon$, which form the connection between the soluble CF_1 and the membrane-embedded CF_O part. It is known that the CF_1 core ($\alpha_3\beta_3$) is stabilized by binding of the $CF_1\gamma$ subunit, which then allows subsequent interaction with the subunit $CF_1\varepsilon$ (Ketchner et al., 1995; Steinemann et al., 1995; Choquet and Vallon, 2000). Furthermore, both subunits, $CF_1\gamma$ and $CF_1\varepsilon$, are reduced in the mutants (Figure 15A), indicating that Alb4 might function as an assembly factor at this stage of ATP synthase biogenesis.

However, although several ATP synthase subunits are reduced in their protein level, fully assembled and most likely enzymatically functional ATP synthase is detectable in the *alb4* mutants. Obviously, this must occur in an Alb4-independent way. This finding is similar to the results reported for yeast mitochondria, where ATP synthase subunits are less abundant in

the absence of Oxa1 - but assembly of functional ATP synthase takes place nevertheless (Jia et al., 2007). In this case, the loss of Oxa1 in yeast mitochondria does not abolish the formation of homo-oligomers of the CF_OIII homologue Atp9. Moreover, Atp9 oligomers are still able to interact with the F_1 part and form stable intermediate ATP synthase complexes. As mentioned above, only the competence of the Atp9-F_1 sub-complex for subsequent addition of Atp6 is then impaired in absence of Oxa1 (Jia et al., 2007). Thus, the assembly steps downstream of the attachment of the head-group (F_1) to the membrane-embedded sub-complex (F_O), which involve the insertion of later assembly partners like Atp6 in mitochondria or $CF_1\gamma$ in chloroplasts, seem to be similarly dependent on Oxa1 and Alb4.
However, although it is possible that Alb4 and Oxa1 have similar functions in ATP synthase biogenesis, it is noteworthy that Oxa1 has so far only been shown to bind to subunits of the membrane-embedded F_O part, whereas Alb4 could be cross-linked to the $CF_1\alpha/\beta$ subunits of the head-group. It is thus more likely that Alb4 participates either in the stabilisation of CF_1 or in the assembly of CF_1 to CF_O, or both.

7.2.5 Loss of Alb4 results in reduced PSII super-complexes

The results presented in this work strongly indicate that Alb4 is involved in the assembly and/or stabilization of the CF_1CF_O-ATP synthase, one of the four major protein complexes in the thylakoid membrane. However, in addition to components of the ATP synthase, mass spectrometric analysis identified subunits of PSII as well as light-harvesting chlorophyll proteins (LHCPs) to be reduced in the *alb4* mutants (Figure 14 and Table 11). Although the *alb4* phenotype does not directly indicate a defect in photosynthesis, analysis of LHCP complexes revealed a decrease of HMW complexes, most likely corresponding to the PSII-LHCII super-complexes (Figure 20).
Besides the possibility of Alb4 being involved in the assembly or stability of these PSII complexes, it is feasible that this molecular phenotype might be an indirect result of a proton "back-pressure", due to the reduced abundance of ATP synthase in the thylakoid membrane. During photosynthesis protons are accumulated in the thylakoid lumen, thereby creating a transmembrane electrochemical proton gradient. Generally, the CF_1CF_O-ATP synthase uses this gradient for the synthesis of ATP, and in this process, the protons are transferred into the stroma. The reduced levels of ATP synthase in the *alb4* mutants therefore might result in proton stress, since the transmembrane proton gradient is only inefficiently relieved, which in turn could affect the formation or stability of other thylakoidal complexes.
This notion is supported by the swollen appearance of thylakoids in *alb4* mutant chloroplasts (Figure 13). Interestingly, mutants defective in the plastidic ATP synthase were described to

likewise possess disorganized thylakoid membranes with a swollen luminal space (Bosco et al., 2004; Majeran et al., 2001). This phenotype was argued to be caused by a light-dependent high proton gradient across the thylakoid membrane, resulting in an increased influx of osmotically active ions. Moreover, the ATP synthase mutants exhibit altered PSII activity and stability and, as a consequence, are highly sensitive to light. Thus, the reduction of ATP synthase due to the loss of Alb4 might also explain the observed decreased stability of PSII-LHCII complexes.

Since it is known that different kinds of stresses affect especially PSII, most likely by inducing D1 turnover, it is possible that the proton "back-pressure" has similar effects. During D1 repair, PSII super-complexes are thought to disassemble to allow the replacement of the damaged D1 protein. A higher rate of assembly and disassembly might therefore be a reason for the decreased amount of HMW super-complexes detected in the *alb4* mutants. In 2D BN/SDS-PAGE of mutant thylakoids, some preliminary indications for a higher D1 turnover could be found (data not shown). However, further experiments are needed to confirm these observations.

Mass spectrometric analysis indicated a reduction of CP24 (Lhcb6) and Lhcb4.1 in the *alb4* mutants (Figure 14, Table 11). Assembled CP24 represents a core pigment sub-complex of the peripheral antenna complex LHCII (for review see Green and Durnford, 1996). Interestingly, plants deficient in CP24 are smaller than the WT and show major changes in the macro-organization of PSII, but have no differences in the pigment or protein content of thylakoids (Kovacs et al., 2006), reminiscent to the phenotype observed by the loss of Alb4. It might therefore be possible that the reduction of PSII super-complexes detected in the Alb4 mutants is a result of reduced CP24. Nevertheless, it can not be excluded that Alb4 is directly involved in the assembly or stabilization of PSII or even has a special role in the addition of LHC proteins to pre-assembled photosystems.

A direct involvement in the assembly of photosystems was already demonstrated for the two Alb3 homologues in *Chlamydomonas* . Alb3.2 seems to be essential for the assembly and/or maintenance of the photosystems at the level of photosystem core proteins, whereas Alb3.1 is mainly involved in the assembly of LHCPs (Bellafiore et al., 2002; Ossenbühl et al., 2004; Göhre et al., 2006). Similar to Alb3.1, *Arabidopsis* Alb3 mediates the integration of LHC proteins. However, small quantities of LHCPs appear to be inserted into the thylakoid membranes even in absence of Alb3. Nothing is known about this alternative pathway so far. It is possible that these LHCPs integrate spontaneously or via the chloroplast Sec pathway,

but it is also thinkable that Alb4 might be involved in the integration of residual LHCPs (Gerdes et al., 2006; Asakura et al., 2008).

Therefore, although PSII subunits are clearly affected in the *alb4* mutants, further studies are necessary to clarify whether this is a direct effect of the loss of Alb4 protein or an indirect effect due to accumulating protons in the thylakoid lumen.

7.2.6 Alb4 is a functional member of the Alb3/Oxa1/YidC family

As mentioned above, Oxa1 from yeast and YidC from *E. coli* act as insertases as well as assembly chaperones in the biogenesis of membrane proteins. The analysis of the *alb4* phenotype, however, is in better agreement with a role for Alb4 as an assembly or stabilization factor than as an insertase, even though this latter function cannot be excluded based on the present data. However, by complementation analyses, at least some indications could be collected, demonstrating that Alb4 has maintained the ability to act as an insertase, and thus represents a fully functional member of the Alb3/Oxa1/YidC family (Funes et al., 2004a; Prof. A. Kuhn, personal communication). First, expression of a chimeric Alb4 protein, containing a mitochondrial targeting sequence and the conserved transmembrane region of Alb4, was found to partially substitute for Oxa1 in yeast mitochondria (Funes et al., 2004a). Additionally, in recent experiments in which an *E. coli* YidC depletion strain was transformed with a full-length *ALB4* cDNA, cell growth was restored to nearly WT levels (data not shown; Prof. A. Kuhn, personal communication).

Successful complementation among the Alb3/Oxa1/YidC family has been demonstrated in several independent studies (Jiang et al., 2002; Funes et al., 2004ab; van Bloois et al., 2005; Preuss et al., 2005). The mitochondrial homologue Oxa1 for example was shown to substitute for YidC in *E. coli* (van Bloois et al., 2005), and in return, *E. coli* YidC variants can replace Oxa1 and Oxa2 in yeast mitochondria (Preuss et al., 2005), indicating a high degree of functional conservation between the diverse members of this family. Nevertheless, in these studies, also a major difference between the two close homologues Alb3 and Alb4 could be revealed. While complementation of the *yidC* phenotype with *ALB4* cDNA is possible (Prof. A. Kuhn, personal communication), complementation fails in case the full-length *ALB3* cDNA gene is used (Jiang et al., 2002). Only when the N-terminal region of Alb3 is replaced by the first 57 amino acids of the YidC sequence, successful complementation is achieved (Jiang et al., 2002), indicating a problem in the correct targeting of Alb3 in the host organism. This discrepancy in the complementation behavior between Alb3 and Alb4 is quite surprising, since both proteins are highly similar in terms of amino acid sequence and membrane topology. The main differences can be found in the N-terminal transit peptides and especially

at the C-terminus, which is longer in the Alb4 protein (Gerdes et al., 2006). Interestingly in this respect is that *E. coli* cells expressing a truncated Alb4 protein lacking the C-terminal region, fail to grow under the same conditions as the full-length cDNA construct (Prof. A. Kuhn, personal communication). Obviously, the C-terminal segment of Alb4 is important for functional substitution of YidC. If, and moreover how, this extended C-terminal sequence might be responsible for the functional difference between Alb3 and Alb4, remains to be investigated in the future.

7.2.7 *De novo* synthesis and assembly of chloroplast-encoded proteins is not impaired by loss of Alb4

The complementation experiments already indicated that Alb4 can partially take over the function of other family members and therefore has the capacity to function as an integrase for membrane proteins, at least in the heterologeous systems. However, from these results it cannot be directly concluded that Alb4 also functions in the insertion of membrane proteins into the thylakoid membrane *in planta.*

Oxa1 in yeast and YidC in bacteria are known to be involved in both, the co- and post-translational insertion of membrane proteins (He and Fox, 1997; Hell et al., 1998; Hell et al., 2001). The same has been proposed for the thylakoidal Alb3 protein in several studies (Moore et al., 2000; Woolhead et al., 2001; Klostermann et al., 2002). Furthermore, the C-terminus of Alb4 is predicted to possess a coiled-coil structure similar to the ribosome binding domain of Oxa1 (Preuss et al., 2005). Although it has not been demonstrated so far, it was possible that Alb4 might be able to bind to ribosomes and thereby promotes the co-translational insertion of membrane proteins. This hypothesis was tested in a newly established *Arabidopsis* "*in organello"* translation system, in which the effect of Alb4 depletion on *de novo* synthesis, thylakoid insertion and assembly of chloroplast-encoded proteins was investigated (Figures 21 and 22). However, the results of the *in organello* translation did not reveal any specific defect in the production, integration or assembly of the photosynthetic complexes, in contrast to the steady-state results (Figure 15). This finding indicates that the co-translational insertion and assembly of chloroplast-encoded thylakoid proteins does not strictly depend on the function of Alb4. Thus, its function might be limited to the post-translational pathway or to the stabilization of fully assembled complexes composed of both nuclear- and plastid-encoded subunits, which could however not be resolved in this approach. Alternatively, since the overall signal intensity was still sub-optimal, minor differences that could accumulate to a more severe phenotype in the steady-state situation, might not have been visible under the conditions applied.

In summary, the results obtained in this work demonstrate that Alb4 plays a role in the biogenesis of thylakoids. Although it cannot be explicitly excluded that Alb4 functions as an integrase or assembly factor in the thylakoids, there are several indications that Alb4 is rather required for the stabilization of the high molecular weight CF_1CF_O-ATP synthase complexes and possibly also of PSII super-complexes.

References

Aldridge C, Cain P, Robinson C (2009) Protein transport in organelles: Protein transport into and across the thylakoid membrane. *FEBS J* 276: 1177-1186

Altamura N, Capitanio N, Bonnefoy N, Papa S, Dujardin G (1996) The *Saccharomyces cerevisiae* OXA1 gene is required for the correct assembly of cytochrome c oxidase and oligomycin-sensitive ATP synthase. *FEBS Lett* 382: 111-115

Altschul SF, Gish W, Miller W, Myers EW, Lipman DJ (1990) Basic local alignment search tool. *J Mol Biol* 215: 403-410

Altschul SF, Koonin EV (1998) Iterated profile searches with PSI-BLAST--a tool for discovery in protein databases. *Trends Biochem Sci* 23: 444-447

Arnon DJ (1949) Copper enzymes in isolated chloroplasts. Polyphenoloxidase in *Beta vulgaris*. *Plant Physiol* 24: 42-45

Aro EM, Suorsa M, Rokka A, Allahverdiyeva Y, Paakkarinen V, Saleem A, Battchikova N, Rintamaki E (2005) Dynamics of photosystem II: a proteomic approach to thylakoid protein complexes. *J Exp Bot* 56: 347-356

Aronsson H, Jarvis P (2002) A simple method for isolating import-competent Arabidopsis chloroplasts. *FEBS Lett* 529: 215-220

Asakura Y, Kikuchi S, Nakai M (2008) Non-identical contributions of two membrane-bound cpSRP components, cpFtsY and Alb3, to thylakoid biogenesis. *Plant J* 56: 1007-1017

Bauer M, Behrens M, Esser K, Michaelis G, Pratje E (1994) PET1402, a nuclear gene required for proteolytic processing of cytochrome oxidase subunit 2 in yeast. *Mol Gen Genet* 245: 272-278

Beardslee TA, Roy-Chowdhury S, Jaiswal P, Buhot L, Lerbs-Mache S, Stern DB, Allison LA (2002) A nuclear-encoded maize protein with sigma factor activity accumulates in mitochondria and chloroplasts. *Plant J* 31: 199-209

Beck K, Eisner G, Trescher D, Dalbey RE, Brunner J, Muller M (2001) YidC, an assembly site for polytopic Escherichia coli membrane proteins located in immediate proximity to the SecYE translocon and lipids. *EMBO Rep* 2: 709-714

Becker T, Gebert M, Pfanner N, van der Laan LM (2009) Biogenesis of mitochondrial membrane proteins. *Curr Opin Cell Biol*

Bellafiore S, Ferris P, Naver H, Göhre V, Rochaix JD (2002) Loss of albino3 leads to the specific depletion of the light-harvesting system. *Plant Cell* 14: 2303-2314

Ben Shem A, Frolow F, Nelson N (2003) Crystal structure of plant photosystem I. *Nature* 426: 630-635

Blum H, Beier H, Gross HJ (1987) Improved Silver Staining of Plant-Proteins, RNA and DNA in Polyacrylamide Gels. *Electrophoresis* 8: 93-99

Boekema EJ, van Roon H, van Breemen JF, Dekker JP (1999) Supramolecular organization of photosystem II and its light-harvesting antenna in partially solubilized photosystem II membranes. *Eur J Biochem* 266: 444-452

Bonnefoy N, Chalvet F, Hamel P, Slonimski PP, Dujardin G (1994) OXA1, a *Saccharomyces cerevisiae* nuclear gene whose sequence is conserved from prokaryotes to eukaryotes controls cytochrome oxidase biogenesis. *J Mol Biol* 239: 201-212

Bosco CD, Lezhneva L, Biehl A, Leister D, Strotmann H, Wanner G, Meurer J (2004) Inactivation of the chloroplast ATP synthase gamma subunit results in high non-photochemical fluorescence quenching and altered nuclear gene expression in Arabidopsis thaliana. *J Biol Chem* 279: 1060-1069

Britt RD (1996) Oxygen evolution. Oxygenic photosynthesis: the light reactions. Kluwer Academic Publishers, Dordrecht, The Netherlands,

Carrie C, Giraud E, Whelan J (2009) Protein transport in organelles: Dual targeting of proteins to mitochondria and chloroplasts. *FEBS J* 276: 1187-1195

Carrie C, Murcha MW, Kuehn K, Duncan O, Barthet M, Smith PM, Eubel H, Meyer E, Day DA, Millar AH, Whelan J (2008) Type II NAD(P)H dehydrogenases are targeted to mitochondria and chloroplasts or peroxisomes in Arabidopsis thaliana. *FEBS Lett* 582: 3073-3079

Chen M, Samuelson JC, Jiang F, Muller M, Kuhn A, Dalbey RE (2002) Direct interaction of YidC with the Sec-independent Pf3 coat protein during its membrane protein insertion. *J Biol Chem* 277: 7670-7675

Chew O, Whelan J, Millar AH (2003) Molecular definition of the ascorbate-glutathione cycle in Arabidopsis mitochondria reveals dual targeting of antioxidant defenses in plants. *J Biol Chem* 278: 46869-46877

Choquet Y, Vallon O (2000) Synthesis, assembly and degradation of thylakoid membrane proteins. *Biochimie* 82: 615-634

Clark SA, Theg SM (1997) A folded protein can be transported across the chloroplast envelope and thylakoid membranes. *Mol Biol Cell* 8: 923-934

Cline K, Ettinger WF, Theg SM (1992) Protein-specific energy requirements for protein transport across or into thylakoid membranes. Two lumenal proteins are transported in the absence of ATP. *J Biol Chem* 267: 2688-2696

D'Andrea LD, Regan L (2003) TPR proteins: the versatile helix. *Trends Biochem Sci* 28: 655-662

Dalbey RE, Kuhn A (2000) Evolutionarily related insertion pathways of bacterial, mitochondrial, and thylakoid membrane proteins. *Annu Rev Cell Dev Biol* 16: 51-87

Dalbey RE, Kuhn A (2004) YidC family members are involved in the membrane insertion, lateral integration, folding, and assembly of membrane proteins. *J Cell Biol* 166: 769-774

Di Cola A, Klostermann E, Robinson C (2005) The complexity of pathways for protein import into thylakoids: it's not easy being green. *Biochem Soc Trans* 33: 1024-1027

Douwe dB, Weisbeek PJ (1991) Chloroplast protein topogenesis: import, sorting and assembly. *Biochim Biophys Acta* 1071: 221-253

Drapier D, Girard-Bascou J, Wollman FA (1992) Evidence for Nuclear Control of the Expression of the atpA and atpB Chloroplast Genes in Chlamydomonas. *Plant Cell* 4: 283-295

Drapier D, Rimbault B, Vallon O, Wollman FA, Choquet Y (2007) Intertwined translational regulations set uneven stoichiometry of chloroplast ATP synthase subunits. *EMBO J* 26: 3581-3591

Dyall SD, Brown MT, Johnson PJ (2004) Ancient invasions: from endosymbionts to organelles. *Science* 304: 253-257

Eichacker L, Paulsen H, Rudiger W (1992) Synthesis of chlorophyll a regulates translation of chlorophyll a apoproteins P700, CP47, CP43 and D2 in barley etioplasts. *Eur J Biochem* 205: 17-24

Firlej-Kwoka E, Strittmatter P, Soll J, Bolter B (2008) Import of preproteins into the chloroplast inner envelope membrane. *Plant Molecular Biology* 68: 505-519

Franklin AE, Hoffman NE (1993) Characterization of a chloroplast homologue of the 54-kDa subunit of the signal recognition particle. *J Biol Chem* 268: 22175-22180

Fulgosi H, Gerdes L, Westphal S, Glockmann C, Soll J (2002) Cell and chloroplast division requires ARTEMIS. *Proc Natl Acad Sci U S A* 99: 11501-11506

Funes S, Gerdes L, Inaba M, Soll J, Herrmann JM (2004a) The *Arabidopsis thaliana* chloroplast inner envelope protein ARTEMIS is a functional member of the Alb3/Oxa1/YidC family of proteins. *FEBS Lett* 569: 89-93

Funes S, Hasona A, Bauerschmitt H, Grubbauer C, Kauff F, Collins R, Crowley PJ, Palmer SR, Brady LJ, Herrmann JM (2009) Independent gene duplications of the YidC/Oxa/Alb3 family enabled a specialized cotranslational function. *Proc Natl Acad Sci U S A* 106: 6656-6661

Funes S, Nargang FE, Neupert W, Herrmann JM (2004b) The Oxa2 protein of *Neurospora crassa* plays a critical role in the biogenesis of cytochrome oxidase and defines a ubiquitous subbranch of the Oxa1/YidC/Alb3 protein family. *Mol Biol Cell* 15: 1853-1861

Gasteiger E, Gattiker A, Hoogland C, Ivanyi I, Appel RD, Bairoch A (2003) ExPASy: the proteomics server for in-depth protein knowledge and analysis. *Nucleic Acids Research* 31: 3784-3788

Gathmann S, Ruprecht E, Kahmann U, Schneider D (2008) A conserved structure and function of the YidC homologous protein Slr1471 from Synechocystis sp. PCC 6803. *Journal of microbiology and biotechnology* 18: 1090-1094

Geller BL, Wickner W (1985) M13 procoat inserts into liposomes in the absence of other membrane proteins. *J Biol Chem* 260: 13281-13285

Gerdes L, Bals T, Klostermann E, Karl M, Philippar K, Hunken M, Soll J, Schunemann D (2006) A second thylakoid membrane-localized Alb3/OxaI/YidC homologue is involved in proper chloroplast biogenesis in Arabidopsis thaliana. *J Biol Chem* 281: 16632-16642

Göhre V, Ossenbühl F, Crèvecoeur M, Eichacker LA, Rochaix JD (2006) One of Two Alb3 Proteins Is Essential for the Assembly of the Photosystems and for Cell Survival in *Chlamydomonas*. *Plant Cell*

Goussias C, Boussac A, Rutherford AW (2002) Photosystem II and photosynthetic oxidation of water: an overview. *Philos Trans R Soc Lond B Biol Sci* 357: 1369-1381

Gray MW, Burger G, Lang BF (1999) Mitochondrial evolution. *Science* 283: 1476-1481

Green BR, Durnford DG (1996) The chlorophyll-carotenoid proteins of oxygenic photosynthesis. *Annu Rev Plant Physiol Plant Mol Biol* 47: 685-714

Groth G, Pohl E (2001) The structure of the chloroplast F1-ATPase at 3.2 A resolution. *Journal of Biological Chemistry* 276: 1345-1352

Hamel P, Sakamoto W, Wintz H, Dujardin G (1997) Functional complementation of an oxa1- yeast mutation identifies an *Arabidopsis thaliana* cDNA involved in the assembly of respiratory complexes. *Plant J* 12: 1319-1327

Hanahan D (1983) Studies on transformation of *Escherichia coli* with plasmids. *J Mol Biol* 166: 557-580

He S, Fox TD (1997) Membrane translocation of mitochondrially coded Cox2p: distinct requirements for export of N and C termini and dependence on the conserved protein Oxa1p. *Mol Biol Cell* 8: 1449-1460

Hell K, Herrmann J, Pratje E, Neupert W, Stuart RA (1997) Oxa1p mediates the export of the N- and C-termini of pCoxII from the mitochondrial matrix to the intermembrane space. *FEBS Lett* 418: 367-370

Hell K, Herrmann JM, Pratje E, Neupert W, Stuart RA (1998) Oxa1p, an essential component of the N-tail protein export machinery in mitochondria. *Proc Natl Acad Sci U S A* 95: 2250-2255

Hell K, Neupert W, Stuart RA (2001) Oxa1p acts as a general membrane insertion machinery for proteins encoded by mitochondrial DNA. *EMBO J* 20: 1281-1288

Herrmann JM, Neupert W, Stuart RA (1997) Insertion into the mitochondrial inner membrane of a polytopic protein, the nuclear-encoded Oxa1p. *EMBO J* 16: 2217-2226

Herskovits AA, Bochkareva ES, Bibi E (2000) New prospects in studying the bacterial signal recognition particle pathway. *Mol Microbiol* 38: 927-939

Higgins DG, Sharp PM (1988) CLUSTAL: a package for performing multiple sequence alignment on a microcomputer. *Gene* 73: 237-244

Higgins DG, Sharp PM (1989) Fast and sensitive multiple sequence alignments on a microcomputer. *Comput Appl Biosci* 5: 151-153

Hulford A, Hazell L, Mould RM, Robinson C (1994) Two distinct mechanisms for the translocation of proteins across the thylakoid membrane, one requiring the presence of a stromal protein factor and nucleotide triphosphates. *J Biol Chem* 269: 3251-3256

Hynds PJ, Robinson D, Robinson C (1998) The sec-independent twin-arginine translocation system can transport both tightly folded and malfolded proteins across the thylakoid membrane. *J Biol Chem* 273: 34868-34874

Jarvis P, Robinson C (2004) Mechanisms of protein import and routing in chloroplasts. *Curr Biol* 14: R1064-R1077

Jeanmougin F, Thompson JD, Gouy M, Higgins DG, Gibson TJ (1998) Multiple sequence alignment with Clustal X. *Trends Biochem Sci* 23: 403-405

Jia L, Dienhart M, Schramp M, McCauley M, Hell K, Stuart RA (2003) Yeast Oxa1 interacts with mitochondrial ribosomes: the importance of the C-terminal region of Oxa1. *EMBO J* 22: 6438-6447

Jia L, Dienhart MK, Stuart RA (2007) Oxa1 directly interacts with Atp9 and mediates its assembly into the mitochondrial F1Fo-ATP synthase complex. *Mol Biol Cell* 18: 1897-1908

Jiang F, Yi L, Moore M, Chen M, Rohl T, van Wijk KJ, de Gier JW, Henry R, Dalbey RE (2002) Chloroplast YidC homolog Albino3 can functionally complement the bacterial YidC depletion strain and promote membrane insertion of both bacterial and chloroplast thylakoid proteins. *J Biol Chem* 277: 19281-19288

Keegstra K, Cline K (1999) Protein import and routing systems of chloroplasts. *Plant Cell* 11: 557-570

Keegstra K, Youssif AE (1986) Isolation and characterization of chloroplast envelope membranes. In A Weissbach, H Weissbach, eds, Methods Enzymology - Plant Molecular Biology, Vol 118. Academic Press, USA, pp 316-325

Kermorgant M, Bonnefoy N, Dujardin G (1997) Oxa1p, which is required for cytochrome c oxidase and ATP synthase complex formation, is embedded in the mitochondrial inner membrane. *Curr Genet* 31: 302-307

Ketchner SL, Drapier D, Olive J, Gaudriault S, Girard-Bascou J, Wollman FA (1995) Chloroplasts can accommodate inclusion bodies. Evidence from a mutant of Chlamydomonas reinhardtii defective in the assembly of the chloroplast ATP synthase. *J Biol Chem* 270: 15299-15306

Klionsky DJ, Simoni RD (1985) Assembly of a functional F1 of the proton-translocating ATPase of Escherichia coli. *J Biol Chem* 260: 11200-11206

Klostermann E, Droste GH, I, Carde JP, Schünemann D (2002) The thylakoid membrane protein ALB3 associates with the cpSecY-translocase in *Arabidopsis thaliana*. *Biochem J* 368: 777-781

Kogata N, Nishio K, Hirohashi T, Kikuchi S, Nakai M (1999) Involvement of a chloroplast homologue of the signal recognition particle receptor protein, FtsY, in protein targeting to thylakoids. *FEBS Lett* 447: 329-333

Kovacs L, Damkjaer J, Kereiche S, Ilioaia C, Ruban AV, Boekema EJ, Jansson S, Horton P (2006) Lack of the light-harvesting complex CP24 affects the structure and function of the grana membranes of higher plant chloroplasts. *Plant Cell* 18: 3106-3120

Kuhn A, Stuart R, Henry R, Dalbey RE (2003) The Alb3/Oxa1/YidC protein family: membrane-localized chaperones facilitating membrane protein insertion? *Trends Cell Biol* 13: 510-516

Kurisu G, Zhang H, Smith JL, Cramer WA (2003) Structure of the cytochrome b6f complex of oxygenic photosynthesis: tuning the cavity. *Science* 302: 1009-1014

Laemmli UK (1970) Cleavage of Structural Proteins During Assembly of Head of Bacteriophage-T4. *Nature* 227: 680-&

Laidler V, Chaddock AM, Knott TG, Walker D, Robinson C (1995) A SecY homolog in *Arabidopsis thaliana*. Sequence of a full-length cDNA clone and import of the precursor protein into chloroplasts. *J Biol Chem* 270: 17664-17667

Leister D, Schneider A (2003) From genes to photosynthesis in Arabidopsis thaliana. *Int Rev Cytol* 228: 31-83

Li X, Henry R, Yuan J, Cline K, Hoffman NE (1995) A chloroplast homologue of the signal recognition particle subunit SRP54 is involved in the posttranslational integration of a protein into thylakoid membranes. *Proc Natl Acad Sci U S A* 92: 3789-3793

Lowry OH, Rosebrough NJ, Farr AL, Randall RJ (1951) Protein measurement with the Folin phenol reagent. *J Biol Chem* 193: 265-275

Luirink J, Samuelsson T, de Gier J (2001) YidC/Oxa1p/Alb3: evolutionarily conserved mediators of membrane protein assembly. *FEBS Lett* 501: 1-5

Luirink J, Sinning I (2004) SRP-mediated protein targeting: structure and function revisited. *Biochim Biophys Acta* 1694: 17-35

Luirink J, von Heijne G, Houben E, de Gier JW (2005) Biogenesis of inner membrane proteins in *Escherichia coli*. *Annu Rev Microbiol* 59: 329-355

Lupas A, Van Dyke M, Stock J (1991) Predicting coiled coils from protein sequences. *Science* 252: 1162-1164

Majeran W, Olive J, Drapier D, Vallon O, Wollman FA (2001) The light sensitivity of ATP synthase mutants of Chlamydomonas reinhardtii. *Plant Physiol* 126: 421-433

Mant A, Woolhead CA, Moore M, Henry R, Robinson C (2001) Insertion of PsaK into the thylakoid membrane in a "Horseshoe" conformation occurs in the absence of signal recognition particle, nucleoside triphosphates, or functional albino3. *J Biol Chem* 276: 36200-36206

Marchler-Bauer A, Anderson JB, Chitsaz F, Derbyshire MK, DeWeese-Scott C, Fong JH, Geer LY, Geer RC, Gonzales NR, Gwadz M, He S, Hurwitz DI, Jackson JD, Ke Z, Lanczycki CJ, Liebert CA, Liu C, Lu F, Lu S, Marchler GH, Mullokandov M, Song JS, Tasneem A, Thanki N, Yamashita RA, Zhang D, Zhang N, Bryant SH (2009) CDD: specific functional annotation with the Conserved Domain Database. *Nucleic Acids Res* 37: D205-D210

Marchler-Bauer A, Anderson JB, Derbyshire MK, DeWeese-Scott C, Gonzales NR, Gwadz M, Hao L, He S, Hurwitz DI, Jackson JD, Ke Z, Krylov D, Lanczycki CJ, Liebert CA, Liu C, Lu F, Lu S, Marchler GH, Mullokandov M, Song JS, Thanki N, Yamashita RA, Yin JJ, Zhang D, Bryant SH (2007) CDD: a conserved domain database for interactive domain family analysis. *Nucleic Acids Res* 35: D237-D240

Marques JP, Dudeck I, Klosgen RB (2003) Targeting of EGFP chimeras within chloroplasts. *Mol Genet Genomics* 269: 381-387

Marques JP, Schattat MH, Hause G, Dudeck I, Klosgen RB (2004) In vivo transport of folded EGFP by the DeltapH/TAT-dependent pathway in chloroplasts of Arabidopsis thaliana. *J Exp Bot* 55: 1697-1706

Mattoo AK, Hoffman-Falk H, Marder JB, Edelman M (1984) Regulation of protein metabolism: Coupling of photosynthetic electron transport to in vivo degradation of the rapidly metabolized 32-kilodalton protein of the chloroplast membranes. *Proc Natl Acad Sci U S A* 81: 1380-1384

Michl D, Robinson C, Shackleton JB, Herrmann RG, Klösgen RB (1994) Targeting of proteins to the thylakoids by bipartite presequences: CFoII is imported by a novel, third pathway. *EMBO J* 13: 1310-1317

Mignone F, Gissi C, Liuni S, Pesole G (2002) Untranslated regions of mRNAs. *Genome Biol* 3: Reviews0004

Mollier P, Hoffmann B, Debast C, Small I (2002) The gene encoding Arabidopsis thaliana mitochondrial ribosomal protein S13 is a recent duplication of the gene encoding plastid S13. *Curr Genet* 40: 405-409

Moore M, Goforth RL, Mori H, Henry R (2003) Functional interaction of chloroplast SRP/FtsY with the ALB3 translocase in thylakoids: substrate not required. *J Cell Biol* 162: 1245-1254

Moore M, Harrison MS, Peterson EC, Henry R (2000) Choroplast Oxa1p homolog Albino3 is required for post-translational integration of the light-harvesting chlorophyll-binding protein into thylakoid membranes. *The Journal Of Biological Chemistry* 275: 1529-1532

Mould RM, Shackleton JB, Robinson C (1991) Transport of proteins into chloroplasts. Requirements for the efficient import of two lumenal oxygen-evolving complex proteins into isolated thylakoids. *J Biol Chem* 266: 17286-17289

Murashige T, Skoog F (1962) A revised medium for rapid growth and bio assays with tobacco tissue cultures. *Physiologia Plantarum* 15:

Nagamori S, Smirnova IN, Kaback HR (2004) Role of YidC in folding of polytopic membrane proteins. *J Cell Biol* 165: 53-62

Nakai M, Goto A, Nohara T, Sugita D, Endo T (1994) Identification of the SecA protein homolog in pea chloroplasts and its possible involvement in thylakoidal protein transport. *J Biol Chem* 269: 31338-31341

Nicholas KB, Nicholas HB (1997) GeneDoc: a tool for editing and annotating multiple sequence alignments. *Distributed by the authors*

Nilsson R, Brunner J, Hoffman NE, van Wijk KJ (1999) Interactions of ribosome nascent chain complexes of the chloroplast- encoded D1 thylakoid membrane protein with cpSRP54. *EMBO J* 18: 733-742

Nilsson R, van Wijk KJ (2002) Transient interaction of cpSRP54 with elongating nascent chains of the chloroplast-encoded D1 protein; 'cpSRP54 caught in the act'. *FEBS Lett* 524: 127-133

Ort DR, Yokum CF (1996) Oxygenic Photosynthesis: The light reactions. Kluwer Academic Publishers, Dordrecht, The Netherlands, pp 539-563

Ossenbühl F, Göhre V, Meurer J, Krieger-Liszkay A, Rochaix JD, Eichacker LA (2004) Efficient assembly of photosystem II in *Chlamydomonas reinhardtii* requires Alb3.1p, a homolog of *Arabidopsis* ALBINO3. *Plant Cell* 16: 1790-1800

Ossenbühl F, Hartmann K, Nickelsen J (2002) A chloroplast RNA binding protein from stromal thylakoid membranes specifically binds to the 5' untranslated region of the psbA mRNA. *Eur J Biochem* 269: 3912-3919

Ossenbühl F, Inaba-Sulpice M, Meurer J, Soll J, Eichacker LA (2006) The synechocystis sp PCC 6803 oxa1 homolog is essential for membrane integration of reaction center precursor protein pD1. *Plant Cell* 18: 2236-2246

Pasch JC, Nickelsen J, Schünemann D (2005) The yeast split-ubiquitin system to study chloroplast membrane protein interactions. *Appl Microbiol Biotechnol* 69: 440-447

Pfaffl MW (2001) A new mathematical model for relative quantification in real-time RT-PCR. *Nucleic Acids Res* 29: e45

Preuss M, Ott M, Funes S, Luirink J, Herrmann JM (2005) Evolution of mitochondrial oxa proteins from bacterial YidC: Inherited and acquired functions of a conserved protein insertion machinery. *J Biol Chem*

Pujol C, Marechal-Drouard L, Duchene AM (2007) How can organellar protein N-terminal sequences be dual targeting signals? In silico analysis and mutagenesis approach. *J Mol Biol* 369: 356-367

Rapaport D (2003) Finding the right organelle. Targeting signals in mitochondrial outer-membrane proteins. *EMBO Rep* 4: 948-952

Reynolds ES (1963) Use of Lead Citrate at High Ph As An Electron-Opaque Stain in Electron Microscopy. *Journal of Cell Biology* 17: 208-&

Ridder AN, Morein S, Stam JG, Kuhn A, de Kruijff B, Killian JA (2000) Analysis of the role of interfacial tryptophan residues in controlling the topology of membrane proteins. *Biochemistry* 39: 6521-6528

Rokka A, Suorsa M, Saleem A, Battchikova N, Aro EM (2005) Synthesis and assembly of thylakoid protein complexes: multiple assembly steps of photosystem II. *Biochem J* 388: 159-168

Rudhe C, Chew O, Whelan J, Glaser E (2002) A novel in vitro system for simultaneous import of precursor proteins into mitochondria and chloroplasts. *Plant J* 30: 213-220

Saiki RK, Gelfand DH, Stoffel S, Scharf SJ, Higuchi R, Horn GT, Mullis KB, Erlich HA (1988) Primer-directed enzymatic amplification of DNA with a thermostable DNA polymerase. *Science* 239: 487-491

Sakamoto W, Spielewoy N, Bonnard G, Murata M, Wintz H (2000) Mitochondrial localization of AtOXA1, an *Arabidopsis* homologue of yeast Oxa1p involved in the insertion and assembly of protein complexes in mitochondrial inner membrane. *Plant Cell Physiol* 41: 1157-1163

Sambrook J, Fritsch EF, Maniatis T (1989) Molecular Cloning: A Laboratory Manual. Cold Spring Harbor Laboratory Press New York,

Sambrook J, Russell D (2001) Molecular Cloning: A Laboratory Manual. Cold Spring Harbor Laboratory Press, Cold Spring Harbor, NY,

Samuelson JC, Chen M, Jiang F, Moller I, Wiedmann M, Kuhn A, Phillips GJ, Dalbey RE (2000) YidC mediates membrane protein insertion in bacteria. *Nature* 406: 637-641

Saracco SA, Fox TD (2002) Cox18p is required for export of the mitochondrially encoded Saccharomyces cerevisiae Cox2p C-tail and interacts with Pnt1p and Mss2p in the inner membrane. *Mol Biol Cell* 13: 1122-1131

Schägger H, von Jagow G (1991) Blue native electrophoresis for isolation of membrane protein complexes in enzymatically active form. *Anal Biochem* 199: 223-231

Scholl RL, May ST, Ware DH (2000) Seed and molecular resources for Arabidopsis. *Plant Physiol* 124: 1477-1480

Schünemann D (2004) Structure and function of the chloroplast signal recognition particle. *Curr Genet* 44: 295-304

Schünemann D (2007) Mechanisms of protein import into thylakoids of chloroplasts. *Biol Chem* 388: 907-915

Schünemann D, Amin P, Hartmann E, Hoffman NE (1999) Chloroplast SecY is complexed to SecE and involved in the translocation of the 33-kDa but not the 23-kDa subunit of the oxygen-evolving complex. *J Biol Chem* 274: 12177-12182

Schünemann D, Gupta S, Persello-Cartieaux F, Klimyuk VI, Jones JD, Nussaume L, Hoffman NE (1998) A novel signal recognition particle targets light-harvesting proteins to the thylakoid membranes. *Proc Natl Acad Sci U S A* 95: 10312-10316

Schwacke R, Fischer K, Ketelsen B, Krupinska K, Krause K (2007) Comparative survey of plastid and mitochondrial targeting properties of transcription factors in Arabidopsis and rice. *Mol Genet Genomics* 277: 631-646

Schwacke R, Schneider A, van der GE, Fischer K, Catoni E, Desimone M, Frommer WB, Flugge UI, Kunze R (2003) ARAMEMNON, a novel database for Arabidopsis integral membrane proteins. *Plant Physiol* 131: 16-26

Scotti PA, Urbanus ML, Brunner J, de Gier JW, von Heijne G, van der DC, Driessen AJ, Oudega B, Luirink J (2000) YidC, the *Escherichia coli* homologue of mitochondrial Oxa1p, is a component of the Sec translocase. *EMBO J* 19: 542-549

Seelert H, Poetsch A, Dencher NA, Engel A, Stahlberg H, Muller DJ (2000) Structural biology. Proton-powered turbine of a plant motor. *Nature* 405: 418-419

Sonnhammer EL, von Heijne G, Krogh A (1998) A hidden Markov model for predicting transmembrane helices in protein sequences. *Proc Int Conf Intell Syst Mol Biol* 6: 175-182

Souza RL, Green-Willms NS, Fox TD, Tzagoloff A, Nobrega FG (2000) Cloning and characterization of COX18, a Saccharomyces cerevisiae PET gene required for the assembly of cytochrome oxidase. *J Biol Chem* 275: 14898-14902

Spence E, Bailey S, Nenninger A, Moller SG, Robinson C (2004) A Homolog of Albino3/OxaI Is Essential for Thylakoid Biogenesis in the Cyanobacterium *Synechocystis* sp. PCC6803. *J Biol Chem* 279: 55792-55800

Spurr AR (1969) A low-viscosity epoxy resin embedding medium for electron microscopy. *J Ultrastruct Res* 26: 31-43

Steinemann D, Engelbrecht S, Lill H (1995) Reassembly of Synechocystis sp. PCC 6803 F1-ATPase from its over-expressed subunits. *FEBS Lett* 362: 171-174

Stengel A, Benz P, Balsera M, Soll J, Bolter B (2008) TIC62 redox-regulated translocon composition and dynamics. *J Biol Chem* 283: 6656-6667

Strotmann H, Shavit N, Leu S (1998) *The Molecular Biology of Chloroplast and Mitochondria in Chlamydomonas*. Kluwer Academic Publishers, Norwell, MA, pp 477-500

Stuart R (2002) Insertion of proteins into the inner membrane of mitochondria: the role of the Oxa1 complex. *Biochim Biophys Acta* 1592: 79-87

Sundberg E, Slagter GS, Fridborg I, Cleary SP, Robinson C, Coupland G (1997) Albino3, an *Arabidopsis* nuclear gene essential for chloroplast differentiation, encodes a chloroplast protein that shows homology to proteins present in bacterial membranes yeast mitochondria. *The Plant Cell* 9: 717-730

Szyrach G, Ott M, Bonnefoy N, Neupert W, Herrmann JM (2003) Ribosome binding to the Oxa1 complex facilitates co-translational protein insertion in mitochondria. *EMBO J* 22: 6448-6457

Till BJ, Reynolds SH, Greene EA, Codomo CA, Enns LC, Johnson JE, Burtner C, Odden AR, Young K, Taylor NE, Henikoff JG, Comai L, Henikoff S (2003) Large-scale discovery of induced point mutations with high-throughput TILLING. *Genome Res* 13: 524-530

Towbin H, Staehelin T, Gordon J (1979) Electrophoretic transfer of proteins from polyacrylamide gels to nitrocellulose sheets: procedure and some applications. *Proc Natl Acad Sci U S A* 76: 4350-4354

Tsien RY (1998) The green fluorescent protein. *Annu Rev Biochem* 67: 509-544

van Bloois E, Nagamori S, Koningstein G, Ullers RS, Preuss M, Oudega B, Harms N, Kaback HR, Herrmann JM, Luirink J (2005) The Sec-independent function of Escherichia coli YidC is evolutionary-conserved and essential. *J Biol Chem* 280: 12996-13003

van der Laan LM, Bechtluft P, Kol S, Nouwen N, Driessen AJ (2004) F1FO ATP synthase subunit c is a substrate of the novel YidC pathway for membrane protein biogenesis. *J Cell Biol* 165: 213-222

van Wijk KJ, Bingsmark S, Aro EM, Andersson B (1995) In vitro synthesis and assembly of photosystem II core proteins. The D1 protein can be incorporated into photosystem II in isolated chloroplasts and thylakoids. *J Biol Chem* 270: 25685-25695

Waegemann K, Soll J (1995) Characterization and isolation of the chloroplast protein import machinery. *Methods in Cell Biology, Vol 50* 50: 255-267

Whelan J, Millar AH, Day DA (1996a) The alternative oxidase is encoded in a multigene family in soybean. *Planta* 198: 197-201

Whelan J, O'Mahony P, Harmey MA (1990) Processing of precursor proteins by plant mitochondria. *Arch Biochem Biophys* 279: 281-285

Whelan J, Tanudji MR, Smith MK, Day DA (1996b) Evidence for a link between translocation and processing during protein import into soybean mitochondria. *Biochim Biophys Acta* 1312: 48-54

Wittig I, Braun HP, Schagger H (2006) Blue native PAGE. *Nat Protoc* 1: 418-428

Wollman FA, Minai L, Nechushtai R (1999) The biogenesis and assembly of photosynthetic proteins in thylakoid membranes1. *Biochim Biophys Acta* 1411: 21-85

Woolhead CA, Thompson SJ, Moore M, Tissier C, Mant A, Rodger A, Henry R, Robinson C (2001) Distinct Albino3-dependent and -independent pathways for thylakoid membrane protein insertion. *J Biol Chem* 276: 40841-40846

Yen MR, Harley KT, Tseng YH, Saier MH, Jr. (2001) Phylogenetic and structural analyses of the oxa1 family of protein translocases. *FEMS Microbiol Lett* 204: 223-231

Yi L, Dalbey RE (2005) Oxa1/Alb3/YidC system for insertion of membrane proteins in mitochondria, chloroplasts and bacteria (review). *Mol Membr Biol* 22: 101-111

Yuan J, Henry R, McCaffery M, Cline K (1994) SecA homolog in protein transport within chloroplasts: evidence for endosymbiont-derived sorting. *Science* 266: 796-798

Yuan J, Kight A, Goforth RL, Moore M, Peterson EC, Sakon J, Henry R (2002) ATP stimulates signal recognition particle (SRP)/FtsY-supported protein integration in chloroplasts. *J Biol Chem* 277: 32400-32404

Zhang L, Paakkarinen V, Suorsa M, Aro EM (2001) A SecY homologue is involved in chloroplast-encoded D1 protein biogenesis. *J Biol Chem*

Zhang L, Paakkarinen V, van Wijk KJ, Aro EM (1999) Co-translational assembly of the D1 protein into photosystem II. *J Biol Chem* 274: 16062-16067

Zouni A, Witt HT, Kern J, Fromme P, Krauss N, Saenger W, Orth P (2001) Crystal structure of photosystem II from Synechococcus elongatus at 3.8 A resolution. *Nature* 409: 739-743

Zygadlo A, Robinson C, Scheller HV, Mant A, Jensen PE (2006) The properties of the positively charged loop region in PSI-G are essential for its "spontaneous" insertion into thylakoids and rapid assembly into the photosystem I complex. *J Biol Chem* 281: 10548-10554

Danksagung

Als Erstes möchte ich mich bei Prof. Dr. Soll bedanken, in dessen Arbeitsgruppe ich meine Promotion anfertigen durfte. Seine ständige Unterstützung und Diskussionsbereitschaft haben dieses Projekt stets vorangetrieben.

Desweiteren gilt mein Dank meiner Gruppenleiterin Elisabeth für ihre stete Hilfsbereitschaft, viele gute Gespräche und vor allem auch dafür, dass sie ein wenig Ordnung in unser Labor gebracht hat.

Ein besonderer Dank gilt natürlich auch Lars- für eine nette gemeinsame Zeit im Labor, viele anregende Gespräche und dafür, dass es immer mit Rat und Tat zur Seite stand – auch nachdem er das Labor verlassen hatte.

Vielen Dank auch an Maxi und Inge, für ihre große Hilfe bei vielen Experimenten, der Arbeit mit den Pflanzen, den unzähligen Antikörpertests und die vermutlich weltbesten Protoplasten!

Für das nette Arbeitsklima und die gegenseitige Hilfe bei der Lösung der vielen kleinen und großen Probleme des Laboralltags danke ich allen Mitgliedern der Arbeitsgruppe. Insbesondere auch Birgit, Ingrid und Sabrina für viele lustige Stunden im Labor. Ich hatte viel Spaß - auch wenn es nicht immer danach aussah…

Allen Postdocs (auch Ehemaligen und jetzigen Professoren) der AG Soll danke ich für anregende Diskussionen, guten Rat und vor allem viele gute Ideen. Besonderer Dank gilt dabei Bettina, Ute, Enrico, Katrin and Manu.

Dankbar bin auch auch all denjenigen, die mit Experimenten, Proben oder Gesprächen zu diesem Projekt beigetragen haben: Thomas Bals und Danja Schünemann (Bochum), sowie Andreas Kuhn (Hohenheim) für nette Kooperationen in Sachen Alb4, Irene für die Elektronenmikroskopie, sowie Serena Schwenkert und Jörg Meurer für die ATP Synthase Antikörper.

Vielen Dank auch an Hannes Herrmann für einige nette Konferenzen, viele gute und hilfreiche Gepräche und seine stete Motivation. Dank auch an Heike Bauerschmitt, die immer für eine Kooperation offen war – vielleicht klappt es ja doch noch irgendwann.

Besonderen Dank auch an alle, die mir beim Schreiben und Verbessern dieser Arbeit mit zahlreichen Tipps geholfen haben. Dabei insebesondere Lars und Elisabeth für das schnelle Korrekturlesen.

Ganz besonders danke ich natürlich meinen Eltern und Familie, die immer für mich da waren und mich jederzeit unterstützten.

Curriculum vitae

Personal Details:

Birth Date:	December 20th, 1974
Birth Place:	Salzgitter, Germany
Marital Status:	engaged
Citizenship:	German

Education:

School (1981-1994)

08.1987 – 06.1994:	Gymnasium Groß Ilsede (German secondary school) Graduation: Abitur

Vocational training

08.1994 - 06.1996:	Training as technical assistant of Biology at Technical High School ´Dr. von Morgenstern-Schulen` in Braunschweig
07.1996 - 07.1998:	Work as subject teacher for specialized practice at Technical High ´Dr. von Morgenstern-Schulen` in Braunschweig

University

10.1998 – 09.2000:	Undergraduate studies of Biology at the ´Technische Universität Carolo-Wilhelmina zu Braunschweig`
29.09.2000:	Degree: Prediploma in the subjects Zoology, Genetics, Microbiology, Botany, Mathematics and Organic Chemistry (Average grade: „very good“)
09.2000 – 09.2003:	Graduate studies of Biology: Botany (main subject), Microbiology, Cell Biology (subsidiary subjects)
01.2003 – 09.2003:	Preparation of the Diploma thesis in the lab of Prof. Dr. Brigitte M. Jockusch at the ´Technische Universität Carolo- Wilhelmina zu Braunschweig` Title: „ Analysis of the conformation of the Vinculin tail domain with Electron-Spin-Resonance Spectroscopy“
18.08.2003:	Receiving of the academic degree: Diplom-Biologin (Grade: „passed with distinction“)
11.2003 – 08.2004:	Work experience in the lab of Dr. Ulla Knaus at the ´Scripps Research Institute ` in San Diego, USA
10.2004 – :	PhD graduate student in the lab of Prof. Dr. J. Soll at the ’Ludwig-Maximilians-Universität München’ (LMU München), Munich, Germany

List of publications

Original papers:

Gerdes L., Bals T., Klostermann E., **Karl M.**, Philippar K., Hünken M., Soll J. and Schünemann D. (2006). A second thylakoid membrane localized Alb3/Oxa1/YidC homologue is involved in proper chloroplast biogenesis in *Arabidopsis thaliana*. J.Biol.Chem.281, 16632-16642.

Karl M., Bals T., Gügel I.L., Piotrowski M., Maier U., Kuhn A., Schünemann D., Soll J., Ankele E. (2009). Alb4 of *Arabidopsis* promotes assembly and stabilisation of a none chlorophyll-binding photosynthetic complex, the CF_1CF_0-ATP synthase. In preparation

Reviews:

Karl M., Ankele E. and Soll J. (2009) The role of Alb3/YidC-like proteins in the formation of photosynthetic membranes. Current topics on plant biology. Accepted

Poster:

Oxa-related proteins in *Arabidopsis thaliana*. **Karl M.**, Gerdes L**.** and Soll J.
FEBS Advanced Course on Origin and Evolution of Mitochondria and Chloroplasts, Wildbad-Kreuth, Germany (2005)

Oxa-like proteins in *Arabidopsis thaliana*. **Karl M.**, Gerdes L**.,** Hünken M. and Soll J.
EMBO Conference on Protein Transport Systems: Protein Targeting and Translocation, Gdansk, Poland (2006)

Identification and localization of Oxa-like proteins in *Arabidopsis thaliana.* Karl M., Gerdes L**.,** Hünken M and Soll J. FEBS Advanced Course on Origin and Evolution of Mitochondria and Chloroplasts, Maratea, Italy (2007)

Characterization of Alb4- a second Alb3/Oxa1/YidC homologue in the thylakoid membrane. Karl M., Ankele E., and Soll J. SFB TR1 Conference, Munich, Germany (2008)

Talks

Alb4-a second Alb3/Oxa1/YidC homolog in the thylakoid membrane. (2008)
ISE-G-Meeting, Munich, Germany

Ehrenwörtliche Versicherung

Ich versichere hiermit ehrenwörtlich, dass die vorgelegte Dissertation von mir selbständig und nur unter Verwendung der angegebenen Hilfsmittel und Quellen angefertigt wurde.

München, den

Monique Karl

Erklärung

Hiermit erkläre ich, dass ich zuvor nicht versucht habe, anderweitig eine Dissertation einzureichen oder mich einer Doktorprüfung zu unterziehen. Die vorliegende Dissertation wurde keiner weiteren Prüfungskommission weder in Teilen noch als Ganzes vorgelegt.

München, den

Monique Karl